

AD A 053560

RADC-TR-76-101, Volume VI (of seven)
Phase Report
February 1978



2

APPLICATIONS OF MULTICONDUCTOR TRANSMISSION LINE THEORY
TO THE PREDICTION OF CABLE COUPLING, A Digital Computer
Program for Determining Terminal Currents Induced in a
Multiconductor Transmission Line by an Incident
Electromagnetic Field

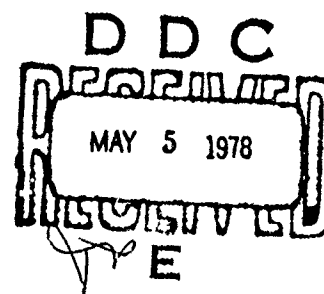
Clayton R. Paul

University of Kentucky

AD NO. _____
DDC FILE COPY

Approved for public release; distribution unlimited.

ROME AIR DEVELOPMENT CENTER
Air Force Systems Command
Griffiss Air Force Base, New York 13441



This report contains a large percentage of machine-produced copy which is not of the highest printing quality but because of economical consideration, it was determined in the best interest of the government that they be used in this publication.

This report has been reviewed by the RADC Information Office (OI) and is releasable to the National Technical Information Service (NTIS). At NTIS it will be releasable to the general public, including foreign nations.

RADC-TR-76-101, Volume VI (of seven) has been reviewed and is approved for publication.

APPROVED:

Jacob Scherer
JACOB SCHERER
Project Engineer

APPROVED:

Lester E. Treankler
LESTER E. TREANKLER, Lt Col, USAF
Assistant Chief
Reliability & Compatibility Division

ACCESSION FOR	
NTIS	Info Section <input checked="" type="checkbox"/>
DDO	Detl Section <input type="checkbox"/>
UNANNOUNCED	<input type="checkbox"/>
JUSTIFICATION	
BY	
DISTRIBUTION/AVAILABILITY	
NO.	AVAIL. NO. or SPECIAL
A	

FOR THE COMMANDER:

John P. Huss
JOHN P. HUSS
Acting Chief, Plans Office

If your address has changed or if you wish to be removed from the RADC mailing list, or if the addressee is no longer employed by your organization, please notify RADC (RBC) Griffiss AFB NY 13441. This will assist us in maintaining a current mailing list.

Do not return this copy. Retain or destroy.

18/RADC 19/TR-76-101-6-VOL-6

UNCLASSIFIED

SECURITY CLASSIFICATION OF THIS PAGE (When Data Entered)

REPORT DOCUMENTATION PAGE		READ INSTRUCTIONS BEFORE COMPLETING FORM
1. REPORT NUMBER RADC-TR-76-101, Vol VI (of seven)	2. GOVT ACCESSION NO.	3. RECIPIENT'S CATALOG NUMBER (9) Phase rept.
4. TITLE (and Subtitle) APPLICATIONS OF MULTICONDUCTOR TRANSMISSION LINE THEORY TO THE PREDICTION OF CABLE COUPLING. A Digital Computer Program for Determining Terminal Currents Induced in a Multiconductor Transmission Line by an Incident Electromagnetic Field.	5. TYPE OF REPORT & PERIOD COVERED Phase Report	6. PERFORMING ORG. REPORT NUMBER N/A
7. AUTHOR(s) Clayton R./Paul	8. CONTRACT OR GRANT NUMBER(s) F30602-75-C-0113	9. PROGRAM ELEMENT, PROJECT, TASK AREA & WORK UNIT NUMBERS 6270274 23380305 17/43
10. PERFORMING ORGANIZATION NAME AND ADDRESS University of Kentucky Department of Electrical Engineering Lexington KY 40506	11. CONTROLLING OFFICE NAME AND ADDRESS Roe Air Development Center (RBC) Griffiss AFB NY 13441	12. NUMBER OF PAGES 185
13. MONITORING AGENCY NAME & ADDRESS (if different from Controlling Office) Same	14. SECURITY CLASS. (of this report) UNCLASSIFIED 12/197p	15. DECLASSIFICATION/DOWNGRADING SCHEDULE N/A
16. DISTRIBUTION STATEMENT (of this Report) Approved for public release; distribution unlimited.		
17. DISTRIBUTION STATEMENT (of the abstract entered in Block 20, if different from Report) Same		
18. SUPPLEMENTARY NOTES RADC Project Engineer: Jacob Scherer (RBC)		
19. KEY WORDS (Continue on reverse side if necessary and identify by block number) Electromagnetic Compatibility Wire-to-Wire Coupling Cable Coupling Crosstalk Transmission Lines Field-to-Wire Multiconductor Transmission Lines Incident Electromagnetic Field.		
20. ABSTRACT (Continue on reverse side if necessary and identify by block number) The report describes a digital computer program which is designed to compute the terminal currents induced in a multiconductor transmission line by an incident electromagnetic field. Sinusoidal steady state behavior of the line is assumed. The transmission line is uniform and consists of n wires and a reference conductor immersed in a homogeneous, lossless, linear, isotropic medium. The n wires and the reference conductor are assumed to be lossless. The reference conductor may be a wire, an infinite ground plane or an overall, cylindrical shield. The incident electromagnetic field may be a uniform plane wave or		

DD FORM 1 JAN 73 1473 EDITION OF 1 NOV 65 IS OBSOLETE

UNCLASSIFIED

SECURITY CLASSIFICATION OF THIS PAGE (When Data Entered)

444 722

Shil

UNCLASSIFIED

SECURITY CLASSIFICATION OF THIS PAGE(When Data Entered)

cont.

a general nonuniform field. The primary restriction on the program validity is that the cross sectional dimensions of the line, e.g., wire separation, must be much less than a wavelength.



UNCLASSIFIED

SECURITY CLASSIFICATION OF THIS PAGE(When Data Entered)

PREFACE

This effort was conducted by The University of Kentucky under the sponsorship of the Rome Air Development Center Post-Doctoral Program for RADC's Compatibility Branch. Mr. Jim Brodock of RADC was the task project engineer and provided overall technical direction and guidance.

The RADC Post-Doctoral Program is a cooperative venture between RADC and some sixty-five universities eligible to participate in the program. Syracuse University (Department of Electrical Engineering), Purdue University (School of Electrical Engineering), Georgia Institute of Technology (School of Electrical Engineering), and State University of New York at Buffalo (Department of Electrical Engineering) act as prime contractor schools with other schools participating via sub-contracts with the prime schools. The U.S. Air Force Academy (Department of Electrical Engineering), Air Force Institute of Technology (Department of Electrical Engineering), and the Naval Post Graduate School (Department of Electrical Engineering, also participate in the program.

The Post-Doctoral Program provides an opportunity for faculty at participating universities to spend up to one year full time on exploratory development and problem-solving efforts with the post-doctorals splitting their time between the customer location and their educational institutions. The program is totally customer-funded with current projects being undertaken for Rome Air Development Center (RADC), Space and Missile Systems Organization (SANSO), Aeronautical Systems Division (ASD), Electronics Systems Division (ESD), Air Force Avionics Laboratory (AFAL), Foreign Technology Division (FTD), Air Force Weapons Laboratory (AFWL), Armament Development and Test Center (ADTC), Air Force Communications Service (AFCS), Aerospace

Defense Command (ADC), Hq USAF, Defense Communications Agency (DCA), Navy, Army, Aerospace Medical Division (AMD), and Federal Aviation Administration (FAA).

Further information about the RADC Post-Doctoral Program can be obtained from Mr. Jacob Scherer, RADC/RBC, Griffiss AFB, NY, 13441, telephone Autovon 587-2543, commercial (315)330-2543.

The author of this report is Clayton R. Paul. He received the BSEE degree from The Citadel (1963), the MSEE degree from Georgia Institute of Technology (1964), and the Ph.D. degree from Purdue University (1970). He is currently an Associate Professor with the Department of Electrical Engineering, University of Kentucky, Lexington, Kentucky 40506.

The author wishes to acknowledge the capable efforts of Ms. Donna Tomlin in typing this manuscript.

TABLE OF CONTENTS

	<u>Page</u>
I. INTRODUCTION -----	1
II. MODEL DERIVATIONS -----	4
2.1 Derivation of the Multiconductor Transmission Line Equations -----	6
2.2 Derivation of the Equivalent Induced Source Vectors, $\underline{V}_s(\underline{z})$ and $\underline{I}_s(\underline{z})$ for TYPE 1 Structures -----	13
2.3 Determining the Per-Unit-Length Inductance Matrix, \underline{L} , for TYPE 1 Structures -----	25
2.4 Determination of the Equivalent Induced Source Vectors and the Per-Unit-Length Inductance Matrix for TYPE 2 Structures -----	29
2.5 Determination of the Equivalent Induced Source Vectors and the Per-Unit-Length Inductance Matrix for TYPE 3 Structures -----	32
2.6 Determining the Entries in the Termination Network Impedance (Admittance) Matrices -----	34
III. DERIVATION OF THE EXCITATION SOURCES FOR UNIFORM PLANE WAVE AND NONUNIFORM FIELD EXCITATIONS -----	43
3.1 Basic Integrals -----	44
3.2 Derivation of the Source Vectors for Uniform Plane Wave Illumination and TYPE 1 Structures -----	46
3.3 Derivation of the Source Vectors for Uniform Plane Wave Illumination and TYPE 2 Structures -----	54
3.4 Calculation of the Source Vectors for Nonuniform Fields -----	61
IV. COMPUTER PROGRAM DESCRIPTION -----	70
4.1 Main Program Description -----	70
4.2 Subroutine LEQTIC -----	78
4.3 Function Subprograms E1 and E2 -----	79

TABLE OF CONTENTS (continued)

	<u>Page</u>
V. USER'S MANUAL -----	86
5.1 Transmission Line Structure Characteristics Cards, Group I -----	87
5.2 The Termination Network Characterization Cards, Group II -----	91
5.3 The Field Specification Cards, Group III -----	98
5.3.1 Uniform Plane Wave Illumination, FSO = 1 -----	98
5.3.2 Nonuniform Field Illumination, FSO = 2 -----	101
VI. EXAMPLES OF PROGRAM USAGE -----	112
6.1 Example I -----	112
6.1.1 Two Wires Above a Ground Plane -----	112
6.1.2 Two Wires Above a Ground Plane by the Method of Images -----	115
6.1.3 Comparison of the Two Solutions -----	131
6.2 Example II -----	132
6.2.1 Use of the Nonuniform Field Specification Option, FSO = 2 -----	138
VII. SUMMARY -----	150
REFERENCES -----	151
APPENDIX A -----	153
APPENDIX B -----	158
APPENDIX C -----	181

LIST OF ILLUSTRATIONS

<u>FIGURE</u>		<u>PAGE</u>
2-1	Cross-sections of the transmission line structures. -----	5
2-2	The per-unit-length model. -----	8
2-3	The termination networks. -----	10
2-4	-----	14
2-5	-----	27
2-6	-----	30
2-7	-----	33
2-8	-----	36
2-9	-----	38
3-1	The TYPE 1 structure. -----	48
3-2	Definition of the uniform plane wave parameters. -----	49
3-3	-----	53
3-4	The TYPE 2 structure. -----	55
3-5	-----	59
3-6	(a) Nonuniform field specification for TYPE 1 structures. -----	63
	(b) Nonuniform field specification for TYPE 2 structures. -----	64
	(c) Nonuniform field specification for TYPE 3 structures. -----	65
3-7	Piecewise-linear field specification. -----	66
5-1	The TYPE 1 structure. -----	88
5-2	The TYPE 2 structure. -----	89
5-3	The TYPE 3 structure. -----	90
5-4	Definition of the uniform plane wave parameters. -----	99

LIST OF ILLUSTRATIONS (continued)

<u>FIGURE</u>		<u>PAGE</u>
5-5	(a) Nonuniform field specification for TYPE 1 structures. -----	103
	(b) Nonuniform field specification for TYPE 2 structures. -----	104
	(c) Nonuniform field specification for TYPE 3 structures. -----	105
5-6	Ordering of Card Groups in Group III for FSO = 2. -----	107
6-1	Example I. -----	113
6-2 (a)	Data cards for the problem in Figure 6-1 with $E_m = 1 \text{ V/m}$, $\theta_E = 30^\circ$, $\theta_p = 150^\circ$, $\phi_p = 40^\circ$. -----	116
6-2 (b)	Data cards for the problem in Figure 6-1 with $E_m = 1 \text{ V/m}$, $\theta_E = 0^\circ$, $\theta_p = 90^\circ$, $\phi_p = 90^\circ$. -----	117
6-2 (c)	Data cards for the problem in Figure 6-1 with $E_m = 1 \text{ V/m}$, $\theta_E = 0^\circ$, $\theta_p = 180^\circ$, $\phi_p = 90^\circ$. -----	118
6-3 (a)	The problem in Figure 6-1. -----	119
6-3 (b)	The problem in Figure 6-1. -----	120
6-3 (c)	The problem in Figure 6-1. -----	121
6-4	Example I, the image problem for Figure 6-1. -----	122
6-5 (a)	Data cards for the problem in Figure 6-4 with $E_m = 1 \text{ V/m}$, $\theta_E = 30^\circ$, $\theta_p = 150^\circ$, $\phi_p = 40^\circ$. -----	125
6-5 (b)	Data cards for the problem in Figure 6-4 with $E_m = 1 \text{ V/m}$, $\theta_E = 0^\circ$, $\theta_p = 90^\circ$, $\phi_p = 90^\circ$. -----	126
6-5 (c)	Data cards for the problem in Figure 6-4 with $E_m = 1 \text{ V/m}$, $\theta_E = 0^\circ$, $\theta_p = 180^\circ$, $\phi_p = 90^\circ$. -----	127
6-6 (a)	The problem in Figure 6-4. -----	128
6-6 (b)	The problem in Figure 6-4. -----	129
6-6 (c)	The problem in Figure 6-4. -----	130
6-7	-----	133
6-8	Example II. -----	134

LIST OF ILLUSTRATIONS (continued)

<u>FIGURE</u>		<u>PAGE</u>
6-9	Data cards for the problem in Figure 6-8 with $E_m = 1 \text{ V/m}$, $\theta_E = 180^\circ$, $\theta_p = 0^\circ$, $\phi_p = 90^\circ$, $FSO = 1$. -----	136
6-10	The problem in Figure 6-8 with $FSO = 1$. -----	137
6-11	Data cards for the problem in Figure 6-8 with $E_m = 1 \text{ V/m}$, $\theta_E = 0^\circ$, $\theta_p = 90^\circ$, $\phi_p = 90^\circ$, $FSO = 1$. -----	139
6-12	The problem in Figure 6-5 with $FSO = 1$. -----	140
6-13	Data cards for the problem in Figure 6-8 with $E_m = 1 \text{ V/m}$, $\theta_E = 180^\circ$, $\theta_p = 0^\circ$, $\phi_p = 90^\circ$, $FSO = 2$. Sheet 1 of 3 -----	142
	Sheet 2 of 3 -----	143
	Sheet 3 of 3 -----	144
6-14	The problem of Figure 6-8 using the nonuniform field specification option. -----	145
6-15	Data cards for the problem in Figure 6-8 with $E_m = 1 \text{ V/m}$, $\theta_E = 0^\circ$, $\theta_p = 90^\circ$, $\phi_p = 90^\circ$, $FSO = 2$. Sheet 1 of 3 -----	146
	Sheet 2 of 3 -----	147
	Sheet 3 of 3 -----	148
6-16	The problem of Figure 6-8 using the nonuniform field specification option. -----	149
A-1	Illustration of common mode and differential mode currents. -----	154

LIST OF TABLES

<u>TABLES</u>		<u>PAGE</u>
1	Format of the Structure Characteristics Cards, Group I -----	92
2	Format of the Termination Network Characterization Cards, Group II	
	Group II (a) -----	95
	Group II (b) -----	96
3	Format of the Field Specification Cards, Group III, for Uniform Plane Wave Illumination, FSO = 1--	100
4	Format of the Field Specification Cards, Group III, for Nonuniform Fields, FSO = 2.	
	Sheet 1 of 4 -----	108
	Sheet 2 of 4 -----	109
	Sheet 3 of 4 -----	110
	Sheet 4 of 4 -----	111

I. INTRODUCTION

The problem of determining the currents induced in termination networks at the ends of a multiconductor transmission line by an incident electromagnetic field is obviously quite important in determining the electromagnetic compatibility of electronic systems. The digital computer program described in this report is intended to be used for this purpose.

The special case of a transmission line consisting of two wires (cylindrical conductors) immersed in a general, nonuniform field was considered by Taylor, Satterwhite and Harrison [3]. The equations for the terminal currents obtained in [3] were placed in a more convenient form by Smith [4]. The special case of a uniform plane wave incident on a three-wire line (the three wires lie in a plane) in the transverse direction (perpendicular to the transmission line longitudinal (x) axis) with the electric field intensity vector polarized parallel to the line axis was obtained by Harrison in [5]. Paul has extended these special case results to (n+1) conductor (multiconductor) lines for an arbitrary incident electromagnetic field [1,6].

This report describes a digital computer program, WIRE, which is designed to calculate the sinusoidal, steady state, terminal currents induced at the ends of a uniform, multiconductor transmission line which is illuminated by an incident electromagnetic field. Three types of transmission line structures are considered. TYPE 1 structures consist of (n+1) parallel wires. TYPE 2 structures consist of n wires above an infinite ground plane. TYPE 3 structures consist of n wires within an overall, cylindrical shield.

For each structure type, one of the conductors is designated as the reference conductor for the line voltages. For TYPE 1 structures, the

reference conductor is one of the $(n+1)$ wires. For TYPE 2 structures, the reference conductor is the ground plane. For TYPE 3 structures, the reference conductor is the overall, cylindrical shield.

All of the transmission lines are considered to be uniform in the sense that there is no variation in the cross-sections of the $(n+1)$ conductors along the transmission line axis and all $(n+1)$ conductors are parallel to each other. All conductors are considered to be perfect conductors and the surrounding medium is considered to be homogeneous, linear, isotropic and lossless.

The incident field can be in the form of a uniform plane wave for TYPE 1 and TYPE 2 structures or a nonuniform field for all structure types. The uniform plane wave excitation is specified by data entries describing the magnitude of the electric field intensity vector, the orientation of this vector and the direction of propagation. These quantities will be made precise in the following chapters. For the nonuniform field, the data entries are the values of the incident electric field intensity (magnitude and phase) at points along the axes of the conductors and along contours between the wires at the two ends of the line. Piecewise-linear behavior of the fields (magnitude and phase) is assumed between these data points.

The primary restrictions on the program are that the cross-sectional dimensions of the line, e.g., conductor separations, are much smaller than a wavelength at the frequency in question and the ratios of conductor separation to wire radii are greater than approximately 5. The first restriction is imposed to insure (in a qualitative fashion) that only the TEM mode of propagation is significant, i.e., the higher order modes are non-propagating. This requirement that the cross-sectional dimensions of the

line are electrically small must also be imposed to insure that the definition of voltage is independent of path if the incident field is not curl free in the line's cross-sectional plane. (See Chapter II.) The second restriction is necessary to insure the validity of the entries in the per-unit-length transmission line inductance and capacitance matrices. The entries in these matrices are derived by assuming that the per-unit-length charge distributions on the wires are essentially constant around the peripheries of the wires, i.e., the wires are separated from each other sufficiently to insure that proximity effect is not a factor.

General termination structures are provided for at the ends of the transmission line. These terminations are assumed to be linear.

Chapter II contains the derivation of the equations for general field excitations. Chapter III contains a derivation of the equivalent sources induced in the structure types by uniform plane waves as well as nonuniform fields. Chapter IV contains a discussion of the contents of the program. Chapter V contains a User's Manual and Chapter VI contains examples which are used to check the program operation.

II. MODEL DERIVATIONS

Cross-sections of the three basic types of structures considered by the program are shown in Figure 2-1. The axis of the line is the x coordinate and the (n+1) conductors are perpendicular to the y,z plane as indicated in Figure 2-1. The TYPE 1 structure consists of (n+1) wires in which one of the wires is designated as the reference conductor for the line voltages. The TYPE 2 structure consists of n wires above an infinite ground plane where the ground plane is the reference conductor for the line voltages. The TYPE 3 structure consists of n wires within an overall cylindrical shield. In this case, the shield is the reference conductor.

All conductors are considered to be perfect conductors and the surrounding medium is considered to be homogeneous, linear, isotropic and lossless. The surrounding medium (homogeneous) is characterized by a permittivity ϵ and a permeability μ . Throughout this report, the permeability and permittivity of free space will be denoted by $\mu_v = 4\pi \times 10^{-7}$ and $\epsilon_v \cong (1/36\pi) \times 10^{-9}$, respectively, and the permeability and permittivity of the medium are related to the free space values by the relative permeability, μ_r , and relative permittivity (relative dielectric constant), ϵ_r , as $\mu = \mu_r \mu_v$ and $\epsilon = \epsilon_r \epsilon_v$, respectively. For structure TYPE 1 and TYPE 2, a logical choice for ϵ_r and μ_r would be 1 (free space). For structure TYPE 3, a logical choice for the relative permeability, μ_r , would be 1 as is typical of dielectrics. The program, however, allows for any ϵ_r and μ_r for all structure types.

The n wires are labeled from 1 to n and the radius of the i-th wire is denoted by r_{wi} . The reference conductor is designated as the zero-th conductor. For TYPE 1 structures, the reference wire has radius r_{w0} and the

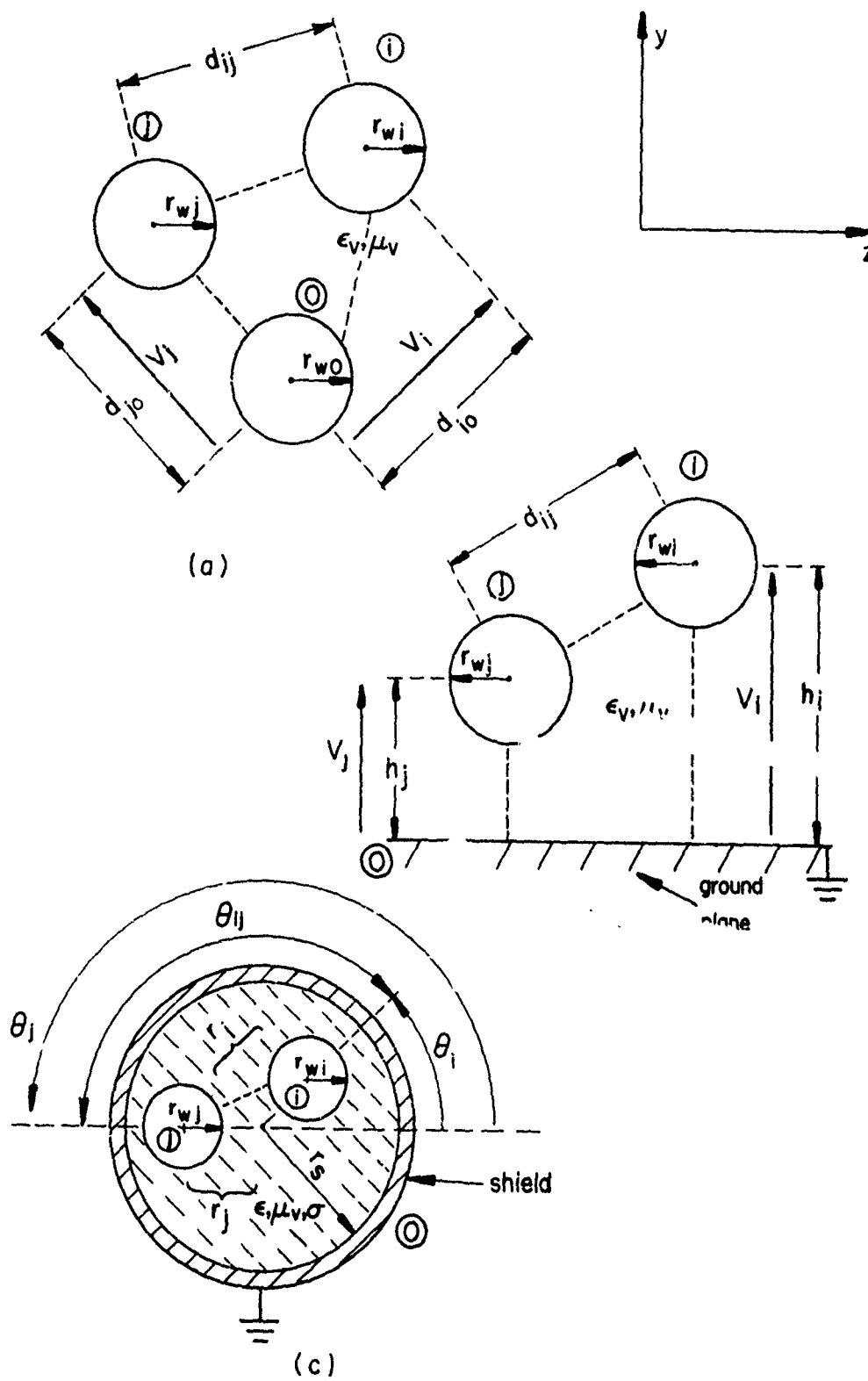


Figure 2-1. Cross-sections of the transmission line structures.

center-to-center separation between the i -th and j -th wires is designated as d_{ij} . For TYPE 2 structures, the i -th wire is at a height h_i about the ground plane with a center-to-center separation between the i -th and j -th wires of d_{ij} . For TYPE 3 structures, the interior radius of the cylindrical shield is designated by r_s , the i -th wire is at a distance r_i from the shield center and the angular separation between the i -th and j -th wires is designated by θ_{ij} .

Implicit in the following is the requirement for the transmission line to be uniform. Transmission lines considered here are uniform in the sense that all $(n+1)$ conductors have uniform cross-sections along the line axis and all n wires are parallel to each other and the reference conductor.

2.1 Derivation of the Multiconductor Transmission Line Equations

The distributed parameter transmission line equations for multiconductor lines with incident field illumination can be derived and are similar (with matrix notation employed) to the familiar equations for two-conductor lines [1,2,6,7,8]. Assuming sinusoidal excitation at a radian frequency $\omega=2\pi f$, the electric field intensity vector, $\vec{E}(x,y,z,t)$, and the magnetic field intensity vector, $\vec{H}(x,y,z,t)$, are written as $\vec{E}(x,y,z,t) = \vec{E}(x,y,z)e^{j\omega t}$ and $\vec{H}(x,y,z,t) = \vec{H}(x,y,z)e^{j\omega t}$. The complex vectors $\vec{E}(x,y,z)$ and $\vec{H}(x,y,z)$ are the phasor quantities. Line voltages, $V_i(x,t) = V_i(x)e^{j\omega t}$, of the i -th conductor with respect to the zeroth conductor (the reference conductor) are defined as the line integral of \vec{E} between the two conductors along a path in the y,z plane. $V_i(x)$ is the complex phasor voltage. The line current, $I_i(x,t) = I_i(x)e^{j\omega t}$ associated with the i -th conductor and directed in the x direction is defined as the line integral of \vec{H} along a closed contour in the y,z plane encircling only the i -th conductor and $I_i(x)$ is the complex phasor current.

The current in the reference conductor, $I_0(x, t) = I_0 e^{j\omega t}$, satisfies $I_0 = \sum_{i=1}^n (-I_i(x))$.

It is convenient to consider the effects of the spectral components of the incident field as per-unit-length distributed sources along the line. The sources appear as series voltage sources and shunt current sources as indicated in Figure 2-2 for an "electrically small" Δx section of the line. The multiconductor transmission line equations may then be derived for the Δx subsection in Figure 2-2 in the limit as $\Delta x \rightarrow 0$ as a set of $2n$ coupled, complex, ordinary differential equations [1],

$$\frac{d}{dx} \underline{V}(x) + j\omega \underline{L} \underline{I}(x) = \underline{V}_s(x) \quad (2-1a)$$

$$\frac{d}{dx} \underline{I}(x) + j\omega \underline{C} \underline{V}(x) = \underline{I}_s(x) \quad (2-1b)$$

A matrix \underline{M} with m rows and n columns is denoted as $m \times n$ and the element in the i -th row and j -th column is denoted by $[M]_{ij}$. $\underline{V}(x)$ and $\underline{I}(x)$ are $n \times 1$ vectors of the line voltages and currents, respectively. The elements in the i -th rows are $[\underline{V}(x)]_i = V_i(x)$ and $[\underline{I}(x)]_i = I_i(x)$ and $[\underline{V}'(x)]_i = (d/dx)V_i(x)$. The $n \times n$ real, symmetric, constant matrices \underline{L} and \underline{C} are the per-unit-length inductance and capacitance matrices, respectively. From Figure 2-2 one can derive (2-1) and the entries in \underline{L} and \underline{C} become [1]

$$[\underline{L}]_{ii} = \ell_i + \ell_0 - 2m_{i0} \quad (2-2a)$$

$$[\underline{L}]_{ij} = \ell_0 + m_{ij} - m_{i0} - m_{j0} \quad (2-2b)$$

$i \neq j$

and

$$[\underline{C}]_{ii} = c_{i0} + \sum_{\substack{j=1 \\ i \neq j}}^n c_{ij} \quad (2-3a)$$

$$[\underline{C}]_{ij} = -c_{ij} \quad (2-3b)$$

$i \neq j$

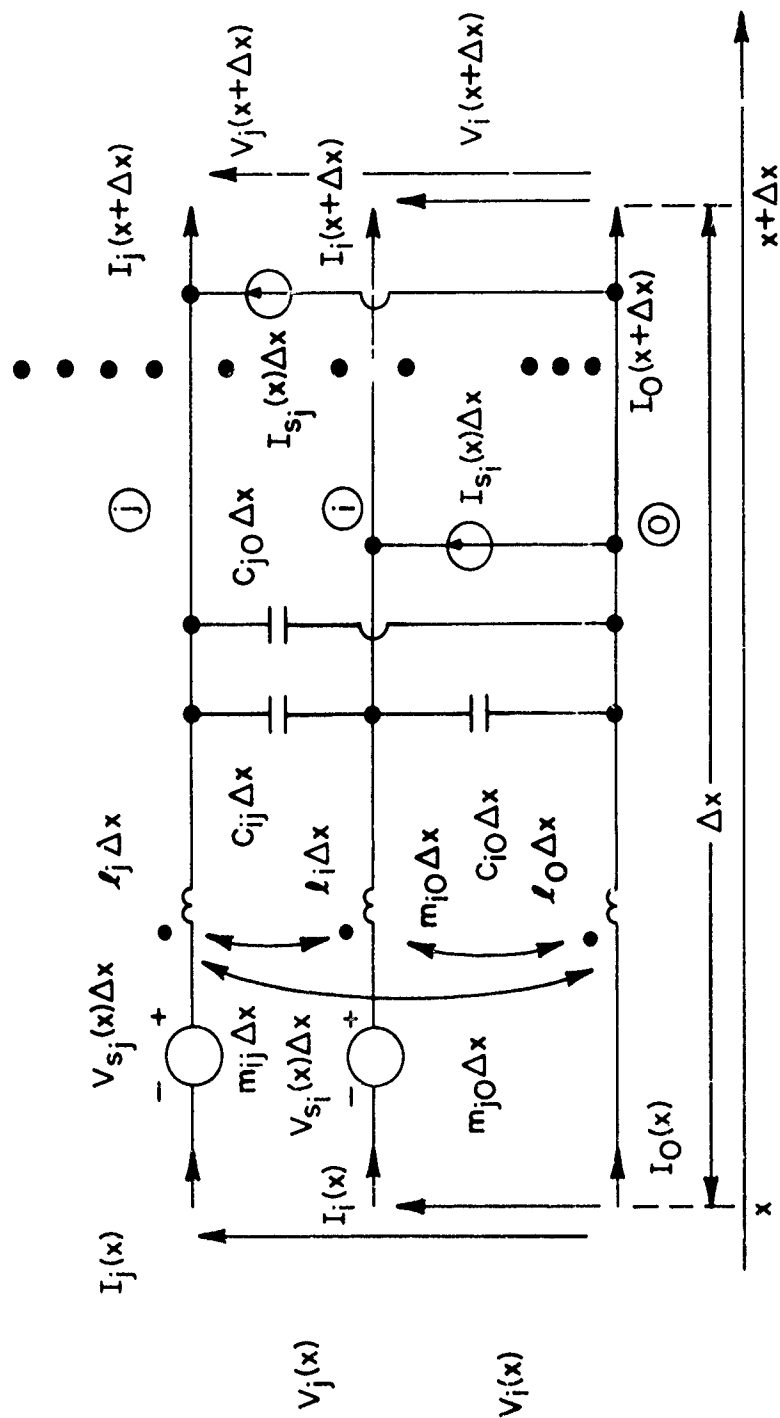


Figure 2-2. The per-unit-length model.

The entries in $\underline{V}_s(x)$ and $\underline{I}_s(x)$ are the per-unit-length distributed sources along the line induced by the incident field, i.e., $[\underline{V}_s(x)] = V_{si}(x)$ and $[\underline{I}_s(x)] = I_{si}(x)$, as shown in Figure 2-2.

In order to consider general termination networks (and allowing independent sources in these networks) we may characterize these as generalized Thevenin equivalents [1]. For a line of total length l , the equations for the termination networks at $x = 0$ and $x = l$ are

$$\underline{V}(0) = \underline{V}_0 - \underline{Z}_0 \underline{I}(0) \quad (2-4a)$$

$$\underline{V}(l) = \underline{V}_l + \underline{Z}_l \underline{I}(l) \quad (2-4b)$$

where \underline{V}_0 and \underline{V}_l are $n \times 1$ vectors of equivalent open circuit port excitation voltages, $[\underline{V}_0]_i = V_{0i}$ and $[\underline{V}_l]_i = V_{li}$, and \underline{Z}_0 and \underline{Z}_l are $n \times n$ symmetric impedance matrices as shown in Figure 2-3. This is, of course, a completely general and arbitrary characterization of these linear termination networks. The entries in these termination equations can be easily determined for a given network by considering $V_i(0)$ and $V_i(l)$ (the termination port voltages) as independent sources, and writing the loop current equations for each network where $I_i(0)$ and $I_i(l)$ are subsets of the loop currents in each network. (See Section 2.6.)

With the line immersed in a homogeneous medium with permittivity ϵ and permeability μ , the product of \underline{L} and \underline{C} becomes [1]

$$\underline{LC} = \underline{CL} = \mu \epsilon \underline{1}_n \quad (2-5)$$

where $\underline{1}_n$ is the $n \times n$ identity matrix with ones on the main diagonal and zeros elsewhere, i.e., $[\underline{1}_n]_{ii} = 1$, and $[\underline{1}_n]_{ij} = 0$, $i \neq j$. For this case, the solution to (2-1) and (2-4) is in a simple form [1]

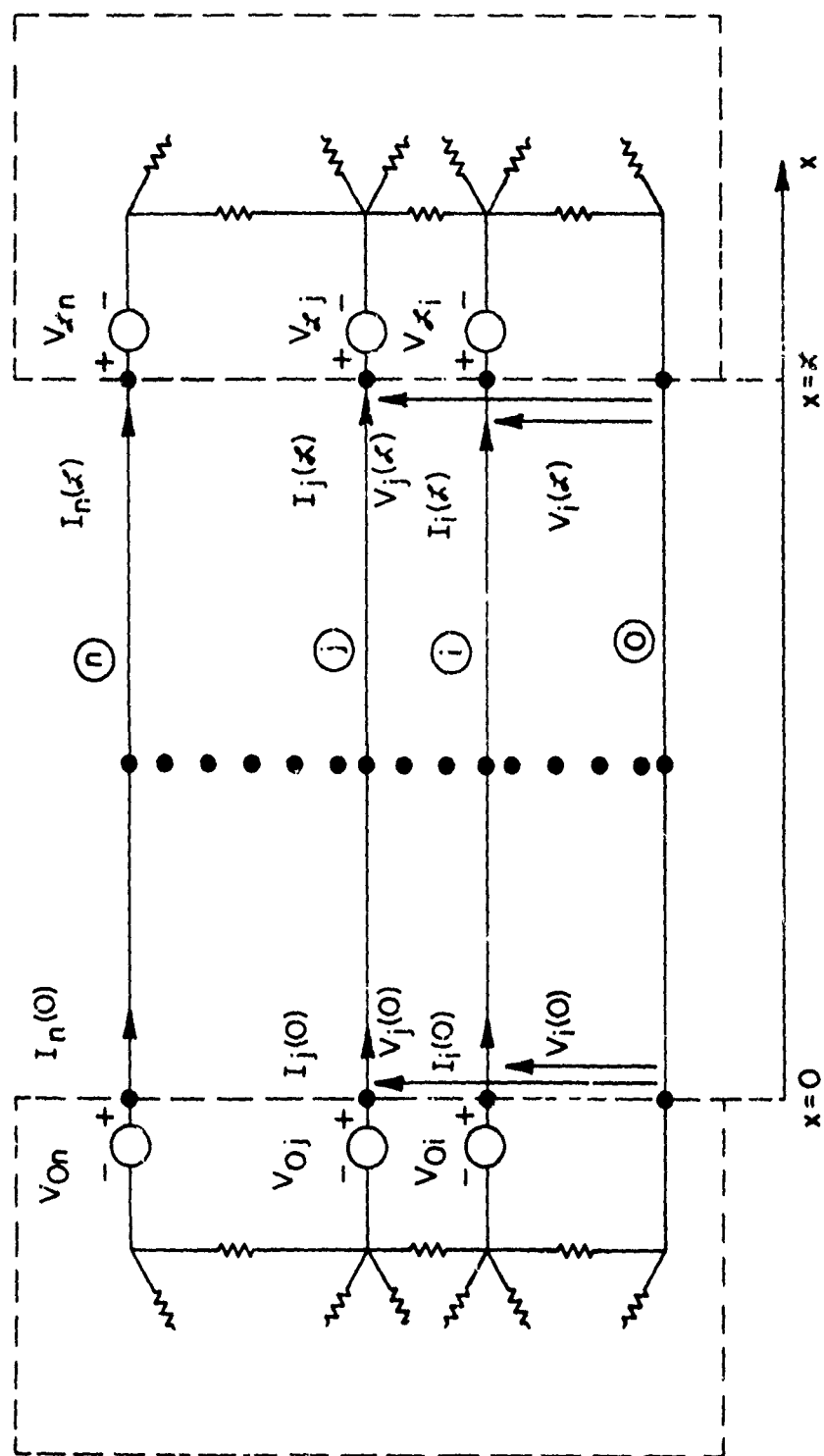


Figure 2-3. The termination networks.

$$\begin{aligned}
& [\cos(kz) \{ \underline{Z}_0 + \underline{Z}_I \} + j \sin(kz) \{ \underline{Z}_C + \underline{Z}_I \underline{Z}_C^{-1} \underline{Z}_0 \}] \underline{I}(0) \\
& = -\underline{V}_I + [j \sin(kz) \underline{Z}_I \underline{Z}_C^{-1} + \cos(kz) \underline{1}_n] \underline{V}_0 \\
& \quad + \hat{\underline{V}}_s(z) - \underline{Z}_I \hat{\underline{I}}_s(z)
\end{aligned} \tag{2-6a}$$

$$\begin{aligned}
\underline{I}(z) & = -j \sin(kz) \underline{Z}_C^{-1} \underline{V}_0 \\
& + [\cos(kz) \underline{1}_n + j \sin(kz) \underline{Z}_C^{-1} \underline{Z}_0] \underline{I}(0) + \hat{\underline{I}}_s(z)
\end{aligned} \tag{2-6b}$$

where the wavenumber is $k = 2\pi/\lambda$, $\lambda = v/f$, $v = 1/\sqrt{\mu\epsilon} = v_0/\sqrt{\mu_r \epsilon_r}$, $v_0 = 1/\sqrt{\mu_0 \epsilon_0}$ and the $n \times n$ characteristic impedance matrix, \underline{Z}_C , is [1]

$$\underline{Z}_C = v \underline{L} \tag{2-7}$$

The inverse of an $n \times n$ matrix \underline{M} is denoted by \underline{M}^{-1} and $\hat{\underline{V}}_s(z)$ and $\hat{\underline{I}}_s(z)$ in (2-6) are given by [1]

$$\begin{aligned}
\hat{\underline{V}}_s(z) & = \int_0^z \{ \cos(k(z-x)) \underline{V}_s(x) \\
& \quad - j \sin(k(z-x)) \underline{Z}_C \underline{I}_s(x) \} dx
\end{aligned} \tag{2-8a}$$

$$\begin{aligned}
\hat{\underline{I}}_s(z) & = \int_0^z \{ \cos(k(z-x)) \underline{I}_s(x) \\
& \quad - j \sin(k(z-x)) \underline{Z}_C^{-1} \underline{V}_s(x) \} dx.
\end{aligned} \tag{2-8b}$$

Solution of (2-6a) for the current vector, $\underline{I}(0)$, requires the solution of n complex equations in n unknowns ($\underline{I}_1(0)$). Once (2-6a) is solved, (2-6b) yields the currents $\underline{I}(z)$ directly.

In this report, no independent excitation sources in the termination networks will be considered. The program XTALK described in Vol. VII of

this series [2] can be used to compute the contribution to the response due to these sources. Thus the source vectors in the generalized Thevenin equivalent representations in (2-4) will be zero, i.e., $\underline{V}_0 = \underline{V}_{\mathcal{L}} = 0$ where the $m \times p$ zero matrix, $\underline{0}$, has zeros in every position, i.e., $[\underline{0}]_{m \times p}^{ij} = 0$ for $i = 1, \dots, m$ and $j = 1, \dots, p$. Thus the generalized Thevenin equivalent representation becomes

$$\underline{V}(0) = -\underline{Z}_0 \underline{I}(0) \quad (2-9a)$$

$$\underline{V}(\mathcal{L}) = \underline{Z}_{\mathcal{L}} \underline{I}(\mathcal{L}) \quad (2-9b)$$

and the equations for the terminal currents in (2-6) become

$$[\cos(k\mathcal{L}) \{ \underline{Z}_0 + \underline{Z}_{\mathcal{L}} \} + j \sin(k\mathcal{L}) \{ \underline{Z}_C + \underline{Z}_{\mathcal{L}} \underline{Z}_C^{-1} \underline{Z}_0 \}] \underline{I}(0) = \hat{\underline{V}}_s(\mathcal{L}) - \underline{Z}_{\mathcal{L}} \hat{\underline{I}}_s(\mathcal{L}) \quad (2-10a)$$

$$\underline{I}(\mathcal{L}) = [\cos(k\mathcal{L}) \underline{1}_n + j \sin(k\mathcal{L}) \underline{Z}_C^{-1} \underline{Z}_0] \underline{I}(0) + \hat{\underline{I}}_s(\mathcal{L}) \quad (2-10b)$$

As an alternate formulation, a generalized Norton equivalent representation may be used to characterize the termination networks. If we define $\underline{Y}_0 = \underline{Z}_0^{-1}$ and $\underline{Y}_{\mathcal{L}} = \underline{Z}_{\mathcal{L}}^{-1}$ the generalized Norton equivalent representation becomes

$$\underline{I}(0) = -\underline{Y}_0 \underline{V}(0) \quad (2-11a)$$

$$\underline{I}(\mathcal{L}) = \underline{Y}_{\mathcal{L}} \underline{V}(\mathcal{L}) \quad (2-11b)$$

Equations (2-10) can then be written as

$$[\cos(k\mathcal{L}) \{ \underline{Y}_0 + \underline{Y}_{\mathcal{L}} \} + j \sin(k\mathcal{L}) \{ \underline{Y}_{\mathcal{L}} \underline{Z}_C \underline{Y}_0 + \underline{Z}_C^{-1} \}] \underline{V}(0) = \hat{\underline{I}}_s(\mathcal{L}) - \underline{Y}_{\mathcal{L}} \hat{\underline{V}}_s(\mathcal{L}) \quad (2-12a)$$

$$\underline{I}(\mathcal{L}) = -[\cos(k\mathcal{L}) \underline{Y}_0 + j \sin(k\mathcal{L}) \underline{Z}_C^{-1}] \underline{V}(0) + \hat{\underline{I}}_s(\mathcal{L}) \quad (2-12b)$$

where $\underline{I}(0)$ can be recovered from $\underline{V}(0)$ via (2-11a).

There remain two basic problems: determining the entries in the per-unit-length inductance and capacitance matrices, \underline{L} and \underline{C} , and determining the equivalent source vectors, $\hat{\underline{V}}_s(\underline{x})$ and $\hat{\underline{I}}_s(\underline{x})$, which are induced by the incident electromagnetic field. The derivations of \underline{L} and \underline{C} for the three structure types have been given previously [1,9] and will be summarized in the following sections. It will become clear in the following section that once the equivalent source vectors, $\hat{\underline{V}}_s(\underline{x})$ and $\hat{\underline{I}}_s(\underline{x})$, are determined for the TYPE 1 structure, they can be immediately obtained for the TYPE 2 and TYPE 3 structures with a parallel development. Thus the basic problem is the determination of these equivalent source vectors for the TYPE 1 structure.

2.2 Derivation of the Equivalent Induced Source Vectors, $\hat{\underline{V}}_s(\underline{x})$ and $\hat{\underline{I}}_s(\underline{x})$, for TYPE 1 Structures

In order to determine the equivalent induced sources, $\underline{V}_{s1}(\underline{x})$ and $\underline{I}_{s1}(\underline{x})$, consider Figure 2-4. The method used in [3] can be adapted here in a similar fashion. Faraday's law in integral form becomes

$$\oint_{C_1} \vec{E} \cdot d\vec{C}_1 = -j\omega\mu \int_{S_1} \vec{H} \cdot \vec{n} dS_1 \quad (2-13)$$

where S_1 is a flat, rectangular surface in the x,y plane between wire 1 and wire 0 and between x and $x + \Delta x$ as shown in Figure 2-4. The unit normal \vec{n} is $\vec{n} = \vec{z}$ where \vec{z} is the unit vector in the z direction, $dS_1 = dx dy$ and C_1 is a contour encircling S_1 in the proper direction (counter-clockwise according to the right-hand rule). Equation (2-13) becomes for the indicated integration¹

¹In integrating from $y=0$ to $y=d_{10}$, we are implicitly assuming that the wires are sufficiently separated so that they may be replaced by infinitesimally small filaments of current (charge).

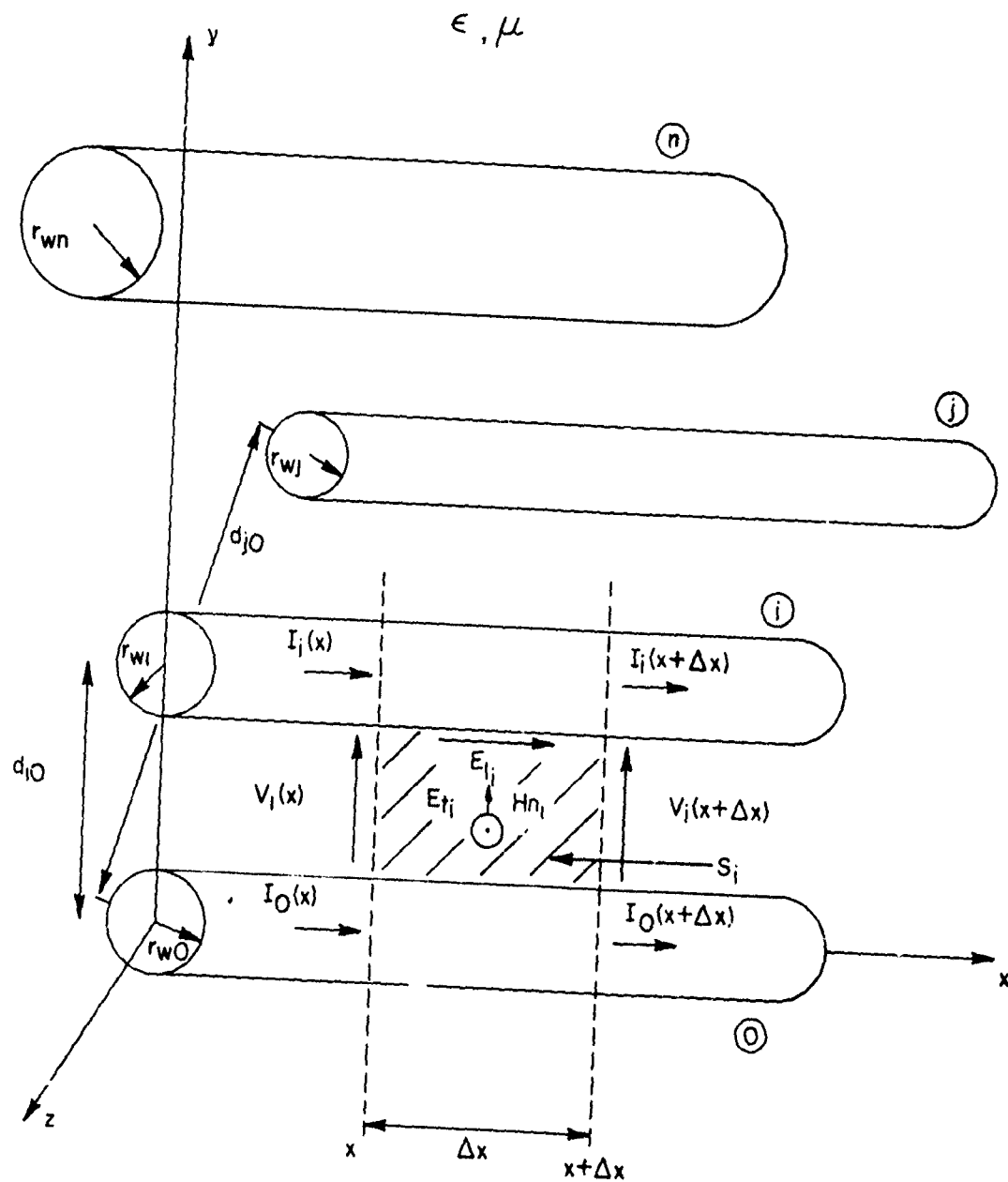


Figure 2-4.

$$\begin{aligned}
& \int_0^{d_{10}} [E_{ti}(y, x + \Delta x) - E_{ti}(y, x)] dy \\
& - \int_x^{x+\Delta x} [E_{li}(d_{10}, x) - E_{li}(0, x)] dx \\
& = -j\omega\mu \int_0^{x+\Delta x} \int_0^{d_{10}} H_{ni}(y, x) dy dx \quad (2-14)
\end{aligned}$$

where E_{ti} is the component of the total electric field (incident plus scattered) transverse to the line axis and lying along a straight line joining the two conductors i.e., $E_{ti} = E_y$; E_{li} is the component of the total electric field along the longitudinal axis of the line, i.e., $E_{li} = E_x$; and H_{ni} is the component of the total magnetic field perpendicular to the plane formed by the two wires, i.e., $H_{ni} = H_z$.

Defining the voltage between the two wires as

$$V_i(x) = - \int_0^{d_{10}} E_{ti}(y, x) dy \quad (2-15)$$

then

$$- \frac{dV_i(x)}{dx} = \lim_{\Delta x \rightarrow 0} \frac{1}{\Delta x} \int_0^{d_{10}} [E_{ti}(y, x + \Delta x) - E_{ti}(y, x)] dy \quad (2-16)$$

The total electric field along the wire surfaces is zero since we assume perfect conductors. (One can straightforwardly include finite conductivity conductors through a surface impedance as was done in [3]). Therefore (2-14) becomes in the limit as $\Delta x \rightarrow 0$

$$\frac{dV_i(x)}{dx} = j\omega\mu \int_0^d i_0 H_{ni}(y,x) dy. \quad (2-17)$$

The total magnetic field is the sum of an incident and a scattered field

$$\begin{aligned} H_{ni}(y,x) &= H_z(y,x) \\ &= \underbrace{H_z^{(scat)}(y,x)}_{\text{scattered}} + \underbrace{H_z^{(inc)}(y,x)}_{\text{incident}} \end{aligned} \quad (2-18)$$

and the scattered field here is considered to be produced by the transmission line currents. The scattered flux passing between the two conductors per unit of line length is directly related to the scattered magnetic field and the per-unit-length inductance matrix, \underline{L} , as

$$\begin{aligned} \phi_i^{(scat)}(x) &= - \int_0^d i_0 \mu H_{ni}^{(scat)}(y,x) dy \\ &= [\ell_{i1}, \ell_{i2}, \dots, \ell_{in}] \begin{bmatrix} I_1(x) \\ I_2(x) \\ \vdots \\ I_n(x) \end{bmatrix} \end{aligned} \quad (2-19)$$

where $\ell_{ij} = [\underline{L}]_{ij}$. Substituting (2-19) and (2-18) into (2-17) and arranging for $i = 1, \dots, n$ yields

$$\underline{\dot{V}}(x) + j\omega \underline{L} \underline{I}(x) = \begin{bmatrix} \vdots \\ j\omega\mu \int_0^d i_0 H^{(inc)}(y,x) dy \\ \vdots \end{bmatrix} \quad (2-20)$$

and the source vector $\underline{V}_s(x)$ in (2-1) is easily identified by comparing (2-20) and (2-1).

For transmission line theory to apply, the cross-sectional dimensions of the line (wire spacing, etc.) must be electrically small, i.e., $kd_{10} \ll 1$. Thus the result indicates that the voltage, V_{si} , induced in the loop between the i th conductor and the zeroth conductor and between x and $x + \Delta x$ is equal to the rate of change of the incident flux penetrating this "electrically small" loop which, of course, makes sense.

Ampere's law yields

$$E_y = \frac{1}{j\omega\epsilon} \left[\frac{\partial H_x}{\partial z} - \frac{\partial H_z}{\partial x} \right] \quad (2-21)$$

E_y will consist of scattered and incident field components and is written as

$$E_{ti}(y, x) = E_y(y, x) \quad (2-22)$$

$$= \underbrace{E_y^{(scat)}(y, x)}_{\text{scattered}} + \underbrace{E_y^{(inc)}(y, x)}_{\text{incident}}$$

Substituting (2-21) into (2-15) we have

$$V_i(x) = - \int_0^{d_{10}} E_y(y, x) dy$$

$$= \frac{1}{j\omega\epsilon} \int_0^{d_{10}} \left\{ \frac{\partial H_z^{(scat)}(y, x)}{\partial x} + \frac{\partial H_z^{(inc)}(y, x)}{\partial x} - \frac{\partial H_x^{(scat)}(y, x)}{\partial z} - \frac{\partial H_x^{(inc)}(y, x)}{\partial z} \right\} dy. \quad (2-23)$$

Utilizing (2-19) we obtain

$$V_i(x) = -\frac{1}{j\omega\mu\epsilon} \frac{d}{dx} \{[\ell_{i1}, \ell_{i2}, \dots, \ell_{in}] \underline{I}(x)\} \\ - \frac{1}{j\omega\epsilon} \int_0^{d_{i0}} \frac{\partial H_x^{(scat)}(y, x)}{\partial z} dy - \int_0^{d_{i0}} E_{ti}^{(inc)}(y, x) dy. \quad (2-24)$$

If we assume that the currents on the wires are directed only in the x direction, i.e., there are no transverse components of the currents on the wire surfaces, then $H_x^{(scat)}(y, x) = 0$ and (2-24) becomes

$$V_i(x) = -\frac{1}{j\omega\mu\epsilon} \frac{d}{dx} \{[\ell_{i1}, \ell_{i2}, \dots, \ell_{in}] \underline{I}(x)\} \\ - \int_0^{d_{i0}} E_{ti}^{(inc)}(y, x) dy. \quad (2-25)$$

Arranging these equations for $i = 1, \dots, n$ we obtain the second transmission line equation

$$\underline{\dot{I}}(x) + j\omega\mu\epsilon \underline{L}^{-1} \underline{V}(x) \\ = -j\omega\mu\epsilon \underline{L}^{-1} \begin{bmatrix} \int_0^{d_{10}} E_{t1}^{(inc)}(y, x) dy \\ \vdots \\ \int_0^{d_{n0}} E_{tn}^{(inc)}(y, x) dy \end{bmatrix}. \quad (2-26)$$

Utilizing (2-5) in (2-26) ($C = \mu\epsilon \underline{L}^{-1}$) we obtain by comparing (2-20) and (2-26) to (2-1)

$$\underline{V}_S(x) = j\omega\mu \begin{bmatrix} \int_0^{d_{10}} H_{n1}^{(inc)}(y, x) dy \\ \vdots \\ \int_0^{d_{n0}} H_{n1}^{(inc)}(y, x) dy \end{bmatrix} \quad (2-27a)$$

$$\underline{I}_s(x) = -j\omega C \int_0^{d_{10}} \begin{bmatrix} (inc) \\ E_{ti}(y,x) \\ \vdots \end{bmatrix} dy \quad (2-27b)$$

The shunt current sources in $\underline{I}_s(x)$ are therefore a result of the line voltage induced by the incident electric field being applied across the per-unit-length line-to-line capacitances which, of course, satisfies our intuition.

The final problem remaining is to obtain simplified versions of $\hat{\underline{V}}_s$ and $\hat{\underline{I}}_s$ in (2-8) to be directly used in (2-10) and (2-12). First consider the determination of $\hat{\underline{V}}_s(z)$. Substituting (2-27) into (2-8a) yields

$$\begin{aligned} \hat{\underline{V}}_s(z) = & j\omega\mu \int_0^z \left\{ \cos(k(z-x)) \right. \\ & \times \left[\int_0^{d_{10}} \begin{bmatrix} (inc) \\ H_{ni}(y,x) \\ \vdots \end{bmatrix} dy \right] \Big\} dx \\ & - k \int_0^z \left\{ \sin(k(z-x)) \right. \\ & \times \left[\int_0^{d_{10}} \begin{bmatrix} (inc) \\ E_{ti}(y,x) \\ \vdots \end{bmatrix} dy \right] \Big\} dx. \end{aligned} \quad (2-28)$$

From Faraday's law we obtain

$$H_{ni}^{(inc)} = \frac{1}{j\omega\mu} \left[\frac{\partial E_{ti}^{(inc)}}{\partial y} - \frac{\partial E_{ti}^{(inc)}}{\partial x} \right]. \quad (2-29)$$

Substituting this into (2-28) yields

$$\begin{aligned}
 \hat{\underline{v}}_s(\mathcal{L}) = & \int_0^{\mathcal{L}} \left\{ \cos(k(\mathcal{L} - x)) \begin{bmatrix} \text{(inc)} \\ E_{li}(d_{i0}, x) \\ \vdots \\ \text{(inc)} \\ E_{li}(0, x) \end{bmatrix} \right\} dx \\
 & - \int_0^{\mathcal{L}} \left\{ \cos(k(\mathcal{L} - x)) \right. \\
 & \quad \times \left[\int_0^{d_{i0}} \frac{\partial E_{ti}(y, x)}{\partial x} dy \right. \\
 & \quad \quad \left. \left. \begin{bmatrix} \text{(inc)} \\ \vdots \\ \vdots \end{bmatrix} \right] \right\} dx \\
 & - k \int_0^{\mathcal{L}} \left\{ \sin(k(\mathcal{L} - x)) \right. \\
 & \quad \times \left[\int_0^{d_{i0}} \begin{bmatrix} \text{(inc)} \\ E_{ti}(y, x) \\ \vdots \end{bmatrix} dy \right] \left. \right\} dx.
 \end{aligned} \tag{2-30}$$

Utilizing Leibnitz's rule (see [10, p. 219]), (2-30) is equivalent to

$$\begin{aligned}
 \hat{\underline{v}}_s(\mathcal{L}) = & \int_0^{\mathcal{L}} \left\{ \cos(k(\mathcal{L} - x)) \right. \\
 & \quad \times \left[\begin{bmatrix} \text{(inc)} \\ E_{li}(d_{i0}, x) \\ \vdots \\ \text{(inc)} \\ E_{li}(0, x) \end{bmatrix} \right] \left. \right\} dx \\
 & - \int_0^{\mathcal{L}} \frac{\partial}{\partial x} \left\{ \cos(k(\mathcal{L} - x)) \right. \\
 & \quad \times \left[\int_0^{d_{i0}} \begin{bmatrix} \text{(inc)} \\ E_{ti}(y, x) \\ \vdots \end{bmatrix} dy \right] \left. \right\} dx
 \end{aligned} \tag{2-31}$$

and this may be written as

$$\begin{aligned}
 \hat{\underline{v}}_s(\underline{z}) = & \int_0^{\underline{z}} \left\{ \cos(k(\underline{z} - x)) \right. \\
 & \times \left[\begin{array}{c} \text{(inc)} \\ E_{\ell 1}(d_{10}, x) - E_{\ell 1}(0, x) \\ \vdots \\ \text{(inc)} \end{array} \right] \Bigg\} dx \\
 & - \left[\int_0^{d_{10}} \begin{array}{c} \text{(inc)} \\ E_{t1}(y, \underline{z}) \\ \vdots \\ \text{(inc)} \end{array} dy \right] \\
 & + \cos(k\underline{z}) \left[\int_0^{d_{10}} \begin{array}{c} \text{(inc)} \\ E_{t1}(y, 0) \\ \vdots \\ \text{(inc)} \end{array} dy \right] \quad (2-32)
 \end{aligned}$$

Similarly $\hat{\underline{i}}_s(\underline{z})$ may be obtained as

$$\begin{aligned}
 \hat{\underline{i}}_s(\underline{z}) = & -j\underline{z}_C^{-1} \int_0^{\underline{z}} \left\{ \sin(k(\underline{z} - x)) \right. \\
 & \times \left[\begin{array}{c} \text{(inc)} \\ E_{\ell 1}(d_{10}, x) - E_{\ell 1}(0, x) \\ \vdots \\ \text{(inc)} \end{array} \right] \Bigg\} dx \\
 & - j\underline{z}_C^{-1} \left\{ \sin(k\underline{z}) \left[\int_0^{d_{10}} \begin{array}{c} \text{(inc)} \\ E_{t1}(y, 0) \\ \vdots \\ \text{(inc)} \end{array} dy \right] \right\} \quad (2-33)
 \end{aligned}$$

The important quantity in (2-10a) is $\hat{\underline{v}}_s(\underline{z}) - \underline{z}_C \hat{\underline{i}}_s(\underline{z})$. Combining (2-32) and (2-33), this becomes

$$\begin{aligned}
& \hat{\underline{V}}_{-s}(\underline{z}) - \underline{Z}_{\underline{z}} \hat{\underline{I}}_{-s}(\underline{z}) \\
&= \int_0^{\underline{z}} \left\{ [\cos(k(\underline{z} - x)) \underline{1}_n + j \sin(k(\underline{z} - x)) \underline{Z}_{\underline{z}} \underline{Z}_C^{-1}] \right. \\
&\quad \times \left[\begin{array}{c} \text{(inc)} \\ E_{\ell 1}(d_{i0}, x) - E_{\ell 1}(0, x) \\ \vdots \end{array} \right] \Big\} dx \\
&\quad - \left[\int_0^{d_{i0}} \begin{array}{c} \text{(inc)} \\ E_{t1}(y, \underline{z}) \\ \vdots \end{array} \right] dy \\
&\quad + [\cos(k\underline{z}) \underline{1}_n + j \sin(k\underline{z}) \underline{Z}_{\underline{z}} \underline{Z}_C^{-1}] \\
&\quad \times \left[\int_0^{d_{i0}} \begin{array}{c} \text{(inc)} \\ E_{t1}(y, 0) \\ \vdots \end{array} \right] dy.
\end{aligned} \tag{2-34}$$

Note that the equivalent forcing function on the right-hand side of (2-10a), $\hat{\underline{V}}_{-s}(\underline{z}) - \underline{Z}_{\underline{z}} \hat{\underline{I}}_{-s}(\underline{z})$, given in (2-34) is simply determined as a convolution of differences of the incident electric field vector along the wire axes, $\text{(inc)} E_{\ell 1}(d_{i0}, x) - E_{\ell 1}(0, x)$, and a linear combination of integrals of components of the electric field vectors at the endpoints of the line which are transverse to the line, $\text{(inc)} E_{t1}(y, \underline{z})$ and $\text{(inc)} E_{t1}(y, 0)$. This is, of course, precisely the result obtained by Smith [4] for two conductor lines. Substituting (2-34) into (2-10a) one can verify that the result reduces for two conductor lines ($n = 1$) to the result given by Smith [4] since $\underline{Z}_C, \underline{Z}_{\underline{z}}, \underline{Z}_0$ become scalars for two conductor lines and (2-10a) becomes one equation in only one unknown $I(0)$.

The final equations for the line currents then become (substituting (2-34) into (2-10))

$$\begin{aligned}
 & [\cos(kz) \{z_0 + z_z\} + j \sin(kz) \{z_c + z_z z_c^{-1} z_0\}] \underline{I}(0) = \\
 & \int_0^z \{ [\cos(k(z-x)) \underline{1}_n \\
 & + j \sin(k(z-x)) z_z z_c^{-1}] \underline{E}_\ell^{(inc)}(x) \} dx - \underline{E}_t^{(inc)}(z) \\
 & + \{ [\cos(kz) \underline{1}_n + j \sin(kz) z_z z_c^{-1}] \underline{E}_t^{(inc)}(0) \}
 \end{aligned} \tag{2-35a}$$

$$\begin{aligned}
 \underline{I}(z) &= [\cos(kz) \underline{1}_n + j \sin(kz) z_c^{-1} z_0] \underline{I}(0) \\
 &- j z_c^{-1} \int_0^z \{ \sin(k(z-x)) \underline{E}_\ell^{(inc)}(x) \} dx \\
 &- j z_c^{-1} \{ \sin(kz) \underline{E}_t^{(inc)}(0) \}
 \end{aligned} \tag{2-35b}$$

where $\underline{E}_\ell^{(inc)}(x)$, $\underline{E}_t^{(inc)}(z)$, and $\underline{E}_t^{(inc)}(0)$ are $n \times 1$ column vectors with the entries in the i -th rows given by

$$[\underline{E}_\ell^{(inc)}(x)]_i = E_{\ell i}^{(inc)}(d_{i0}, x) - E_{\ell i}^{(inc)}(0, x) \tag{2-36a}$$

$$[\underline{E}_t^{(inc)}(z)]_i = \int_0^{d_{i0}} E_{ti}^{(inc)}(\rho_i, z) d\rho_i \tag{2-36b}$$

$$[\underline{E}_t^{(inc)}(0)]_i = \int_0^{d_{i0}} E_{ti}^{(inc)}(\rho_i, 0) d\rho_i \tag{2-36c}$$

for $i = 1, \dots, n$.

A word of caution in the interpretation of the notation is in order. Although it should be clear from the derivation, the reader should nevertheless be reminded that the integration path for the component $E_{ti}^{(inc)}$ is in the y direction when the i -th conductor is concerned. When other conductors are concerned, the integration path is a straight line in the y, z plane which joins the conductor and the zeroth conductor and is perpendicular to these two conductors. This is designated as ρ_i in (2-36) and replaces the y variable for the path associated with conductors i and 0 . The notation may be cumbersome but the idea and the implementation are quite simple.

Defining the vectors

$$\underline{M} = \int_0^z \cos(k(z-x)) \underline{E}_x^{(inc)}(x) dx \quad (2-37a)$$

$$\underline{N} = \int_0^z \sin(k(z-x)) \underline{E}_x^{(inc)}(x) dx \quad (2-37b)$$

we may write (2-35) as

$$\begin{aligned} & [\cos(kz) \{ \underline{Z}_0 + \underline{Z}_z \} + j \sin(kz) \{ \underline{Z}_C + \underline{Z}_z \underline{Z}_C^{-1} \underline{Z}_0 \}] \underline{I}(0) \\ &= \underline{M} + j \underline{Z}_z \underline{Z}_C^{-1} \underline{N} - \underline{E}_t^{(inc)}(z) \end{aligned} \quad (2-38a)$$

$$\begin{aligned} & + [\cos(kz) \underline{1}_n + j \sin(kz) \underline{Z}_z \underline{Z}_C^{-1}] \underline{E}_t^{(inc)}(0) \\ \underline{I}(z) &= [\cos(kz) \underline{1}_n + j \sin(kz) \underline{Z}_C^{-1} \underline{Z}_0] \underline{I}(0) \\ & - j \underline{Z}_C^{-1} \underline{N} - j \underline{Z}_C^{-1} \{ \sin(kz) \underline{E}_t^{(inc)}(0) \} \end{aligned} \quad (2-38b)$$

For the generalized Norton equivalent representation, equations (2-38) can be written as

$$\begin{aligned} & [\cos(kz) \{Y_0 + Y_z\} + j \sin(kz) \{Y_z Z_C^{-1} Y_0 + Z_C^{-1}\}] [-V(0)] = \\ & Y_z M + j Z_C^{-1} N - Y_z [E_t^{(inc)}(z)] \\ & + [\cos(kz) Y_z + j \sin(kz) Z_C^{-1}] [E_t^{(inc)}(0)] \end{aligned} \quad (2-39a)$$

$$\begin{aligned} I(z) &= [\cos(kz) Y_0 + j \sin(kz) Z_C^{-1}] [-V(0)] \\ &\quad - j Z_C^{-1} N - j Z_C^{-1} \{\sin(kz) E_t^{(inc)}(0)\} \end{aligned} \quad (2-39b)$$

and $I(0)$ is obtained from $I(0) = -Y_0 V(0) = Y_0 [-V(0)]$.

2.3 Determining the Per-Unit-Length Inductance Matrix, L , for TYPE 1

Structures

For TYPE 1 structures, one final calculation remains; the determination of the per-unit-length inductance matrix, L , which is related to the characteristic impedance, Z_C , via (2-7). Ordinarily this is a difficult calculation [11]. However, if we assume that the wires are separated sufficiently such that the charge distribution around the periphery of each wire is constant, then the wires can be replaced by filamentary lines of charge. Typically, this will be accurate if the smallest ratio of wire separation to wire radius is greater than approximately 5 [11]. In this case, the entries in L for TYPE 1 structures are given by [1,9]

$$[L]_{ii} = \mu \epsilon [C]_{ii} = \frac{\mu}{2\pi} \ln \left(\frac{d_{i0}^2}{r_{wi} r_{w0}} \right) \quad (2-40a)$$

$$[L]_{ij} = \mu \epsilon [C]_{ij} = \frac{\mu}{2\pi} \ln \left(\frac{d_{i0} d_{j0}}{r_{w0} d_{ij}} \right) \quad (2-40b)$$

For closer wire spacings, proximity effect will alter the charge distribution from constant ones and numerical approximations must be employed to find C and L [11]. Although the entries in L have been derived elsewhere, we shall show a direct derivation which relates the scattered flux passing between the wires to the wire currents as was used in (2-19).

The matrix L relates the scattered flux $\phi^{(scat)}$ passing between the wires to the wire currents as

$$\begin{matrix} (scat) \\ \phi \end{matrix} = \begin{bmatrix} \phi_1^{(scat)} \\ \cdot \\ \cdot \\ \cdot \\ \phi_n^{(scat)} \end{bmatrix} = \begin{bmatrix} l_{11} & \cdot & \cdot & \cdot & l_{1n} \\ \cdot & & & & \cdot \\ \cdot & & & & \cdot \\ \cdot & & & & \cdot \\ l_{n1} & \cdot & \cdot & \cdot & l_{nn} \end{bmatrix} \begin{bmatrix} I_1 \\ \cdot \\ \cdot \\ \cdot \\ I_n \end{bmatrix} \quad (2-41)$$

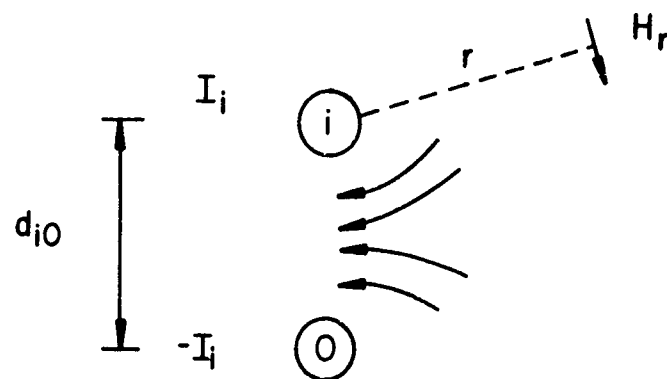
The respective entries are determined as

$$l_{ii} = \frac{\phi_i^{(scat)}}{I_i} \Big|_{I_1, \dots, I_{i-1}, I_{i+1}, \dots, I_n = 0} \quad (2-42a)$$

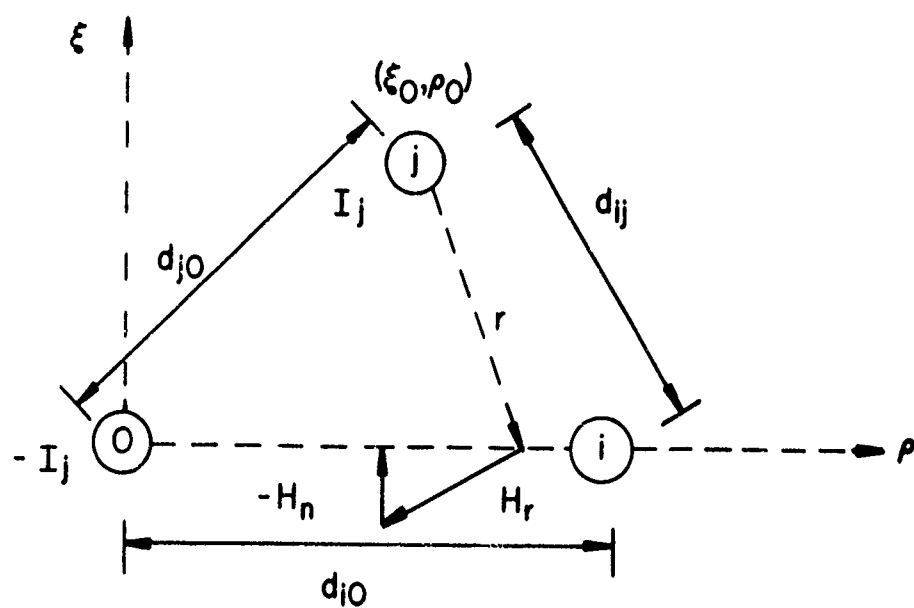
$$l_{ij} = \frac{\phi_i^{(scat)}}{I_j} \Big|_{I_1, \dots, I_{j-1}, I_{j+1}, \dots, I_n = 0} \quad (2-42b)$$

and $l_{ij} = l_{ji}$. Large wire separations are assumed so that the wires may be replaced by filaments of current. When the wires are not widely separated, accurate values for L can be obtained by numerical methods [11].

Consider Figure 2-5(a). The magnitude of the magnetic field intensity



(a)



(b)

Figure 2-5.

vector due to I_i on wire i at a distance $r > r_{wi}$ away from wire i is

$$H_r = \frac{I_i}{2\pi r} \quad (2-43)$$

and the total flux passing between wire i and wire 0 due to both currents is

$$\begin{aligned} \phi_i^{(scat)} &= \frac{\mu I_i}{2\pi} \left\{ \int_{r_{wi}}^{d_{i0}} \frac{1}{r} dr + \int_{r_{w0}}^{d_{i0}} \frac{1}{r} dr \right\} \\ &= \frac{\mu I_i}{2\pi} \ln \left(\frac{d_{i0}^2}{r_{wi} r_{w0}} \right) \end{aligned} \quad (2-44)$$

Thus ℓ_{ii} is easily identified as in (2-40a).

Consider Figure 2-5(b). The portion of the flux $\phi_i^{(scat)}$ passing between wire i and wire 0 due to $-I_j$ in the reference conductor is as above

$$\phi_{i0}^{(scat)} = \frac{\mu I_j}{2\pi} \ln \left(\frac{d_{i0}}{r_{w0}} \right) \quad (2-45)$$

and the portion of the flux passing between wire i and wire 0 due to I_j in the j th conductor can be found to be

$$\begin{aligned} \phi_{ij}^{(scat)} &= -\mu \int_0^{d_{i0}} H_n d\rho \\ &= -\frac{\mu}{2\pi} I_j \left\{ \int_{\rho=0}^{\rho=d_{i0}} \frac{(\rho - \rho_0)}{[\xi_0^2 + (\rho - \rho_0)^2]} d\rho \right\} \\ &= \frac{\mu}{2\pi} I_j \left\{ \frac{1}{2} \ln \left[\frac{(\xi_0^2 + \rho_0^2)}{\xi_0^2 + (d_{i0} - \rho_0)^2} \right] \right\} \end{aligned} \quad (2-46)$$

Combining (2-45) and (2-46) we obtain

$$\phi_i^{(\text{scat})} = \phi_{i0}^{(\text{scat})} + \phi_{ij}^{(\text{scat})} = \frac{\mu I_j}{2\pi} \ln \left(\frac{d_{i0} d_{j0}}{d_{ij} r_{w0}} \right) \quad (2-47)$$

since

$$d_{ij}^2 = \xi_0^2 + (d_{i0} - \rho_0)^2 \quad (2-48a)$$

$$d_{j0}^2 = \xi_0^2 + \rho_0^2 \quad (2-48b)$$

and λ_{ij} is easily identified as in (2-40b).

2.4 Determination of the Equivalent Induced Source Vectors and the Per-Unit-Length Inductance Matrix for TYPE 2 Structures

Consider the system of n wires above an infinite ground plane shown in Figure 2-1(b). The result for $(n+1)$ wires given in (2-35) - (2-39) can be extended to this case with the following observations. Consider Figure 2-6. Clearly we may apply Faraday's law in the previous development to the flat, rectangular surface in the x,y plane shown in Figure 2-6(b) between the ground plane and the i -th wire and between x and $x+\Delta x$. This flat, rectangular surface S_i lies in the x,y plane. Equations (2-35) - (2-39) will again be obtained. Equations (2-36) become for this case

$$[E_z(x)]_i = E_{zi}^{(\text{inc})}(h_i, x) - E_{zi}^{(\text{inc})}(0, x) \quad (2-49a)$$

$$[E_t(x)]_i = \int_0^{h_i} E_{ti}^{(\text{inc})}(\rho_i, x) d\rho_i \quad (2-49b)$$

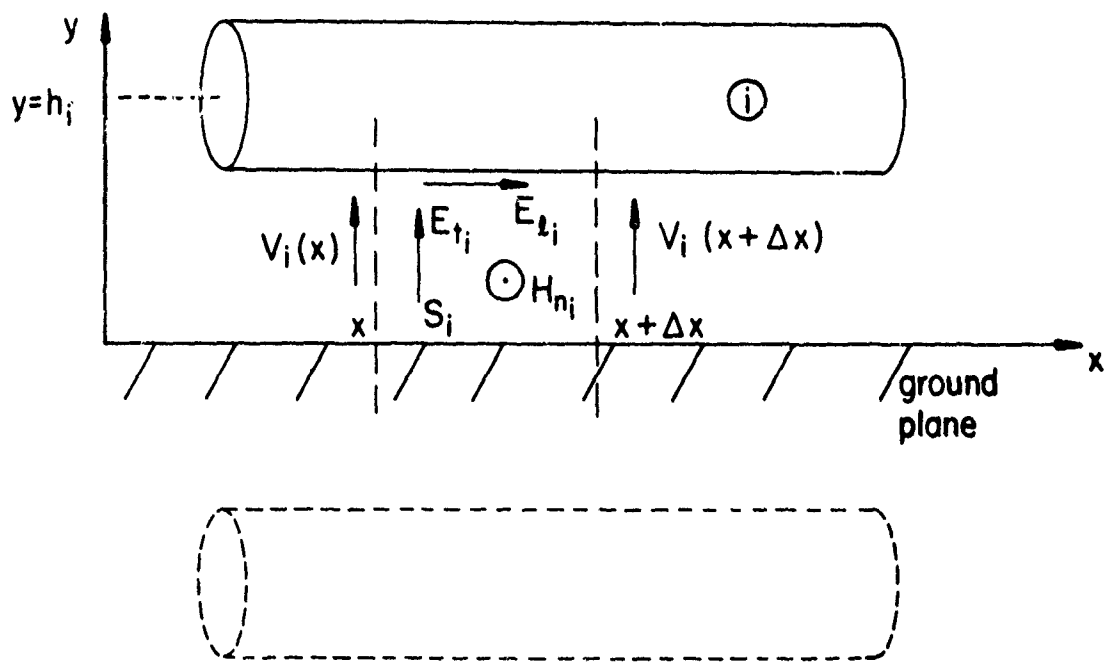
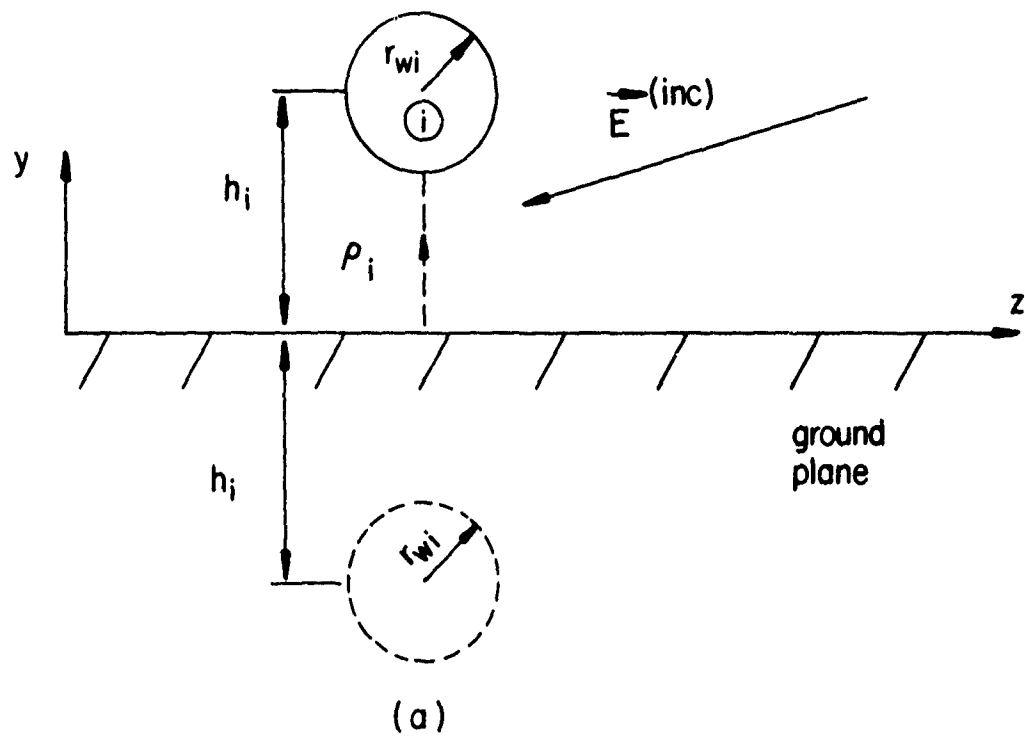


Figure 2-6.

$$[E_t^{(inc)}(0)]_i = \int_0^{h_i} E_{ti}^{(inc)}(\rho_i, 0) d\rho_i \quad (2-49c)$$

where ρ_i is a straight-line contour in the y, z plane between the position of the ground plane, $y=0$, and the i -th wire, and is perpendicular to the ground plane, i.e. $\rho_i = y$. This is indicated in Figure 2-6(a).

$E_{li}^{(inc)}(h_i, x)$ is the component of the incident electric field parallel to the axis of the i -th wire at $y=h_i$ and $E_{li}^{(inc)}(0, x)$ is the component of the incident field parallel to the ground plane directly beneath the i -th wire. In the program, it assumed that the net incident electric field (the vector sum of the incident field in the absence of the ground plane and the portion of this field which is reflected by the ground plane) is obtained. Therefore $F_{li}^{(inc)}(0, x) = 0$. $E_{ti}^{(inc)}$ is the component of the incident electric field parallel to ρ_i and directed in the $+y$ direction.

The per-unit-length inductance matrix, L , can be obtained in a fashion similar to Section 2.3 by determining the scattered magnetic flux passing through the surface S_i between the i -th wire and the position of the ground plane (the ground plane is replaced by image wires) and is given by [1,9]

$$[L]_{ii} = \frac{\mu}{2\pi} \ln \left(\frac{2h_i}{r_{wi}} \right) \quad (2-50a)$$

$$[L]_{ij} = \frac{\mu}{2\pi} \ln \left(\frac{d_{ij}^*}{d_{ij}} \right) \quad (2-50b)$$

$i \neq j$

for $i, j=1, \dots, n$ where

$$d_{ij}^* = \sqrt{d_{ij}^2 + 4h_i h_j} \quad (2-51)$$

2.5 Determination of the Equivalent Induced Source Vectors and the Per-Unit-Length Inductance Matrix for TYPE 3 Structures

Consider the system of n wires within an overall, cylindrical shield shown in Figure 2-1(c). Obviously, a parallel development to that of Section 2-2 and 2-4 can be used to obtain the equations (2-35) - (2-39). The image of the i -th wire (assuming the i -th wire can be replaced by a filament) is located at a distance of r_s^2/r_i from the shield center as shown in Figure 2-7 [1]. Equations (2-36) become for this case

$$[E_{\ell}^{(inc)}(x)]_i = E_{\ell i}^{(inc)}(r_s - r_i, x) - E_{\ell i}^{(inc)}(0, x) \quad (2-52a)$$

$$[E_t^{(inc)}(x)]_i = \int_0^{r_s - r_i} E_{ti}^{(inc)}(\rho_i, x) d\rho_i \quad (2-52b)$$

$$[E_t^{(inc)}(0)]_i = \int_0^{r_s - r_i} E_{ti}^{(inc)}(\rho_i, 0) d\rho_i \quad (2-52c)$$

where ρ_i is a straight-line contour in the y, z plane between the i -th wire and its image and beginning at the interior of the shield. This contour is on a line between the i -th wire and its image.

$E_{\ell i}^{(inc)}(r_s - r_i, x)$ is the component of the incident electric field parallel to the axis of the i -th wire at $y = r_s - r_i$ and $E_{\ell i}^{(inc)}(0, x)$ is the component of the incident field parallel to the axis of the shield on the interior of the surface. In the program, it is assumed that the net incident electric field is obtained so that $E_{\ell i}^{(inc)}(0, x) = 0$. $E_{ti}^{(inc)}$ is the component of the incident electric field parallel to ρ_i and directed in the $+\gamma$ direction.

The per-unit-length inductance matrix, L , can be obtained in a fashion

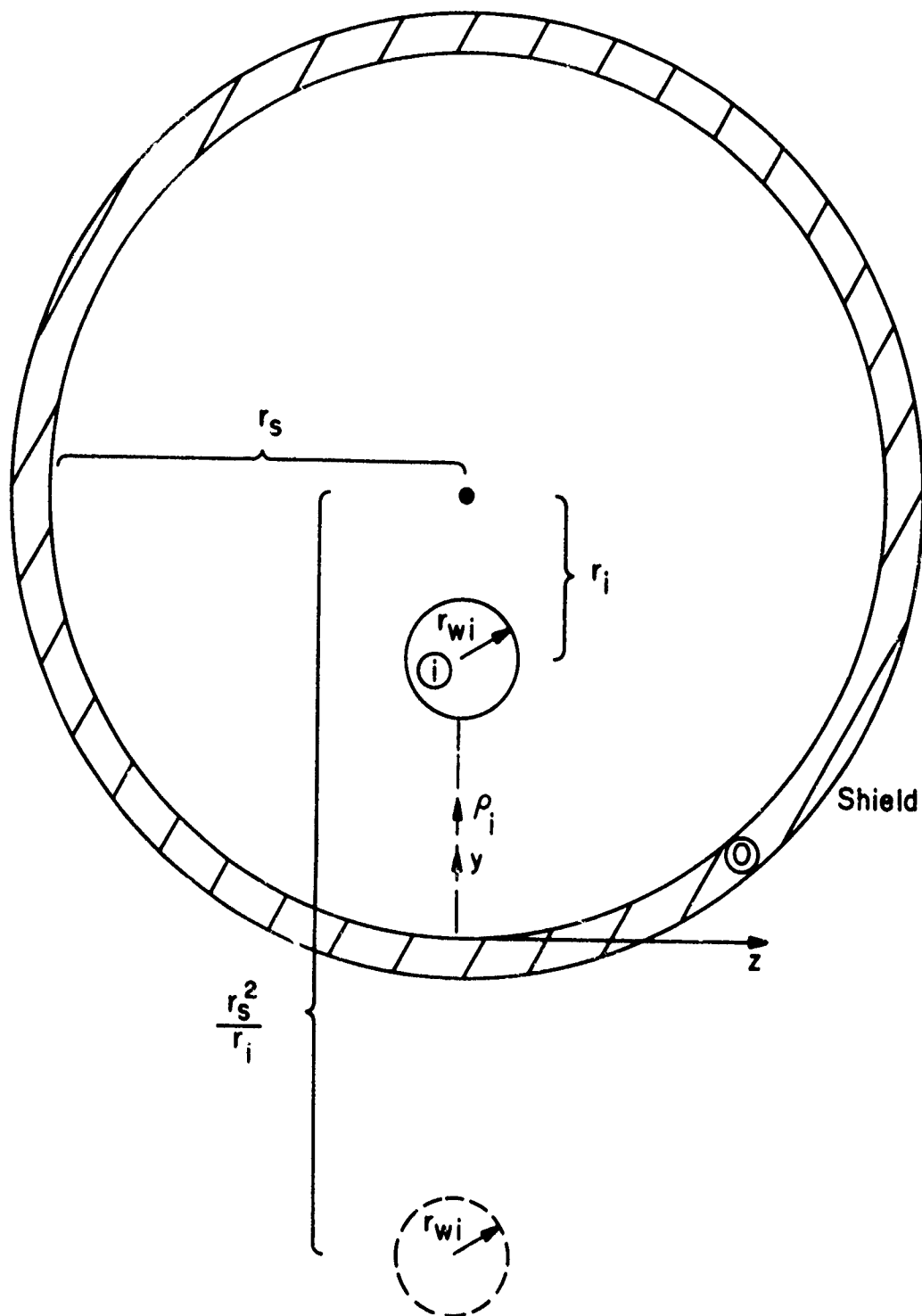


Figure 2-7.

similar to Section 2.3 by determining the scattered magnetic flux passing through a surface between the i-th wire and interior of the shield in the y,x plane and is given by [1,9]

$$[L]_{ii} = \frac{\mu}{2\pi} \ln \left(\frac{r_s^2 - r_i^2}{r_s r_{wi}} \right) \quad (2-53a)$$

$$[L]_{ij} = \frac{\mu}{2\pi} \ln \left\{ \left(\frac{r_i}{r_s} \right) \sqrt{\frac{(r_i r_j)^2 + r_s^4 - 2r_i r_j r_s^2 \cos \theta_{ij}}{(r_i r_j)^2 + r_j^4 - 2r_i r_j^3 \cos \theta_{ij}}} \right\} \quad (2-53b)$$

$i \neq j$

where θ_{ij} is the angular separation between the i-th and j-th wires (see Figure 2-1).

2.6 Determining the Entries in the Termination Network Impedance (Admittance) Matrices

In order to implement this method, one is required to determine the entries in the $n \times n$ terminal impedance (admittance) matrices, Z_0 and Z_L (Y_0 and Y_L), which characterize the termination networks at the two ends of the line as:

$$\left. \begin{aligned} \underline{V}(0) &= -Z_0 \underline{I}(0) \\ \underline{V}(L) &= Z_L \underline{I}(L) \end{aligned} \right\} \quad \text{Thevenin Equivalent} \quad (2-54a)$$

$$\left. \begin{aligned} \underline{I}(0) &= -Y_0 \underline{V}(0) \\ \underline{I}(L) &= Y_L \underline{V}(L) \end{aligned} \right\} \quad \text{Norton Equivalent} \quad (2-54b)$$

In these matrix equations, the entries in the i-th rows of the $n \times 1$ vectors

$\underline{V}(0)$ and $\underline{V}(x)$ are the line voltages of the i -th wire (with respect to the reference conductor) at $x=0$ and $x=x$, respectively. The entries in the i -th rows of the $n \times 1$ vectors $\underline{I}(0)$ and $\underline{I}(x)$ are the line currents in the i -th wire (directed in the $+x$ direction) at $x=0$ and $x=x$, respectively.

The most straightforward situation occurs when each wire is directly connected to the reference conductor via a single impedance as shown in Figure 2-8. In this case we may write

$$V_i(0) = -Z_{0i} I_i(0) \quad (2-55a)$$

$$V_i(x) = Z_{xi} I_i(x) \quad (2-55b)$$

for $i=1, \dots, n$

and may easily identify the entries in \underline{Z}_0 and \underline{Z}_x as

$$\underline{Z}_0 = \begin{bmatrix} Z_{01} & 0 & \cdots & 0 \\ 0 & Z_{02} & \cdots & 0 \\ \vdots & \vdots & \ddots & \vdots \\ 0 & \cdots & 0 & Z_{0n} \end{bmatrix} \quad (2-56a)$$

$$\underline{Z}_x = \begin{bmatrix} Z_{x1} & 0 & \cdots & 0 \\ 0 & Z_{x2} & \cdots & 0 \\ \vdots & \vdots & \ddots & \vdots \\ 0 & \cdots & 0 & Z_{xn} \end{bmatrix} \quad (2-56b)$$

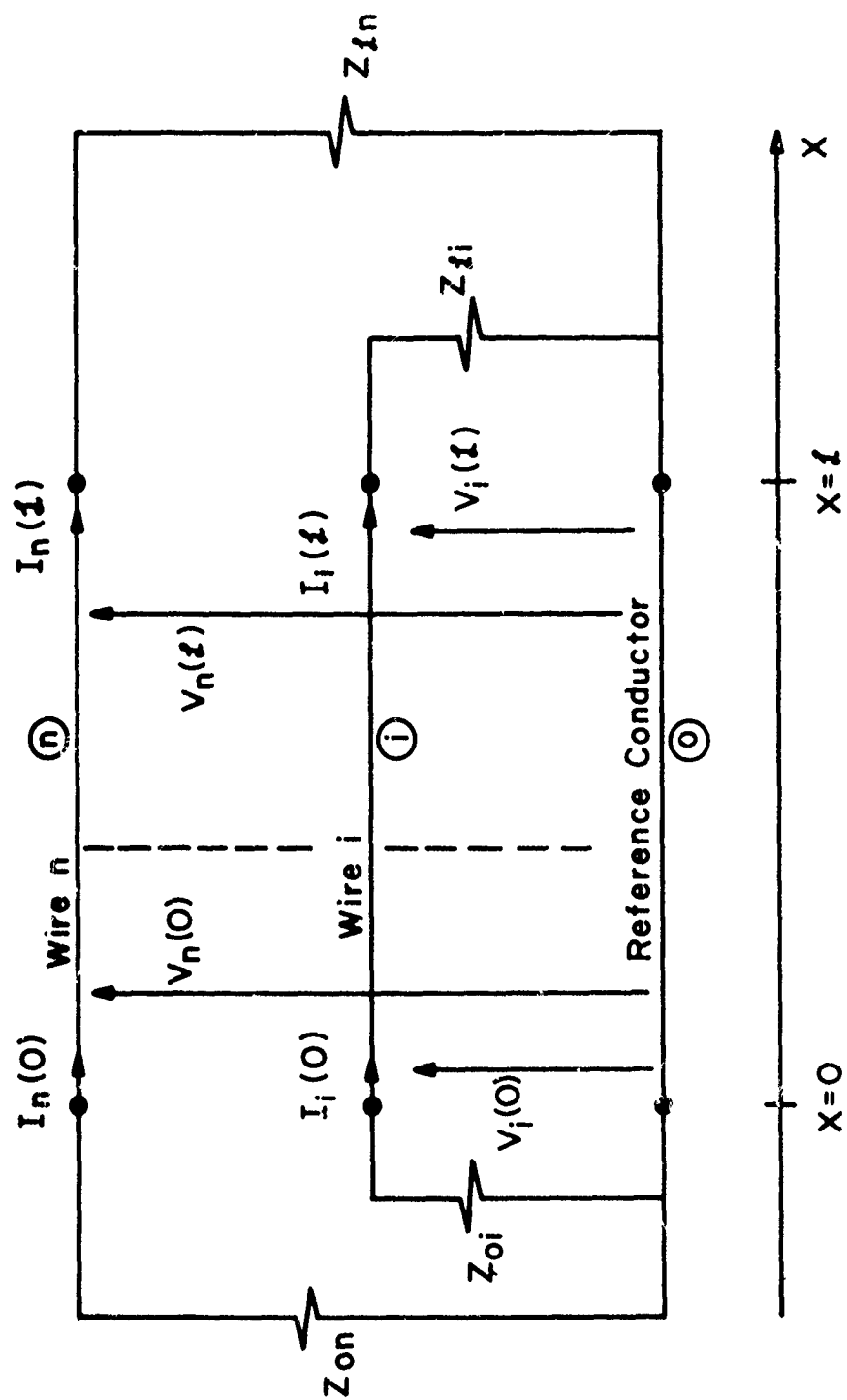


Figure 2-8.

Clearly, the entries in \underline{Y}_0 and \underline{Y}_Z for this case become

$$\underline{Y}_0 = \begin{bmatrix} (1/Z_{01}) & 0 & \cdots & 0 \\ 0 & (1/Z_{02}) & \cdots & 0 \\ \vdots & \vdots & \ddots & \vdots \\ 0 & \cdots & \cdots & (1/Z_{0n}) \end{bmatrix} \quad (2-57a)$$

$$\underline{Y}_Z = \begin{bmatrix} (1/Z_{Z1}) & 0 & \cdots & 0 \\ 0 & (1/Z_{Z2}) & \cdots & 0 \\ \vdots & \vdots & \ddots & \vdots \\ 0 & \cdots & \cdots & (1/Z_{Zn}) \end{bmatrix} \quad (2-57b)$$

Note that $\underline{Y}_0 = \underline{Z}_0^{-1}$ and $\underline{Y}_Z = \underline{Z}_Z^{-1}$. In this case, determining the entries in the terminal impedance (admittance) matrices is a trivial matter and the terminal impedance (admittance) matrices are diagonal.

The more difficult case occurs when each wire is not connected directly to the reference conductor by a single impedance. Two examples which illustrate this situation are shown in Figure 2-9. First consider the situation in Figure 2-9(a). Here it is obviously not possible to obtain terminal impedance (admittance) matrices which are diagonal. The termination impedance matrices can, however, be obtained by defining loop currents in which two of the loop currents so defined are the terminal currents $I_1(0)$ and $I_2(0)$. Writing the required three loop equations we obtain

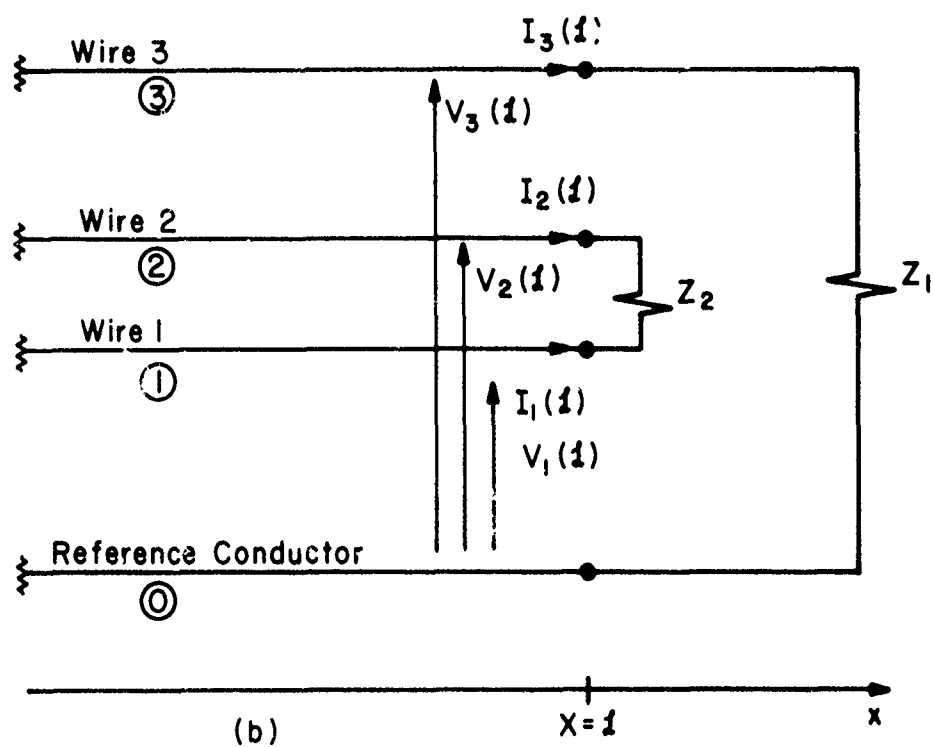
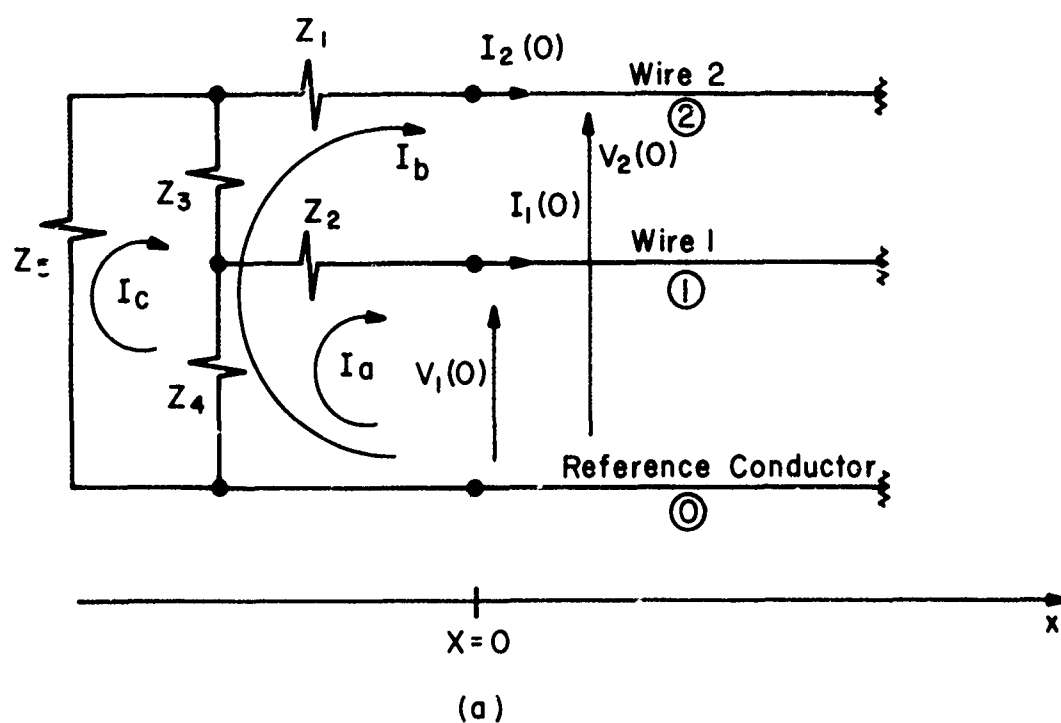


Figure 2-9.

$$V_2(0) = -Z_1 I_b - Z_3(I_b - I_c) - Z_4(I_b + I_a - I_c)$$

$$V_1(0) = -Z_2 I_a - Z_4(I_a + I_b - I_c)$$

$$0 = Z_5 I_c + Z_3(I_c - I_b) + Z_4(I_c - I_a - I_b)$$

The objective is to eliminate the current I_c from these equations leaving $I_a = I_1(0)$ and $I_b = I_2(0)$ as a function of $V_1(0)$ and $V_2(0)$. The third equation yields

$$I_c = \frac{(Z_3 + Z_4) I_b + Z_4 I_a}{(Z_3 + Z_4 + Z_5)}$$

Substituting this result for I_c into the first two equations eliminates the current I_c from these equations and leaves

$$V_1(0) = Z_a I_1(0) + Z_b I_2(0)$$

$$V_2(0) = Z_c I_1(0) + Z_d I_2(0)$$

where Z_a, Z_b, Z_c, Z_d are the resulting combinations of Z_1, Z_2, Z_3, Z_4, Z_5 and we have substituted $I_1(0) = I_a, I_2(0) = I_b$.

This technique can obviously be generalized for any number of wires and additional extraneous loops in the termination networks. Treating the n line voltages as independent sources and writing the required number of loop equations for the terminal network, we may obtain

$$\begin{bmatrix} v_1(0) \\ \vdots \\ v_n(0) \\ 0 \\ \vdots \\ 0 \end{bmatrix} = \begin{bmatrix} \begin{array}{c|c} \tilde{A} & \tilde{B} \\ \hline n \times n & n \times m \end{array} & \begin{array}{c|c} \tilde{C} & \tilde{D} \\ \hline m \times n & m \times m \end{array} \end{bmatrix} \begin{bmatrix} I_1(0) \\ \vdots \\ I_n(0) \\ \hat{I}_1 \\ \vdots \\ \hat{I}_m \end{bmatrix} \quad (2-58)$$

In (2-58) we may eliminate the extraneous loop currents $\hat{I}_1 \dots \hat{I}_m$ by solving the second set of equations to yield

$$\begin{bmatrix} \hat{I}_1 \\ \vdots \\ \hat{I}_m \end{bmatrix} = - \tilde{D}^{-1} \tilde{C} \begin{bmatrix} I_1(0) \\ \vdots \\ I_n(0) \end{bmatrix} \quad (2-59)$$

Substituting this result into the first set of equations we obtain

$$\begin{bmatrix} v_1(0) \\ \vdots \\ v_n(0) \end{bmatrix} = (\tilde{A} - \tilde{B} \tilde{D}^{-1} \tilde{C}) \begin{bmatrix} I_1(0) \\ \vdots \\ I_n(0) \end{bmatrix} \quad (2-60)$$

Clearly, then we may identify

$$\tilde{Z}_0 = - (\tilde{A} - \tilde{B} \tilde{D}^{-1} \tilde{C}) \quad (2-61)$$

The extension of this technique to obtain the Norton Equivalent characterization employs a dual technique. Here we define node voltages (with respect to the reference conductor at either $x=0$ or $x=\mathcal{L}$) of all nodes of the termination network (including the n nodes connected to the line) and write the node voltage equations of the network treating the line currents as independent sources. Therefore we write (for $x=\mathcal{L}$)

$$\begin{bmatrix} I_1(\mathcal{L}) \\ \vdots \\ I_n(\mathcal{L}) \\ 0 \\ \vdots \\ 0 \end{bmatrix} = \begin{bmatrix} \hat{\tilde{A}}_{n \times n} & \hat{\tilde{B}}_{n \times m} \\ \hat{\tilde{C}}_{m \times n} & \hat{\tilde{D}}_{m \times m} \end{bmatrix} \begin{bmatrix} V_1(\mathcal{L}) \\ \vdots \\ V_n(\mathcal{L}) \\ \hat{\tilde{V}}_1 \\ \vdots \\ \hat{\tilde{V}}_m \end{bmatrix} \quad (2-62)$$

Eliminating the extraneous node voltages $\hat{\tilde{V}}_1, \dots, \hat{\tilde{V}}_m$ we obtain

$$\begin{bmatrix} \hat{\tilde{V}}_1 \\ \vdots \\ \hat{\tilde{V}}_m \end{bmatrix} = - \hat{\tilde{D}}^{-1} \hat{\tilde{C}} \begin{bmatrix} V_1(\mathcal{L}) \\ \vdots \\ V_n(\mathcal{L}) \end{bmatrix} \quad (2-63)$$

Substituting we obtain

$$\begin{bmatrix} I_1(z) \\ \vdots \\ I_n(z) \end{bmatrix} = (\hat{A} - \hat{B} \hat{D}^{-1} \hat{C}) \begin{bmatrix} V_1(z) \\ \vdots \\ V_n(z) \end{bmatrix} \quad (2-64)$$

and the terminal admittance matrix is identified as

$$\underline{Y}_T = (\hat{A} - \hat{B} \hat{D}^{-1} \hat{C}) \quad (2-65)$$

As an example of a Norton Equivalent formulation, consider the termination network in Figure 2-9(b). Here we may write

$$I_3(z) = (1/Z_1) V_3(z)$$

$$I_2(z) = (1/Z_2) [V_2(z) - V_1(z)]$$

$$I_1(z) = (1/Z_2) [V_1(z) - V_2(z)]$$

Thus we may identify \underline{Y}_T by writing

$$\begin{bmatrix} I_1(z) \\ I_2(z) \\ I_3(z) \end{bmatrix} = \underbrace{\begin{bmatrix} 1/Z_2 & -1/Z_2 & 0 \\ -1/Z_2 & 1/Z_2 & 0 \\ 0 & 0 & 1/Z_1 \end{bmatrix}}_{\underline{Y}_T} \begin{bmatrix} V_1(z) \\ V_2(z) \\ V_3(z) \end{bmatrix}$$

Note for this example, it is not possible to obtain the Thevenin Equivalent characterization, \underline{Z}_T , since \underline{Y}_T is an obviously singular matrix.

III. DERIVATION OF THE EXCITATION SOURCES FOR UNIFORM PLANE WAVE AND NONUNIFORM FIELD EXCITATIONS

In the previous Chapter, equations for the terminal currents of the line were derived for general forms of the excitation field. In this Chapter, we will derive explicit formulas for the equivalent induced source vectors for uniform plane wave excitation of TYPE 1 and TYPE 2 structures. The coordinate system and reference directions for the incident field which are assumed by the program will be indicated. The formulas for nonuniform field excitation which assume a spatial piecewise linear characterization of the incident field will also be derived.

In the following, some confusion may arise concerning the use of the word "vector". A spatial or physical vector will be denoted as \vec{E} . A matrix or column array vector is denoted by \underline{E} . These two "vectors" are obviously quite different quantities however the word "vector" will be used for both with the distinction between the two, although generally obvious from the context, being denoted by an arrow, \rightarrow , over the symbol or a bar, $-$, under the symbol.

The equations for the terminal currents of the line for all structure types are repeated here for convenient reference. If the Thevenin equivalent characterization of the terminal networks is chosen:

$$\underline{V}(0) = -\underline{Z}_0 \underline{I}(0) \quad (3-1a)$$

$$\underline{V}(x) = \underline{Z}_x \underline{I}(x) \quad (3-1b)$$

then the equations for the terminal currents are

$$\begin{aligned}
& [\cos(kx) \{ \underline{Z}_0 + \underline{Z}_x \} + j \sin(kx) \{ \underline{Z}_C + \underline{Z}_x \underline{Z}_C^{-1} \underline{Z}_0 \}] \underline{I}(0) \\
& = \underline{M} + j \underline{Z}_x \underline{Z}_C^{-1} \underline{N} - \underline{E}_t^{(inc)}(x) + [\cos(kx) \underline{1}_n + j \sin(kx) \underline{Z}_x \underline{Z}_C^{-1}] \underline{E}_t^{(inc)}(0)
\end{aligned} \quad (3-2a)$$

$$\begin{aligned}
\underline{I}(x) &= -j \underline{Z}_C^{-1} \{ \underline{N} + \sin(kx) \underline{E}_t^{(inc)}(0) \} \\
&+ [\cos(kx) \underline{1}_n + j \sin(kx) \underline{Z}_C^{-1} \underline{Z}_0] \underline{I}(0)
\end{aligned} \quad (3-2b)$$

If the Norton equivalent characterization of the terminal networks is chosen:

$$\underline{I}(0) = -\underline{Y}_0 \underline{V}(0) \quad (3-3a)$$

$$\underline{I}(x) = \underline{Y}_x \underline{V}(x) \quad (3-3b)$$

then the equations for the terminal currents are

$$\begin{aligned}
& [\cos(kx) \{ \underline{Y}_0 + \underline{Y}_x \} + j \sin(kx) \{ \underline{Y}_x \underline{Z}_C \underline{Y}_0 + \underline{Z}_C^{-1} \}] [-\underline{V}(0)] \\
& = \underline{Y}_x \underline{M} + j \underline{Z}_C^{-1} \underline{N} - \underline{Y}_x \underline{E}_t^{(inc)}(x) \\
& + [\cos(kx) \underline{Y}_x + j \sin(kx) \underline{Z}_C^{-1}] \underline{E}_t^{(inc)}(0)
\end{aligned} \quad (3-4a)$$

$$\begin{aligned}
\underline{I}(x) &= -j \underline{Z}_C^{-1} \{ \underline{N} + \sin(kx) \underline{E}_t^{(inc)}(0) \} \\
&+ [\cos(kx) \underline{Y}_0 + j \sin(kx) \underline{Z}_C^{-1}] [-\underline{V}(0)]
\end{aligned} \quad (3-4b)$$

The $n \times 1$ induced source vectors \underline{M} , \underline{N} , $\underline{E}_t^{(inc)}(0)$, $\underline{E}_t^{(inc)}(x)$, in these equations are defined in the previous Chapter for the various structure types and the entries in these vectors are due to the incident field. It is the purpose of this Chapter to derive the entries in these vectors for uniform plane wave illumination of TYPE1 and TYPE2 structures and nonuniform field illumination of all structure types.

3.1 Basic Integrals

The entries in the induced source vectors, \underline{M} , \underline{N} , $\underline{E}_t^{(inc)}(0)$, $\underline{E}_t^{(inc)}(x)$, in (3-2) and (3-4) all involve integrals of components of the incident electric field

intensity vector along certain spatial contours. It is, of course, highly desirable for computer implementation to obtain closed form solutions for these integrals. Throughout the following derivations, we will encounter two fundamental integrals which must be evaluated. These are designated as $E1(a,b,k)$ and $E2(a,b,k)$ and are given by

$$E1(a,b,k) = \int_a^b x e^{jkx} dx \quad (3-5a)$$

$$E2(a,b,k) = \int_a^b e^{jkx} dx \quad (3-5b)$$

The straightforward solutions of these integrals are

$$E1(a,b,k) = \left(\frac{be^{jkb} - ae^{jka}}{jk} \right) + \left(\frac{e^{jkb} - e^{jka}}{k^2} \right) \quad (3-6a)$$

$$E2(a,b,k) = \left(\frac{e^{jkb} - e^{jka}}{jk} \right) \quad (3-6b)$$

Note that when $k=0$, evaluation of the solutions in (3-6) will result in obvious problems. Of course, the integrals in (3-5) have well defined solutions for $k=0$ and these are quite obviously

$$E1(a,b,0) = \frac{b^2 - a^2}{2} \quad (3-7a)$$

$$E2(a,b,0) = b-a \quad (3-7b)$$

For values of the argument k equal to zero, the program evaluates (3-7).

The following solutions for the entries in the induced source vectors (inc) (inc) \underline{M} , \underline{N} , $\underline{E}_t(0)$, $\underline{E}_t(z)$ in (3-2) and (3-4) will be written in terms of these integrals and the fundamental integrals are stored in the program as function

subprograms. (See Section 4.2.)

3.2 Derivation of the Source Vectors for Uniform Plane Wave Illumination and TYPE 1 Structures

The basic source vector quantities, \underline{M} , \underline{N} , $\underline{E}_t^{(inc)}(0)$, $\underline{E}_t^{(inc)}(\mathcal{L})$, involved in the equations for the terminal currents in (3-2) and (3-4) for TYPE 1 structures are given in (2-36) and (2-37) which are

$$[\underline{E}_\ell(x)]_i = E_{\ell i}^{(inc)}(d_{i0}, x) - E_{\ell i}^{(inc)}(0, x) \quad (3-8a)$$

$$[\underline{E}_t(\mathcal{L})]_i = \int_0^{d_{i0}} E_{ti}^{(inc)}(\rho_i, \mathcal{L}) d\rho_i \quad (3-8b)$$

$$[\underline{E}_t(0)]_i = \int_0^{d_{i0}} E_{ti}^{(inc)}(\rho_i, 0) d\rho_i \quad (3-8c)$$

$$\underline{M} = \int_0^{\mathcal{L}} \cos(k(\mathcal{L} - x)) \underline{E}_\ell(x) dx \quad (3-8d)$$

$$\underline{N} = \int_0^{\mathcal{L}} \sin(k(\mathcal{L} - x)) \underline{E}_\ell(x) dx \quad (3-8e)$$

where $E_{\ell i}^{(inc)}(d_{i0}, x)$ and $E_{\ell i}^{(inc)}(0, x)$ are the components of the incident electric field in the x direction (along the line axis) along the i-th wire and along the reference wire, respectively. The quantities $E_{ti}^{(inc)}(\rho_i, \mathcal{L})$ and $E_{ti}^{(inc)}(\rho_i, 0)$ are the components of the incident electric field along a straight-line contour joining the i-th wire and the reference wire in planes (y, z) transverse or perpendicular to the line axis at $x=\mathcal{L}$ and $x=0$, respectively. This contour is denoted by ρ_i .

The coordinate system used to define the wire positions and shown in Figure 2-4 is used to define the angle of arrival of the uniform plane wave

and polarization of the incident electric field intensity vector. In defining the wire positions for TYPE 1 structures, an arbitrary rectangular coordinate system is established with the reference wire at the center ($y=0, z=0$) of this coordinate system as shown in Figure 3-1. The i -th wire has coordinates $y=y_i, z=z_i$, relative to this coordinate system. The direction of propagation of the incident wave is defined in Figure 3-2 by the angles θ_p and ϕ_p . The angle θ_E is the angular orientation of the electric field intensity vector, \vec{E} , in the plane containing \vec{E} (which is perpendicular to the direction of propagation) and measured from the projection of the y axis onto this plane. The zero phase reference is taken at the origin of the coordinate system, i.e., $x=0, y=0, z=0$.

The electric field intensity vector can be written in terms of components as [12]

$$\vec{E}^{(inc)} [E_{xm} \vec{x} + E_{ym} \vec{y} + E_{zm} \vec{z}] e^{-j(k_x x + k_y y + k_z z)} \quad (3-9)$$

The items E_{xm}, E_{ym}, E_{zm} are the magnitudes of the projections of $\vec{E}^{(inc)}$ in the x, y and z directions, respectively and $\vec{x}, \vec{y}, \vec{z}$ are unit vectors in the x, y , and z directions, respectively. The quantities k_x, k_y , and k_z are the components of the propagation constant, k , in the x, y and z directions, respectively. To determine these quantities, note that the electric field intensity vector can be most directly related to a spherical coordinate system in terms of the unit vectors $\vec{r}, \vec{\theta}, \vec{\phi}$ as shown in Figure 3-2. In this spherical coordinate system, we may write [12]

$$\vec{E} = (E_{rm} \vec{r} + E_{\theta m} \vec{\theta} + E_{\phi m} \vec{\phi}) e^{-jk \cdot \vec{R}} \quad (3-10)$$

TYPE = 1

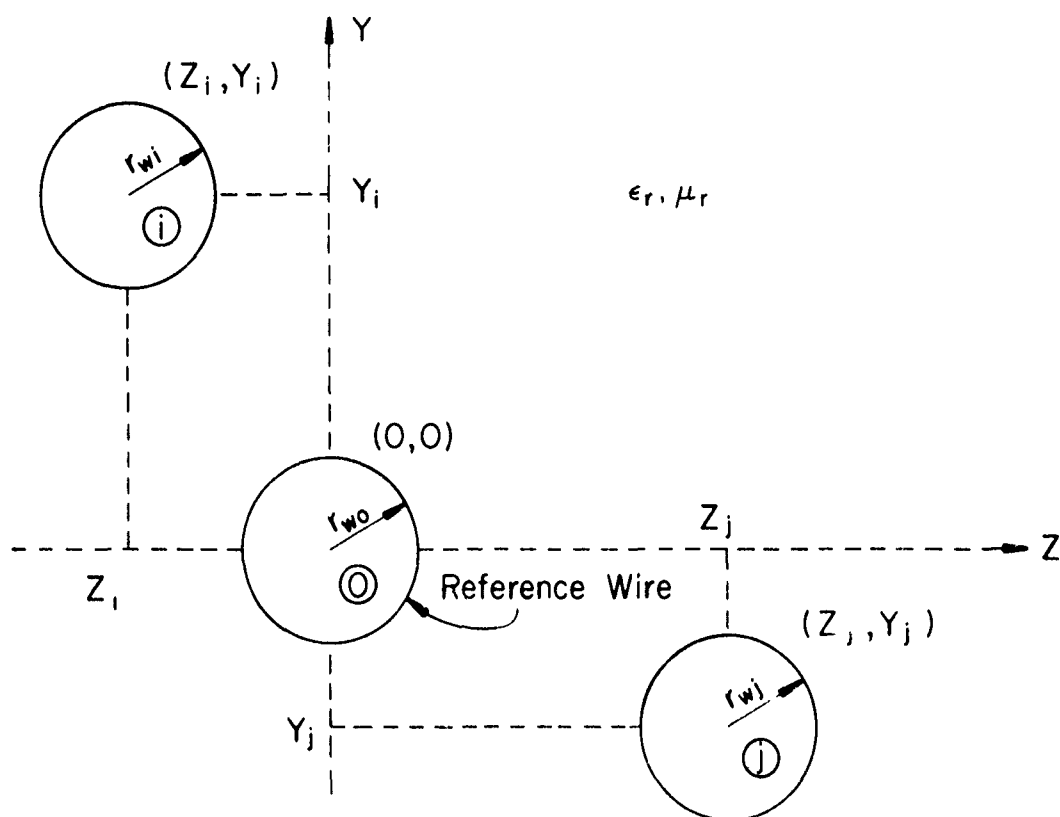
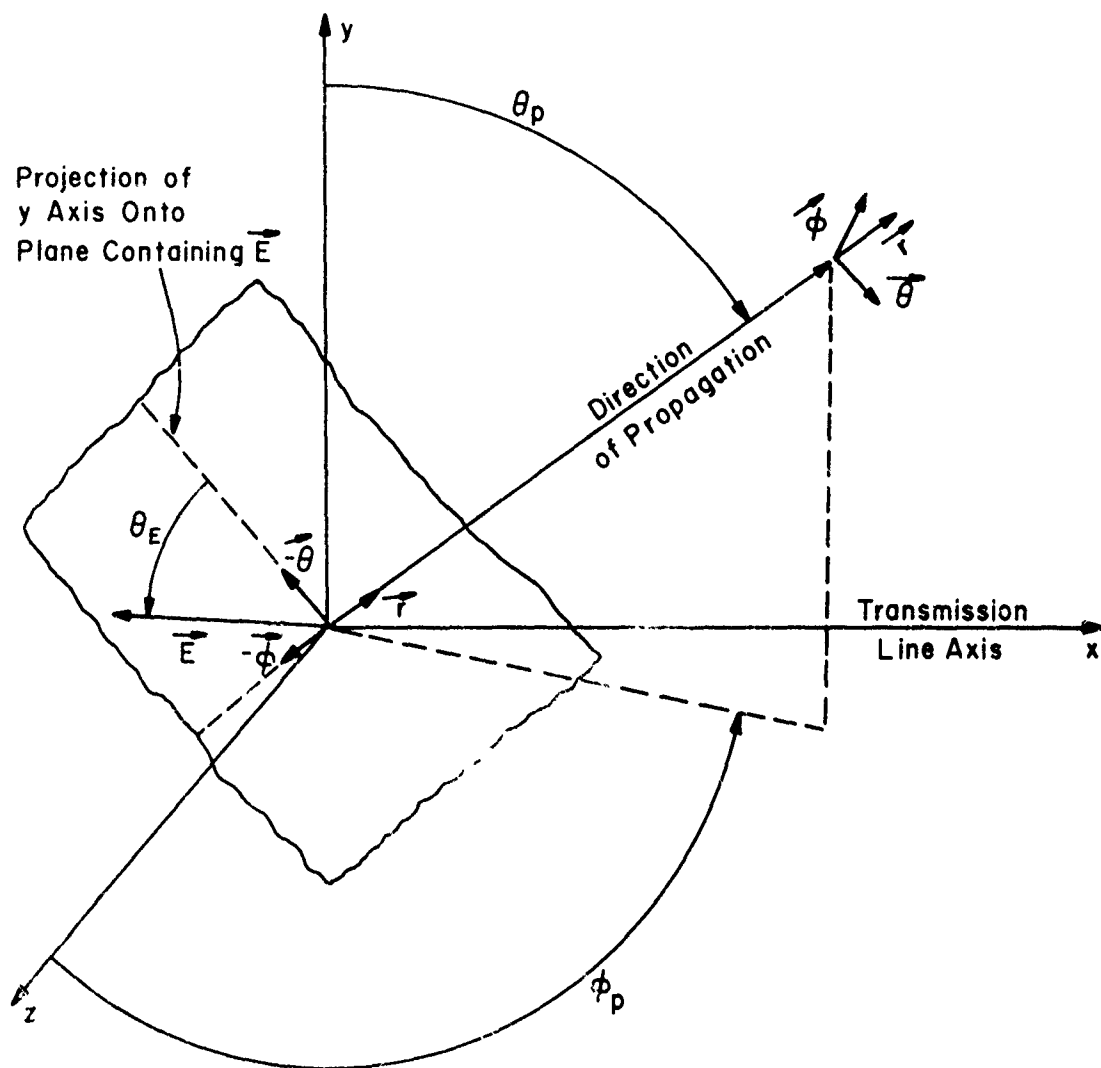


Figure 3-1. The TYPE 1 structure.



Note: Zero Phase Reference Taken at $x=0, y=0, z=0$.

Figure 3-2. Definition of the uniform plane wave parameters.

where from Figure 3-2

$$E_{rm} = 0 \quad (3-11a)$$

$$E_{\theta m} = -E_m \cos \theta_E \quad (3-11b)$$

$$E_{\phi m} = -E_m \sin \theta_E \quad (3-11c)$$

$$\vec{k} = k \vec{r}$$

$$\vec{R} = r \vec{r} = x \vec{x} + y \vec{y} + z \vec{z} \quad (3-11d)$$

\vec{R} is a vector from the origin to a point P and E_m is the magnitude of the electric field intensity. To determine the components E_{xm} , E_{ym} , E_{zm} , k_x , k_y and k_z in (3-9) we simply need the transformation from a spherical coordinate system to a rectangular coordinate system (see reference [12], p.9).

Employing this conversion of coordinate systems, we find

$$E_{xm} = -E_m \cos \theta_E \cos \theta_p \sin \phi_p - E_m \sin \theta_E \cos \phi_p \quad (3-12a)$$

$$E_{ym} = E_m \cos \theta_E \sin \theta_p \quad (3-12b)$$

$$E_{zm} = -E_m \cos \theta_E \cos \theta_p \cos \phi_p + E_m \sin \theta_E \sin \phi_p \quad (3-12c)$$

$$k_x = k \sin \theta_p \sin \phi_p \quad (3-12d)$$

$$k_y = k \cos \theta_p \quad (3-12e)$$

$$k_z = k \sin \theta_p \cos \phi_p \quad (3-12f)$$

Calculation of the quantities in (3-8) proceeds as follows. The i -th entry in the $n \times 1$ vector \underline{M} is

$$[\underline{M}]_i = \int_0^L \cos(k(L-x)) \{E_{\ell 1}^{(inc)}(d_{10}, x) - E_{\ell 1}^{(inc)}(0, x)\} dx \quad (3-13)$$

where

$$\begin{aligned}
 E_{\ell i}^{(inc)}(d_{i0}, x) - E_{\ell i}^{(inc)}(0, x) &= E_x \Big|_{\substack{y=y_i \\ z=z_i}} - E_x \Big|_{\substack{y=0 \\ z=0}} \\
 &= E_{xm} e^{-jk_x x} \{ e^{-j(k_y y_i + k_z z_i)} - 1 \}
 \end{aligned} \tag{3-14}$$

and the i -th wire has y and z coordinates of y_i and z_i , respectively. Substituting (3-14) into (3-13) one can obtain

$$\begin{aligned}
 [M]_i &= E_{xm} \{ e^{-j(k_y y_i + k_z z_i)} - 1 \} \int_0^{\mathcal{L}} \cos(k(\mathcal{L} - x)) e^{-jk_x x} dx \\
 &= E_{xm} \{ e^{-j(k_y y_i + k_z z_i)} - 1 \} \left\{ \frac{e^{jk\mathcal{L}}}{2} \int_0^{\mathcal{L}} e^{-j(k + k_x)x} dx \right. \\
 &\quad \left. + \frac{e^{-jk\mathcal{L}}}{2} \int_0^{\mathcal{L}} e^{j(k - k_x)x} dx \right\}
 \end{aligned} \tag{3-15}$$

This result can be written in terms of the basic integral E2 in Section 3.1 as

$$\begin{aligned}
 [M]_i &= \frac{E_{xm}}{2} \{ e^{-j(k_y y_i + k_z z_i)} - 1 \} \{ e^{jk\mathcal{L}} E2(0, \mathcal{L}, -(k + k_x)) \\
 &\quad + e^{-jk\mathcal{L}} E2(0, \mathcal{L}, (k - k_x)) \}
 \end{aligned} \tag{3-16}$$

Similarly the entries in the $n \times 1$ vector \underline{N} become

$$\begin{aligned}
 [N]_i &= \int_0^{\mathcal{L}} \sin(k(\mathcal{L} - x)) \{ E_{\ell i}^{(inc)}(d_{i0}, x) - E_{\ell i}^{(inc)}(0, x) \} dx \\
 &= -j \frac{E_{xm}}{2} \{ e^{-j(k_y y_i + k_z z_i)} - 1 \} \{ e^{jk\mathcal{L}} E2(0, \mathcal{L}, -(k + k_x)) \\
 &\quad - e^{-jk\mathcal{L}} E2(0, \mathcal{L}, (k - k_x)) \}
 \end{aligned} \tag{3-17}$$

The calculation of the entries in the vectors $\underline{E}_t^{(inc)}(x)$ and $\underline{E}_t^{(inc)}(0)$ proceeds as follows. The i -th entry in $\underline{E}_t^{(inc)}(x)$ is given by

$$[\underline{E}_t^{(inc)}(x)]_i = \int_0^{d_{i0}} E_{ti}(\rho_i, x) d\rho_i \quad (3-18)$$

where ρ_i is a straight-line contour in the y, z plane (at $x=x$) joining the reference wire and the i -th wire. The i -th wire is located at $y=y_i, z=z_i$ and the reference wire is located at $y=0, z=0$. The center-to-center separation between the reference wire and the i -th wire is $d_{i0} = \sqrt{y_i^2 + z_i^2}$. Consider Figure 3-3 which shows this contour and the appropriate components of the electric field along this contour. For this situation, (3-18) becomes

$$[\underline{E}_t^{(inc)}(x)]_i = \int_0^{d_{i0}} (E_{ym} \cos \theta + E_{zm} \sin \theta) e^{-jk_x x} \{ e^{-j(k_y \cos \theta + k_z \sin \theta) \rho_i} \} d\rho_i \quad (3-19)$$

where

$$\cos \theta = \frac{y_i}{d_{i0}} \quad (3-20a)$$

$$\sin \theta = \frac{z_i}{d_{i0}} \quad (3-20b)$$

Therefore, we obtain

$$[\underline{E}_t^{(inc)}(x)]_i = (E_{ym} y_i + E_{zm} z_i) e^{-jk_x x} \frac{(e^{-j(k_y y_i + k_z z_i)} - 1)}{-j(k_y y_i + k_z z_i)} \quad (3-21)$$

This result may be written equivalently in terms of fundamental integral E2

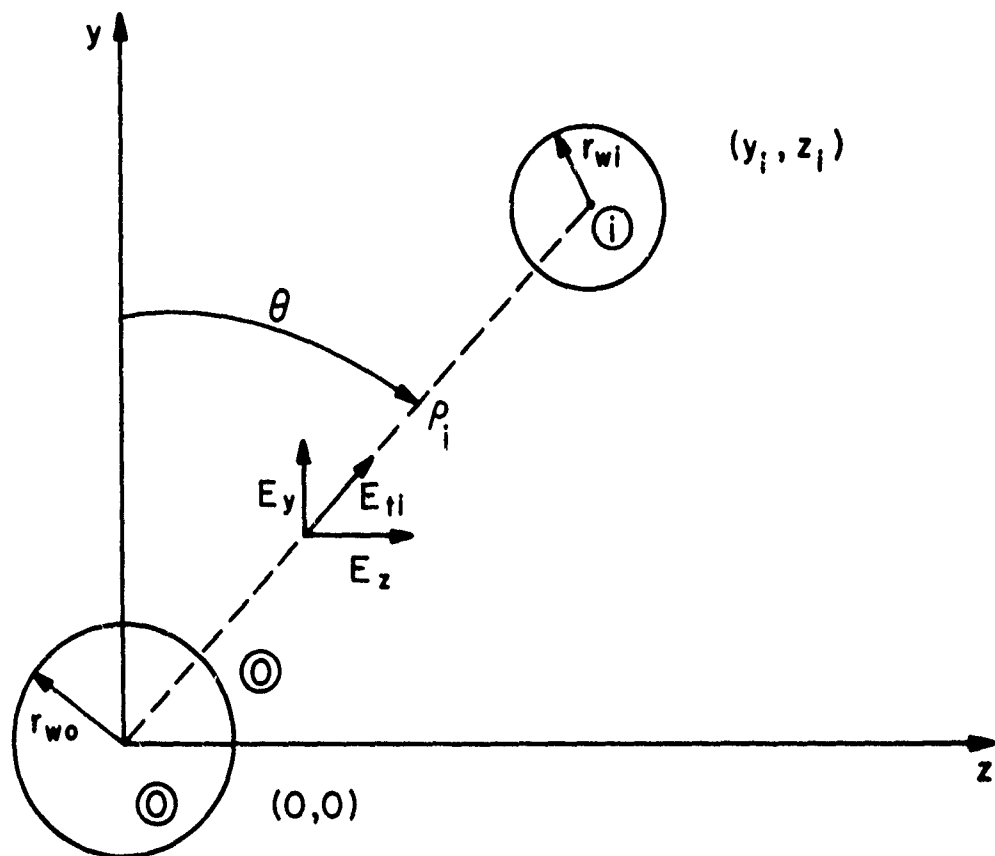


Figure 3-3.

as

$$[E_{-t}^{(inc)}(\mathbf{r})]_i = [E_{ym} y_i + E_{zm} z_i] e^{-jk_x x} E_2(0,1, (k_y y_i + k_z z_i)) \quad (3-22)$$

The i -th entry in the vector $E_{-t}^{(inc)}(0)$ is given by (3-22) with $\mathbf{r} = 0$.

3.3 Derivation of the Source Vectors for Uniform Plane Wave Illumination and TYPE 2 Structures

Derivation of the source vectors, \underline{M} , \underline{N} , $E_y^{(inc)}(0)$, $E_t^{(inc)}(\mathbf{r})$, in (3-2) and (3-4) for uniform plane wave illumination of n wires above a ground plane (TYPE 2 structures) proceeds similarly. Here, we will determine $\vec{E}^{(inc)}$ as the net electric field which is the vector sum of the incident wave and the wave reflected by the perfectly conducting ground plane. In this case, the net electric field tangent to the ground plane will be zero. Therefore $E_{xi}^{(inc)}(0,x)$ in (2-49a) will be zero. Again, an arbitrary rectangular coordinate system is used to define the cross-sectional positions of the wires. The ground plane forms the x,z plane ($y=0$) as shown in Figure 3-4. The zero phase reference for the incident field will be taken to be at the origin of this coordinate system, i.e., $x=0, y=0, z=0$. The various angles defining the direction of propagation of the incident wave and polarization of the electric field intensity vector are the same as for TYPE 1 structures and are shown in Figure 3-2.

The primary problem here is to determine the net electric field parallel to the wire axes and between the i -th wire and the ground plane along a contour perpendicular to the ground plane. This net electric field is the vector sum of the incident field (in the absence of the ground plane) and the portion reflected by the ground plane.

TYPE = 2

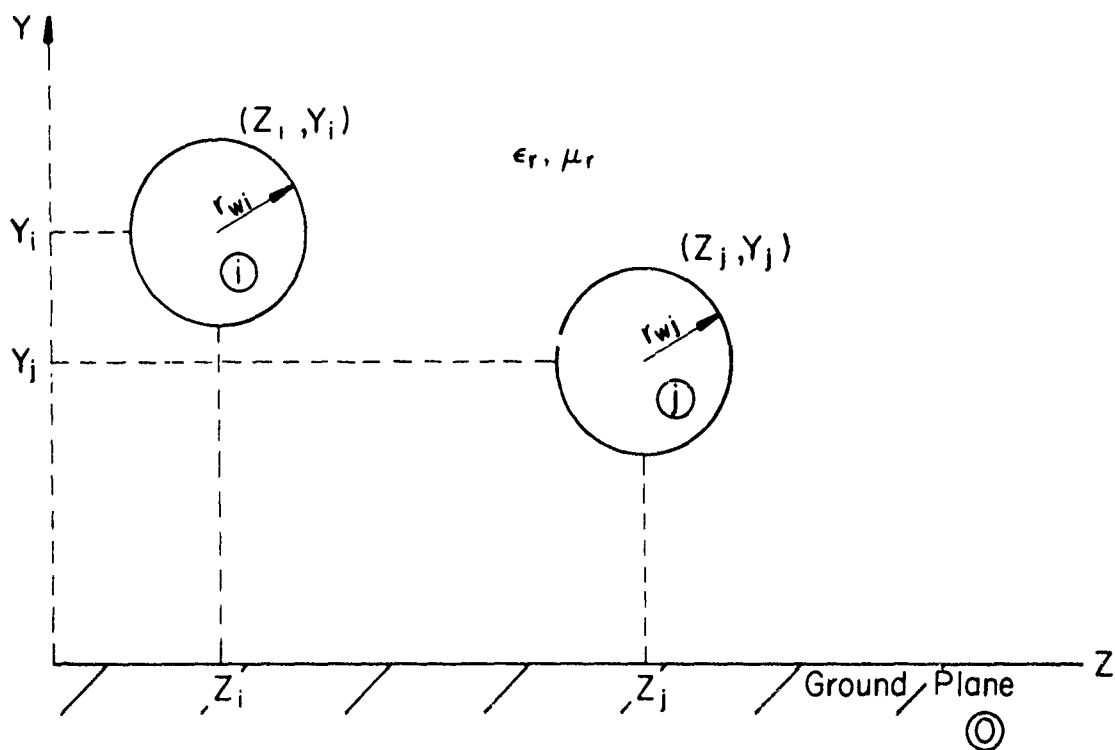


Figure 3-4. The TYPE 2 structure.

We may write the incident electric field

$$\vec{E}^i = (E_{xm}^i \vec{x} + E_{ym}^i \vec{y} + E_{zm}^i \vec{z}) e^{-j(k_x x + k_y y + k_z z)} \quad (3-23)$$

The angle of reflection between the reflected wave and the ground plane is equal to the angle of incidence by Snell's Law [12]. Therefore we may immediately write the form of the reflected wave as

$$\vec{E}^r = (E_{xm}^r \vec{x} + E_{ym}^r \vec{y} + E_{zm}^r \vec{z}) e^{-j(k_x x - k_y y + k_z z)} \quad (3-24)$$

At $y=0$, continuity of the tangential components of the electric field require that

$$E_{xm}^r = -E_{xm}^i \triangleq -E_{xm} \quad (3-25a)$$

$$E_{zm}^r = -E_{zm}^i \triangleq -E_{zm} \quad (3-25b)$$

Consequently, the net x component of the electric field is given by

$$\begin{aligned} E_{x_Total} &= E_{xm}^i e^{-j(k_x x + k_y y + k_z z)} + E_{xm}^r e^{-j(k_x x - k_y y + k_z z)} \\ &= E_{xm} e^{-j(k_x x + k_z z)} \{ e^{-jk_y y} - e^{jk_y y} \} \\ &= -2j E_{xm} \sin(k_y y) e^{-j(k_x x + k_z z)} \end{aligned} \quad (3-26)$$

where E_{xm} is the magnitude of the x component of the incident electric field, i.e., $E_{xm} \triangleq E_{xm}^i$. Similarly, one may show that the net y component of the electric field is given by [12]

$$E_{y\text{Total}} = 2 E_{ym} \cos(k_y y) e^{-j(k_x x + k_z z)} \quad (3-27)$$

The components of the $n \times 1$ vector \underline{M} become

$$\begin{aligned} [\underline{M}]_i &= \int_0^{\mathcal{L}} \cos(k(\mathcal{L} - x)) [\underline{E}_\ell(x)]_i^{(inc)} dx \\ &= \int_0^{\mathcal{L}} \cos(k(\mathcal{L} - x)) E_{x\text{Total}} \Big|_{\substack{y=y_1 \\ z=z_1}} dx \quad (3-28) \\ &= -2jE_{xm} e^{-jk_z z_1} \sin(k_y y_1) \int_0^{\mathcal{L}} \cos(k(\mathcal{L} - x)) e^{-jk_x x} dx \\ &= -jE_{xm} e^{-jk_z z_1} \sin(k_y y_1) \int_0^{\mathcal{L}} \{ e^{jk\mathcal{L}} e^{-jkx} e^{-jk_x x} \\ &\quad + e^{-jk\mathcal{L}} e^{jkx} e^{-jk_x x} \} dx \\ &= -jE_{xm} e^{-jk_z z_1} \sin(k_y y_1) \{ e^{jk\mathcal{L}} E_2(0, \mathcal{L}, -(k + k_x)) \\ &\quad + e^{-jk\mathcal{L}} E_2(0, \mathcal{L}, (k - k_x)) \} \end{aligned}$$

Similarly calculation of the entries in \underline{N} yields

$$\begin{aligned} [\underline{N}]_i &= \int_0^{\mathcal{L}} \sin(k(\mathcal{L} - x)) [\underline{E}_\ell(x)]_i^{(inc)} dx \\ &= \int_0^{\mathcal{L}} \sin(k(\mathcal{L} - x)) E_{x\text{Total}} \Big|_{\substack{y=y_1 \\ z=z_1}} dx \quad (3-29) \\ &= -E_{xm} e^{-jk_z z_1} \sin(k_y y_1) \{ e^{jk\mathcal{L}} E_2(0, \mathcal{L}, -(k + k_x)) \end{aligned}$$

$$-e^{-jk_z} E_2(0, z, (k - k_x)) \} \quad (3-29)$$

The entries in $\underline{E}_t^{(inc)}(z)$ are given by

$$[\underline{E}_t^{(inc)}(z)]_1 = \int_0^{y_1} E_{y_{Total}} \Big|_{\substack{z=z_1 \\ x=z_1}} dy \quad (3-30)$$

$$\begin{aligned} &= \int_0^{y_1} 2E_{ym} \cos(k_y y) e^{-j(k_x z + k_z z_1)} dy \\ &= 2E_{ym} e^{-jk_x z} e^{-jk_z z_1} \int_0^{y_1} \frac{e^{jk_y y} + e^{-jk_y y}}{2} dy \\ &= E_{ym} e^{-jk_x z} e^{-jk_z z_1} \left\{ \int_0^{y_1} e^{jk_y y} dy + \int_0^{y_1} e^{-jk_y y} dy \right\} \\ &= E_{ym} e^{-jk_x z} e^{-jk_z z_1} \left\{ \int_0^{y_1} e^{jk_y y} dy + \int_{-y_1}^0 e^{jk_y y} dy \right\} \\ &= E_{ym} e^{-jk_x z} e^{-jk_z z_1} \{ E_2(-y_1, y_1, k_y) \} \end{aligned}$$

The entries in $\underline{E}_t^{(inc)}(0)$ are those of (3-30) with $z = 0$.

It should be noted that the above quantities can be determined in an alternate fashion. Rather than determining the net electric field as the sum of an incident and a reflected wave, simply replace the ground plane with image wires as shown in Figure 3-5. The entries in the source vectors can then be obtained by using only the incident field and treating the image

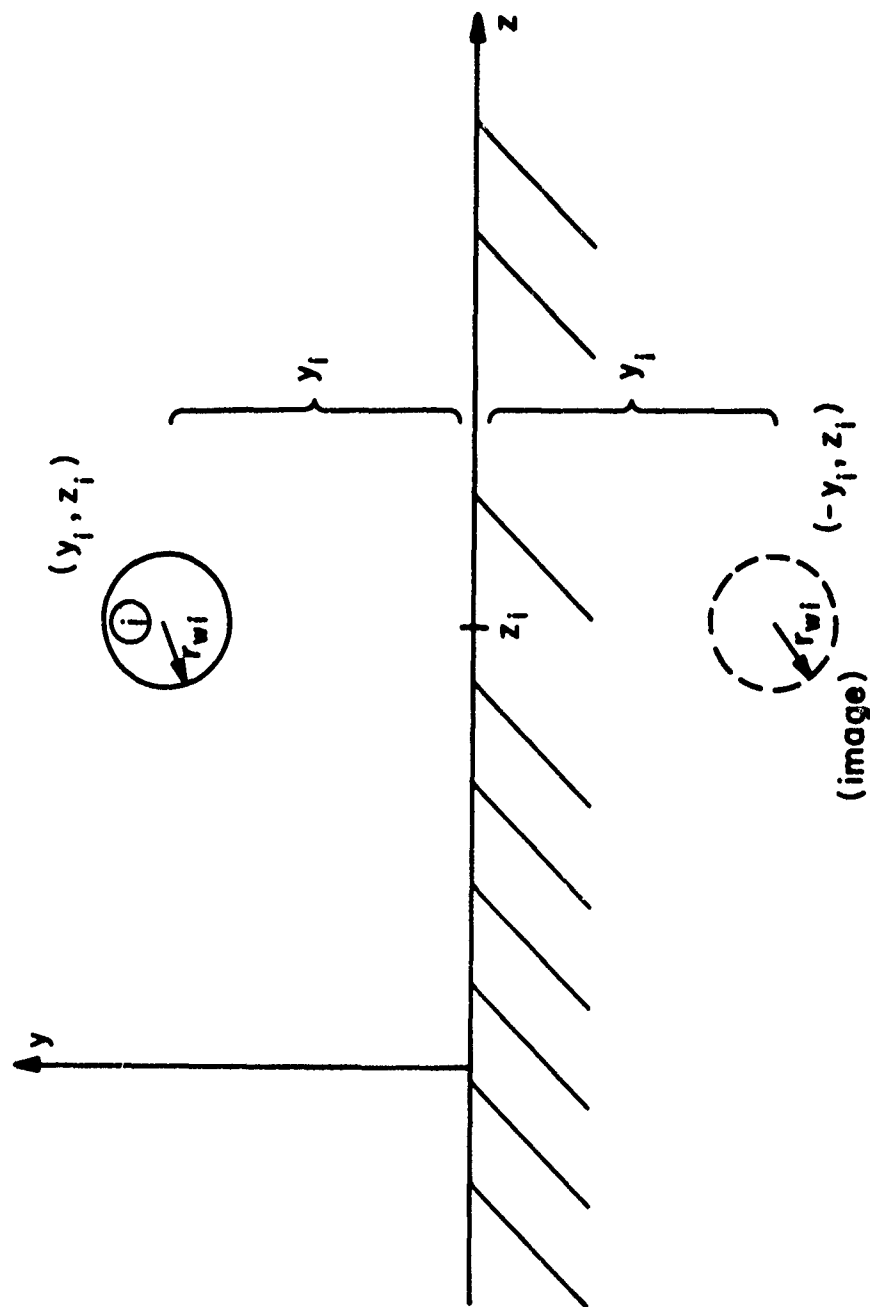


Figure 3-5.

of the i-th wire as the "reference" for the i-th wire as

$$[\underline{M}]_i = \int_0^{\mathcal{L}} \cos(k(\mathcal{L} - x)) \left\{ E_x^{(inc)} \Big|_{\substack{y=y_i \\ z=z_i}} - E_x^{(inc)} \Big|_{\substack{y=-y_i \\ z=z_i}} \right\} dx \quad (3-31a)$$

$$= \int_0^{\mathcal{L}} \cos(k(\mathcal{L} - x)) \{ E_{xm} e^{-j(k_x x + k_y y_i + k_z z_i)} - E_{xm} e^{-j(k_x x - k_y y_i + k_z z_i)} \} dx$$

$$= E_{xm} e^{-jk_z z_i} (e^{-jk_y y_i} - e^{jk_y y_i}) \int_0^{\mathcal{L}} \cos(k(\mathcal{L} - x)) e^{-jk_x x} dx$$

$$= -2j E_{xm} e^{-jk_z z_i} \sin(k_y y_i) \int_0^{\mathcal{L}} \cos(k(\mathcal{L} - x)) e^{-jk_x x} dx$$

$$= -j E_{xm} e^{-jk_z z_i} \sin(k_y y_i) \{ e^{jk\mathcal{L}} E_2(0, \mathcal{L}, -(k + k_x)) + e^{-jk\mathcal{L}} E_2(0, \mathcal{L}, (k - k_x)) \}$$

$$[\underline{N}]_i = \int_0^{\mathcal{L}} \sin(k(\mathcal{L} - x)) \left\{ E_x^{(inc)} \Big|_{\substack{y=y_i \\ z=z_i}} - E_x^{(inc)} \Big|_{\substack{y=-y_i \\ z=z_i}} \right\} dx \quad (3-31b)$$

$$= \int_0^{\mathcal{L}} \sin(k(\mathcal{L} - x)) \{ E_{xm} e^{-j(k_x x + k_y y_i + k_z z_i)} - E_{xm} e^{-j(k_x x - k_y y_i + k_z z_i)} \} dx$$

$$= -E_{xm} e^{-jk_z z_i} \sin(k_y y_i) \{ e^{jk\mathcal{L}} E_2(0, \mathcal{L}, -(k + k_x)) - e^{-jk\mathcal{L}} E_2(0, \mathcal{L}, (k - k_x)) \}$$

$$\begin{aligned}
\stackrel{(inc)}{[E_t(z)]_i} &= \int_{-y_i}^{y_i} E_y^{(inc)} \Big|_{\substack{x=z \\ z=z_i}} dy & (3-31c) \\
&= \int_{-y_i}^{y_i} E_{ym} e^{-j(k_x z + k_y y + k_z z_i)} dy \\
&= E_{ym} e^{-jk_x z} e^{-jk_z z_i} \int_{-y_i}^{y_i} e^{-jk_y y} dy \\
&= E_{ym} e^{-jk_x z} e^{-jk_z z_i} \left\{ \int_{-y_i}^0 e^{-jk_y y} dy + \int_0^{y_i} e^{-jk_y y} dy \right\} \\
&= E_{ym} e^{-jk_x z} e^{-jk_z z_i} \left\{ \int_0^{y_i} e^{jk_y y} dy + \int_{-y_i}^0 e^{jk_y y} dy \right\} \\
&= E_{ym} e^{-jk_x z} e^{-jk_z z_i} \{E2(-y_i, y_i, k_y)\}
\end{aligned}$$

which are precisely the results obtained previously.

3.4 Calculation of the Source Vectors for Nonuniform Fields

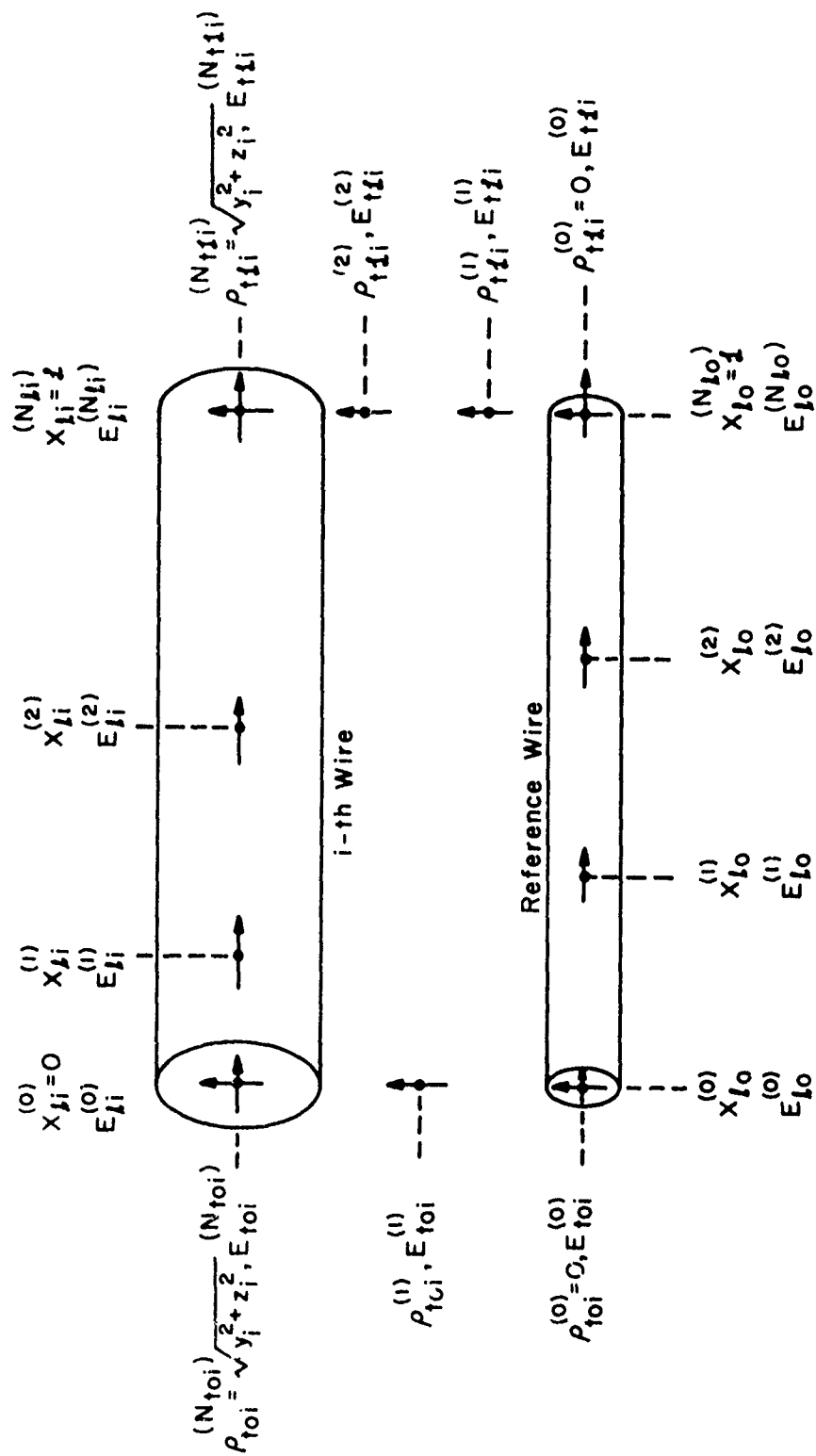
Nonuniform field excitation can be specified for all structure types. The problem here, again, is to evaluate equations of the form in (3-8). This requires that we specify values (magnitude and phase) of the electric field intensity vector along the wires and reference conductor and between each wire and the reference conductor at the endpoints of the line. To accomplish this, we will specify values at a finite number of points along

the appropriate contours and assume piecewise-linear variation of the electric field (magnitude and phase) between the specified points. This is illustrated in Figure 3-6.

For TYPE 1 structures, the values of $\vec{E}_{\ell 0}^{(m)}$, along the reference wires (in the +x direction) at $N_{\ell 0} + 1$ points will be specified as shown in Figure 3-6(a). The values of $\vec{E}_{\ell i}^{(m)}$, along the i-th wire at $N_{\ell i} + 1$ points will be specified. The values of $\vec{E}_{t0}^{(m)}$ and $\vec{E}_{t\ell}^{(m)}$, at $x=0$ and $x=\ell$ along a straight-line contour in the y,z plane joining the reference wire and the i-th wire at $N_{t0} + 1$ and $N_{t\ell} + 1$ points, respectively, will be specified. Similar quantities will be specified for TYPE 2 and TYPE 3 structures as shown in Figure 3-6(b) and Figure 3-6(c), respectively, with the exception that \vec{E} is taken to be zero along the reference conductor for these two cases.

Piecewise-linear variation of the electric field (magnitude and phase) is assumed between these specification points as shown in Figure 3-7 where the magnitude of the appropriate component of the electric field is denoted by $|\cdot|$ and the angle is denoted by \angle . Thus the problem is the determination of quantities of the form in (3-8) for this piecewise-linear variation of the field. The technique is to write linear equations representing the piecewise-linear variation of the magnitude and phase of the field between successive specification points and add the appropriate integrals over the adjacent regions.

The first problem then becomes to characterize the linear magnitude and phase variation between two successive data points. Consider two successive data points, x_m and x_{m+1} , which specify the magnitude of the electric field, E_m and E_{m+1} , and phase, θ_m and θ_{m+1} , respectively. Knowing the end points, one can write linear equations characterizing the linear



(a)

Figure 3-6. Nonuniform field specification for TYPE 1 Structures.

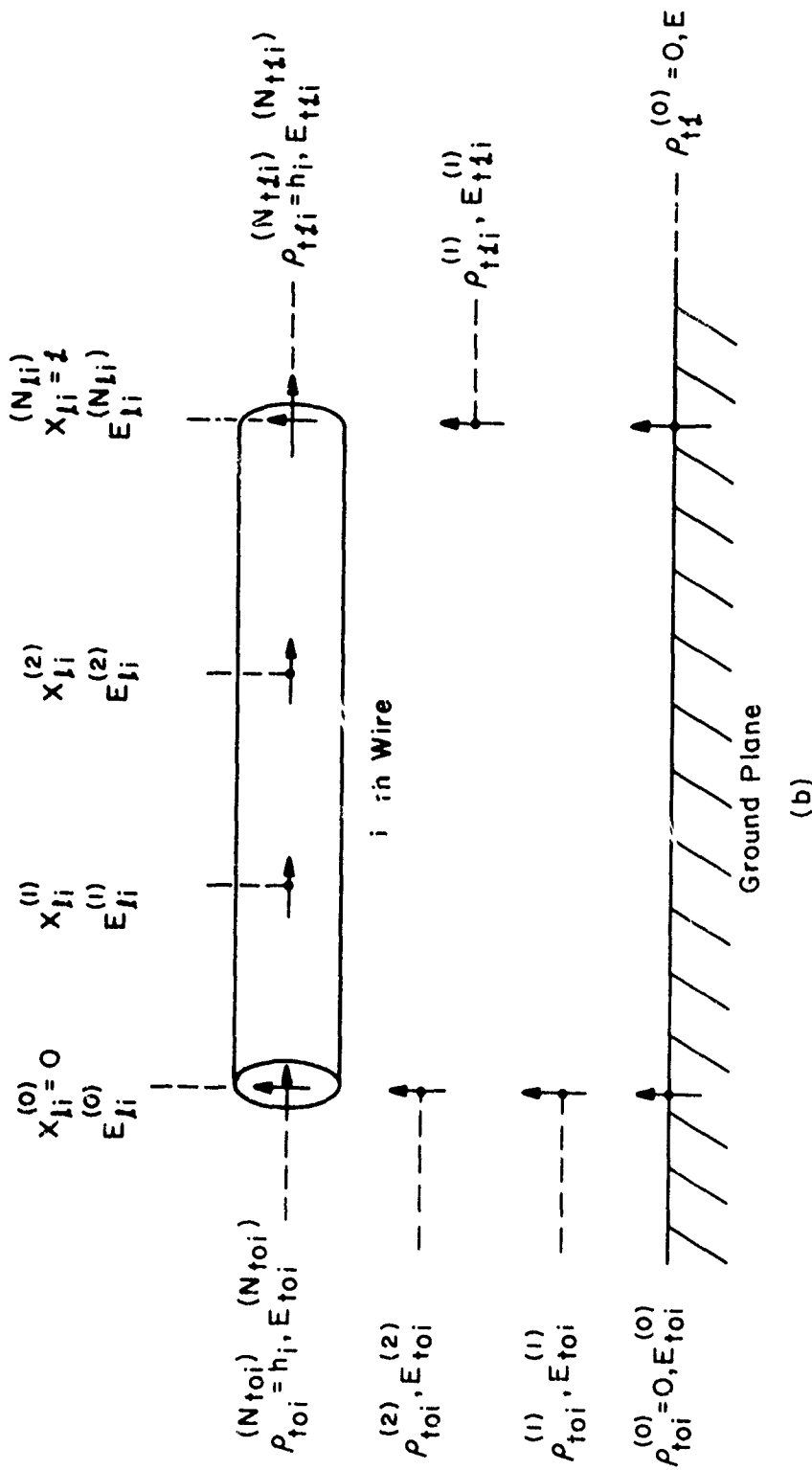


Figure 3-6. Nonuniform field specification for TYPE 2 Structures.

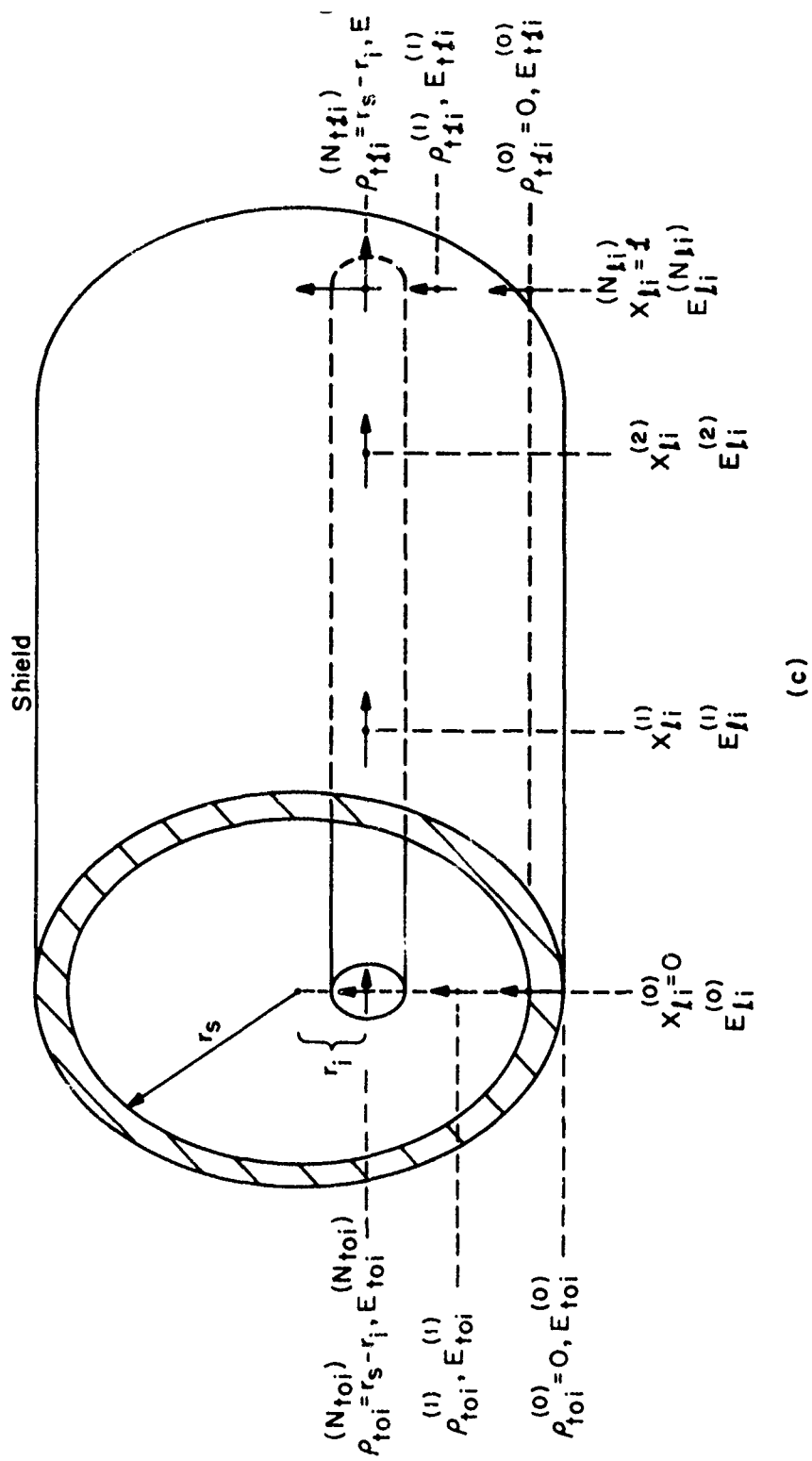


Figure 3-6. Nonuniform field specification for TYPE 3 structures.

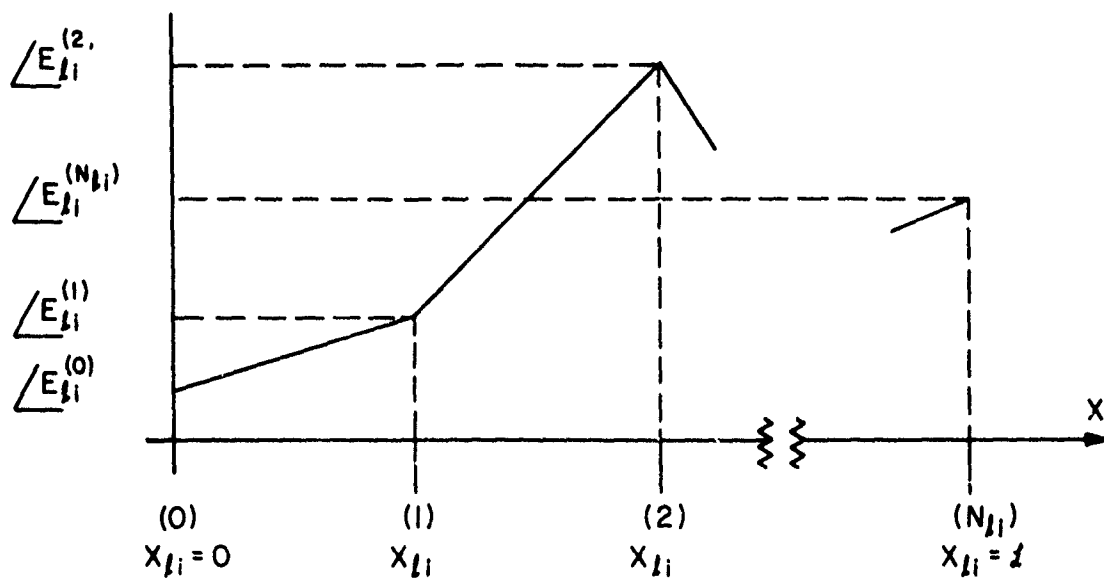
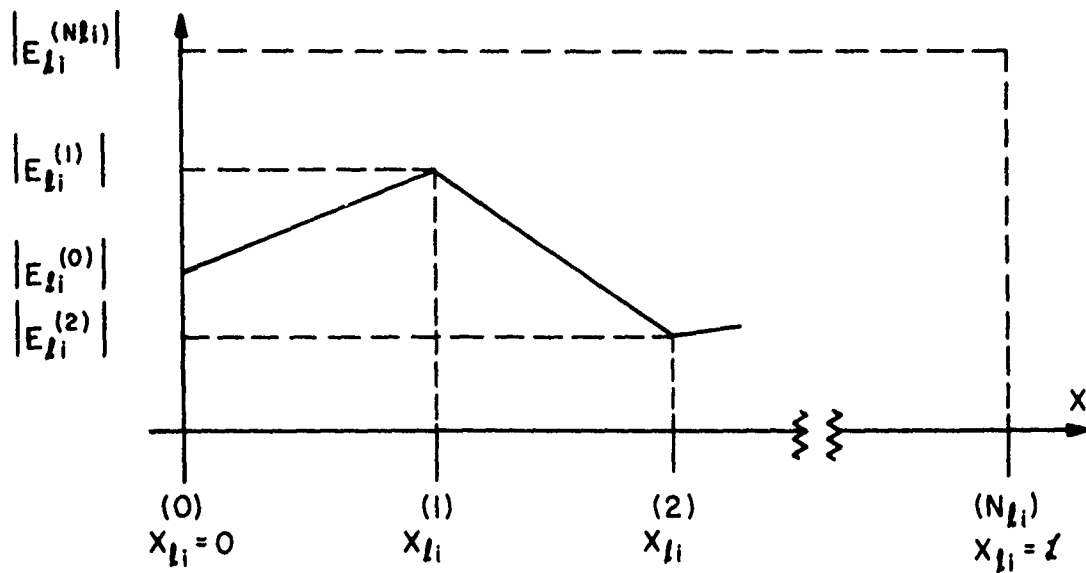


Figure 3-7. Piecewise-linear field specification.

behavior between these successive points as

$$|E_m(x)| = a_m x + b_m \quad (3-32a)$$

$$\theta_m(x) = c_m x + d_m \quad (3-32b)$$

$$a_m = \left\{ \frac{E_{m+1} - E_m}{x_{m+1} - x_m} \right\} \quad (3-33a)$$

$$b_m = \left\{ \frac{E_m x_{m+1} - E_{m+1} x_m}{x_{m+1} - x_m} \right\} \quad (3-33b)$$

$$c_m = \left\{ \frac{\theta_{m+1} - \theta_m}{x_{m+1} - x_m} \right\} \quad (3-33c)$$

$$d_m = \left\{ \frac{\theta_m x_{m+1} - \theta_{m+1} x_m}{x_{m+1} - x_m} \right\} \quad (3-33d)$$

The electric field is then characterized by

$$E_m(x) = |E_m(x)| e^{j\theta_m(x)} \quad (3-34)$$

The quantities of the form in (3-8) which must be evaluated involve certain integrals involving the form (3-32). The first type is of the form in (3-8d) which can be evaluated as

$$\int_{x_m}^{x_{m+1}} \cos(k(\mathcal{Z} - x)) \{a_m x + b_m\} e^{j(c_m x + d_m)} dx \quad (3-35)$$

$$= e^{jd_m} \{a_m \int_{x_m}^{x_{m+1}} \cos(k(\mathcal{Z} - x)) x e^{jc_m x} dx$$

$$+ b_m \int_{x_m}^{x_{m+1}} \cos(k(\mathcal{Z} - x)) e^{jc_m x} dx\}$$

$$= \frac{e^{jd_m}}{2} \{a_m e^{jk\mathcal{Z}} \text{El}(x_m, x_{m+1}, c_m - k)$$

$$+ a_m e^{-jk\mathcal{Z}} \text{El}(x_m, x_{m+1}, c_m + k)$$

$$+ b_m e^{jk\mathcal{Z}} \text{E2}(x_m, x_{m+1}, c_m - k)$$

$$+ b_m e^{-jk\mathcal{Z}} \text{E2}(x_m, x_{m+1}, c_m + k)\}$$

The second form is similar to (3-8e) which can be evaluated as

$$\int_{x_m}^{x_{m+1}} \sin(k(\mathcal{Z} - x)) \{a_m x + b_m\} e^{j(c_m x + d_m)} dx \quad (3-36)$$

$$= \frac{e^{jd_m}}{2j} \{a_m e^{jk\mathcal{Z}} \text{El}(x_m, x_{m+1}, c_m - k)$$

$$- a_m e^{-jk\mathcal{Z}} \text{El}(x_m, x_{m+1}, c_m + k)$$

$$\begin{aligned}
& + b_m e^{jkx} E2(x_m, x_{m+1}, c_m - k) \\
& - b_m e^{-jkx} E2(x_m, x_{m+1}, c_m + k) \}
\end{aligned}$$

The third forms are similar to (3-8b) and (3-8c) which can be evaluated as

$$\int_{x_m}^{x_{m+1}} (a_m x + b_m) e^{j(c_m x + d_m)} dx \quad (3-37)$$

$$\begin{aligned}
& = e^{jd_m} \{ a_m E1(x_m, x_{m+1}, c_m) \\
& + b_m E2(x_m, x_{m+1}, c_m) \}
\end{aligned}$$

The program computes the items in (2-36) and (2-37) for TYPE 1 structures; (2-49) and (2-37) for TYPE 2 structures; and (2-52) and (2-37) for TYPE 3 structures by breaking up the appropriate integrals and adding the integrals between each pair of successive data points. The data points need not be equally spaced along the appropriate contours so that one can model localized, extreme variations in the fields without using an inordinately large number of data points. In specifying the sequence of electric field components along each contour, one must insure that the first and last specification points are at the two ends of the contour and $x_m < x_{m+1}$.

IV. COMPUTER PROGRAM DESCRIPTION

The contents and operation of the code will be described in this Chapter. The cards in the program deck are sequentially numbered in columns 73-80 with the word WIRE in 73-76 and the card number in 77-80. The program is written in Fortran IV language and is double precision. A listing of the program is contained in Appendix B and a general flow chart of the program is given in Appendix B. In this flow chart, the numbers on the left and right of the individual boxes denote the beginning and ending card numbers of the corresponding portion of the code listing, respectively. Changes in the program to convert to single precision arithmetic are indicated in Appendix B. The program has been implemented on an IBM 370/165 digital computer at the University of Kentucky using the Fortran IV G-Level compiler.

The program requires two function subprograms, E1 and E2, and one subroutine, LEQT1C, which must follow the main program and precede the data cards. Subroutine LEQT1C is a general purpose subroutine to solve a set of n , complex, linear simultaneous equations and is a part of the IMSL (International Mathematical and Statistical Library) package [13]. If the IMSL package is not available on the user's system, other appropriate general purpose subroutines may be used. (See Section 4.2 for a discussion of LEQT1C and its argument list.) Listings of function subprograms E1 and E2 are contained in Appendix C.

4.1 Main Program Description

A listing of the WIRE program is contained in Appendix B. Cards 0001 through 0055 contain general comments concerning the applicability of the

program. Cards 0057 through 0060 contain the array dimension information. All vectors and matrices should be dimensioned to be of size N where N is the number of wires exclusive of the reference conductor. These matrices and vectors must be dimensioned appropriately for each problem. Cards 0062 through 0069 declare double precision real and complex variables and dimension the vector and matrix arrays.

Cards 0071 through 0080 define certain constants,

CMTM (conversion from mils to meters)	= 2.54×10^{-5}
MU02PI	= $\mu/2\pi$
ONE	= 1.
P5	= .5
FOUR	= 4.
ONE80	= 180.
ZERO	= 0.
TWO	= 2.
ONEC	= $1. + j0.$
ZEROC	= $0. + j0.$
XJ	= $0. + j1.$
V(velocity of light in free space)	= 2.997925×10^8 m/sec
PI	= π
RADEG(conversion from radians to degrees)	= $180./\pi$

Note that π is computed to the user's machine precision by using the relationship

$$\tan (\pi/4) = 1$$

Cards 0086 through 0145 read and print portions of the input data and perform certain primitive error checks. These cards read the structure type (TYPE=1,2,or3), the load specification option (LS0=11,12,21,or22), the field specification option (FS0=1,or2), the number of wires, N, the relative permittivity of the medium, ER, the relative permeability of the medium, MUR, and the line length, L. In addition, for TYPE 1 structures, the radius of the reference wire, RW0, and for TYPE 3 structures, the interior radius of the overall, cylindrical shield, RS, are read.

Cards 0150 through 0197 read the radii, r_{wi} , and the z_i and y_i coordinates (r_i and θ_i for TYPE 3) for the N wires and compute the entries in the characteristic impedance matrix. The z and y coordinates are stored in the real, $n \times 1$ vectors V3 and V4, respectively:

$$\left\{ \begin{array}{l} z_i \text{ for TYPE 1,2} \\ r_i \text{ for TYPE 3} \end{array} \right\} \rightarrow V3(I)$$

$$\left\{ \begin{array}{l} y_i \text{ for TYPE 1,2} \\ \theta_i \text{ for TYPE 3} \end{array} \right\} \rightarrow V4(I)$$

In addition, the entries in the $n \times n$, real characteristic impedance matrix, Z_C , are temporarily stored in the real parts of the $n \times n$ complex matrix M1. This is done to minimize the required array storage in the program since the matrix M1 will be needed later as a complex matrix.

Matrix

Z_C

Array

M1 (real part)

Cards 0202 through 0211 compute the inverse of \underline{Z}_C , \underline{Z}_C^{-1} , which is stored in the real parts of the $n \times n$, complex arrays M2 and M3. Subroutine LEQTLIC computes this inverse by solving the system of equations $\underline{A}\underline{X} = \underline{1}_n$ where $\underline{1}_n$ is the $n \times n$ identity matrix. The solution \underline{X} is therefore \underline{A}^{-1} . (See Section 4.2 for a more complete discussion of subroutine LEQTLIC.) Since the real part of M1 contains the characteristic impedance matrix, the real part of the $n \times n$, complex solution matrix, M2, will contain \underline{Z}_C^{-1} . Therefore

<u>Matrix</u>	<u>Array</u>
\underline{Z}_C^{-1}	M2 (real part)
\underline{Z}_C^{-1}	M3 (real part)

Cards 0222 through 0254 read and print the entries in the terminal impedance (admittance) matrices at $x = 0$, \underline{Z}_0 (\underline{Y}_0), and at $x = \underline{L}$, \underline{Z}_L (\underline{Y}_L). These are stored in the $n \times n$, complex arrays as

<u>Thevenin Equivalent</u>	<u>Norton Equivalent</u>	<u>Array</u>
\underline{Z}_0	\underline{Y}_0	Y0
\underline{Z}_L	\underline{Y}_L	YL

Cards 0259 through 0267 interchange the entries in arrays M1 and M2 if the Thevenin equivalent characterization is chosen. Thus

<u>Thevenin Equivalent</u>	<u>Norton Equivalent</u>	<u>Array</u>
\underline{Z}_C^{-1}	\underline{Z}_C	M1
\underline{Z}_C	\underline{Z}_C^{-1}	M2
\underline{Z}_C^{-1}	\underline{Z}_C	M3

Cards 0273 through 0292 compute the quantities:

<u>Thevenin Equivalent</u>	<u>Norton Equivalent</u>	<u>Array</u>
$Z_C + Z_L Z_C^{-1} Z_0$	$Y_L Z_C Y_0 + Z_C^{-1}$	M2

The contents of this array M2 will be retained throughout any frequency iteration so that these matrix products need be computed only once.

Cards 0293 and 0294 compute the phase constant for a frequency of one hertz and its product with the line length:

<u>Quantity</u>	<u>Variable</u>
$k _1 \text{ Hertz} = \frac{2\pi}{(v_0/\sqrt{\mu_r \epsilon_r})}$	BB
$kx _1 \text{ Hertz}$	BBL

To obtain the propagation constant at each frequency, BB is multiplied by the appropriate frequency.

Cards 0300 through 0323 read the input data describing the uniform plane wave if FSO = 1, i.e., E_m , θ_E , θ_p , ϕ_p , and compute the x, y, z components of the electric field and propagation constant (for one Hertz) as shown in (3-12).

Cards 0327 through 0333 read the frequency on the first frequency card and compute the propagation constant, k, kx , $\sin(kx)$, $\cos(kx)$:

<u>Quantity</u>	<u>Variable</u>
k	BETA
k \mathcal{L}	BETAL
sin(k \mathcal{L})	DS
cos(k \mathcal{L})	DC

If uniform plane wave field specification is selected (FSO = 1), cards 0342 through 0351 compute certain preliminary quantities to be used in computing the induced source vectors \underline{M} , \underline{N} , $\underline{E}_t^{(inc)}(0)$, $\underline{E}_t^{(inc)}(\mathcal{L})$. If TYPE 1 structures are selected, cards 0357 through 0370 compute the items in these induced source vectors as:

<u>Vector</u>	<u>Array</u>
\underline{M} (3-16)	V1
\underline{N} (3-17)	V2
$\underline{E}_t^{(inc)}(0)$ (3-22, $\mathcal{L} = 0$)	ETO
$\underline{E}_t^{(inc)}(\mathcal{L})$ (3-22)	ETL

If TYPE 2 structures are selected, the items in the induced source vectors are computed in cards 0375 through 0386 as;

<u>Vector</u>	<u>Array</u>
\underline{M} (3-28)	V1
\underline{N} (3-29)	V2
$\underline{E}_t^{(inc)}(0)$ (3-30, $\mathcal{L} = 0$)	ETO
$\underline{E}_t^{(inc)}(\mathcal{L})$ (3-30)	ETL

If nonuniform field excitation (FS0=2) is selected, cards 0399 through 0542 compute the entries in the induced source vectors \underline{M} , \underline{N} , $\underline{E}_t^{(inc)}(0)$, $\underline{E}_t^{(inc)}(z)$. Cards 0399 through 0439 read the magnitude and phase of the incident electric field at specification points along the reference wire and compute the portions of \underline{M} and \underline{N} along the reference wire if TYPE 1 structures are selected. If TYPE 2 or TYPE 3 structures are selected, this computation is bypassed since for these types of structures it is assumed that the total electric fields tangent to the ground plane and the interior wall of the cylindrical shield are zero. Cards 0444 through 0479 read the magnitude and phase of the incident electric field at specification points along the wires and compute the entries in \underline{M} and \underline{N} for each wire which are stored in arrays V1 and V2, respectively. (The i-th entries contain the results for the i-th wire.) Cards 0484 through 0510 read the magnitude and phase of the incident electric field at specification points along contours in the y, z plane between the reference conductor and the i-th wire at x=0 and compute the entries in $\underline{E}_t^{(inc)}(0)$ which are stored in array ETO. (The electric field is tangent to these contours.) Cards 0515 through 0542 repeat this calculation for x=z and compute the entries in $\underline{E}_t^{(inc)}(z)$ which are stored in array ETL.

Cards 0548 through 0592 form the equations

$$\begin{aligned} & [\cos(kz) \{ \underline{Z}_0 + \underline{Z}_z \} + j \sin(kz) \{ \underline{Z}_C + \underline{Z}_z \underline{Z}_C^{-1} \underline{Z}_0 \}] \underline{I}(0) = \\ & = \underline{M} + j \underline{Z}_z \underline{Z}_C^{-1} \underline{N} = \underline{E}_t^{(inc)}(z) + [\cos(kz) \underline{1}_n + j \sin(kz) \underline{Z}_z \underline{Z}_C^{-1}] \underline{E}_t^{(inc)}(0) \end{aligned}$$

for the Thevenin Equivalent specification (LS0=11,12) or

$$\begin{aligned}
& [\cos(kx) \{ Y_0 + Y_x \} + j \sin(kx) \{ Y_x Z_C^{-1} Y_0 + Z_C^{-1} \}] [-V(0)] = \\
& = Y_x M + j Z_C^{-1} N - Y_x E_t^{(inc)}(x) + [\cos(kx) Y_x + j \sin(kx) Z_C^{-1}] E_t^{(inc)}(0)
\end{aligned}$$

for the Norton Equivalent specification (LS0=21,22). The coefficient matrix is stored in array A and the right-hand side vector of the equations is stored in array B. The arrays V1, V2, ETO, ETL contain

<u>Vector</u>	<u>Array</u>
$M - E_t^{(inc)}(x)$	V1
$Z_C^{-1} E_t^{(inc)}(0)$	ETL
$E_t^{(inc)}(0)$	ETO
N	V2

The main diagonal entries in the array M1 contain $Z_C^{-1} N$

<u>Vector</u>	<u>Array</u>
$Z_C^{-1} N$	M1 (on main diagonal)

Subroutine LEQTL0 is called for the solution of these equations in card 0596 and the solution vector ($I(0)$ for LS0=11,12 or $-V(0)$ for LS0=21,22) is returned in array B.

The terminal currents are computed in cards 0610 through 0641. Cards 0610 through 0618 compute the quantities:

Thevenin EquivalentNorton EquivalentArray

$$Z_0 \underline{I}(0)$$

$$\underline{I}(0) = Y_0 [-V(0)]$$

WA

Cards 0619 through 0631 compute the terminal currents at $x=z$ for the Thevenin Equivalent from

$$\underline{I}(z) = -j Z_C^{-1} \{ \underline{N} + \sin(kz) \overset{(inc)}{\underline{E}_t(0)} \} + [\cos(kz) \underline{1}_n + j \sin(kz) Z_C^{-1} Z_0] \underline{I}(0)$$

and for the Norton Equivalent from

$$\underline{I}(z) = -j Z_C^{-1} \{ \underline{N} + \sin(kz) \overset{(inc)}{\underline{E}_t(0)} \} + [\cos(kz) Y_0 + j \sin(kz) Z_C^{-1}] [-V(0)]$$

4.2 Subroutine LEQT1C

Subroutine LEQT1C is a general subroutine for solving a system of n simultaneous complex equations. The program is a part of the IMSL (International Mathematical and Statistical Library) package [13].

The subroutine solves the system of equations

$$\underline{A} \underline{X} = \underline{B} \quad (4-1)$$

where \underline{A} is an $n \times n$ complex matrix, \underline{B} is an $n \times m$ complex matrix and \underline{X} is an $n \times m$ complex matrix whose columns, \underline{X}_i , are solutions to

$$\underline{A} \underline{X}_i = \underline{B}_i \quad (4-2)$$

where \underline{B}_i is the i -th column of \underline{B} .

The calling statement is

CALL LEQT1C(A,N,N,B,N,M,WA,IER)

where

$$\underline{A} \rightarrow \underline{A}$$
$$\underline{B} \rightarrow \underline{B}$$
$$N \rightarrow n$$
$$M \rightarrow m$$

and WA is a complex working vector of length n. IER is an error parameter which is returned as¹

IER = 128 \rightarrow no solution error

IER = 129 \rightarrow \underline{A} is algorithmically singular [13].

The solution \underline{X} is returned in array B and the contents of array A are destroyed.

Subroutine LEQT1C can be used to find the inverse of an $n \times n$ matrix by computing

$$\underline{A} \underline{X} = \underline{1}_n \quad (4-3)$$

where $\underline{1}_n$ is the $n \times n$ identity matrix. Thus the solution is $\underline{X} = \underline{A}^{-1}$. LEQT1C is used in numerous places to invert real matrices by defining the real part of \underline{A} to be the matrix and the imaginary part to be zero. Upon solution, the real part of \underline{X} is the inverse of the real matrix, \underline{A} .

4.3 Function Subprograms E1 and E2

Function subprograms E1 and E2 are used to evaluate (in closed form) the

¹ The solution error parameter is printed out whenever A is singular. The error is IER-128 so that the solution error will be 1 when \underline{A} is singular.

commonly occurring integrals:¹

$$E1(a,b,k) = \int_a^b x e^{jkx} dx \quad (4-4)$$

$$E2(a,b,k) = \int_a^b e^{jkx} dx \quad (4-5)$$

Function E2 can be evaluated as

$$E2(a,b,k) = \frac{e^{jkb} - e^{jka}}{jk} \quad (4-6)$$

which can be written in an alternate form as

$$\begin{aligned} E2(a,b,k) &= e^{\frac{jk(b+a)}{2}} \left(\frac{e^{\frac{jk(b-a)}{2}} - e^{-\frac{jk(b-a)}{2}}}{jk} \right) \quad (4-7) \\ &= e^{\frac{jk(b+a)}{2}} \left(\frac{e^{\frac{jk(b-a)}{2}} - e^{-\frac{jk(b-a)}{2}}}{jk \frac{(b-a)}{2}} \right) \frac{(b-a)}{2} \\ &= (b-a) \frac{\sin\left\{\frac{k(b-a)}{2}\right\}}{\frac{k(b-a)}{2}} e^{\frac{jk(b+a)}{2}} \end{aligned}$$

This form of E2 is more attractive from a computational standpoint since the $\sin(X)/X$ expression in the final result can be computed quite accurately for small values of the argument whereas the form in (4-6) may suffer from roundoff errors when k is small. In fact, a test was conducted on the IBM 370/165 in double precision by computing the function $\sin(X)/X$ for values of $X=1, .1, .01, .001, \dots, 10^{-78}$ until exponential underflow occurred.

The results converged to the expected value of 1. In fact, for values of X from 10^{-8} to 10^{-78} the result was .9)-----9.
15 digits

¹ Note that these integrals can be analogously viewed as Fourier Transforms. Although this concept is interesting, it provides no significant help since the evaluation of these integrals can be easily obtained in a straightforward manner without resorting to a table of transforms.

The function E2 is computed in the function subprogram E2 with argument list

E2 (A, B, X)

The quantity DIF=B-A is computed as well as the quantities $FA=\frac{X}{2}$ DIF and $FB=\frac{X}{2} (B+A)$. If FA=0, the program evaluates $E2=DIF$ since $\sin(FA)/FA = 1$. If not, the program evaluates $E2=DIF \{ \sin(FA)/FA \} e^{jFB}$.

Finding a more suitable computational form for E1 is considerably more complicated. E1 can be evaluated as

$$E1(a, b, k) = \int_a^b x e^{jkx} dx \quad (4-8)$$

$$= \frac{b e^{jkb} - a e^{jka}}{jk} + \frac{e^{jkb} - e^{jka}}{k^2}$$

This result can be separated into a real and imaginary part, i.e.,

$$E1(a, b, k) = RE + j IM \quad (4-9)$$

where

$$RE = \frac{\cos(kb) + kb \sin(kb) - \cos(ka) - ka \sin(ka)}{k^2} \quad (4-10a)$$

$$IM = \frac{\sin(kb) - kb \cos(kb) - \sin(ka) + ka \cos(ka)}{k^2} \quad (4-10b)$$

The real part can be written as

$$RE = \frac{1}{2} \left[2 \sin\left\{\frac{k(b+a)}{2}\right\} \sin\left\{\frac{k(a-b)}{2}\right\} \right] \quad (4-11)$$

$$\begin{aligned} &+ \frac{b \sin(kb) - a \sin(ka)}{k} \\ &= - \frac{(b^2 - a^2)}{2} \left[\frac{\sin\left\{\frac{k(b+a)}{2}\right\}}{\frac{k(b+a)}{2}} - \frac{\sin\left\{\frac{k(b-a)}{2}\right\}}{\frac{k(b-a)}{2}} \right] \\ &+ b^2 \frac{\sin(kb)}{kb} - a^2 \frac{\sin(ka)}{ka} \end{aligned}$$

Note that this form of the real part of E1 contains only sin(X)/X expressions and can be computed very accurately for small X. Notice that as $k \rightarrow 0$, the real part becomes

$$RE_{k \rightarrow 0} = \frac{b^2 - a^2}{2} \quad (4-12)$$

which is precisely the value of E1(a, b, k) when $k=0$. Therefore the imaginary part of E1 must go to zero as k goes to zero.

The imaginary part of E1 can be written as

$$\begin{aligned} IM &= \frac{\sin(kb) - kb \cos(kb) - \sin(ka) + ka \cos(ka)}{k^2} \\ &= \frac{a \left\{ \cos(ka) - \frac{\sin(ka)}{ka} \right\} - b \left\{ \cos(kb) - \frac{\sin(kb)}{kb} \right\}}{k} \end{aligned} \quad (4-13)$$

Note that as $k \rightarrow 0$ there is a distinct possibility of roundoff error in computing the function

$$\cos(\psi) - \frac{\sin(\psi)}{\psi} \quad (4-14)$$

$$RE = \frac{1}{k^2} \left[2 \sin\left\{ \frac{k(b+a)}{2} \right\} \sin\left\{ \frac{k(a-b)}{2} \right\} \right] \quad (4-11)$$

$$+ \frac{b \sin(kb) - a \sin(ka)}{k}$$

$$= - \frac{(b^2 - a^2)}{2} \left[\frac{\sin\left\{ \frac{k(b+a)}{2} \right\}}{\frac{k(b+a)}{2}} - \frac{\sin\left\{ \frac{k(b-a)}{2} \right\}}{\frac{k(b-a)}{2}} \right]$$

$$+ b^2 \frac{\sin(kb)}{kb} - a^2 \frac{\sin(ka)}{ka}$$

Note that this form of the real part of E1 contains only sin(X)/X expressions and can be computed very accurately for small X. Notice that as $k \rightarrow 0$, the real part becomes

$$RE_{k \rightarrow 0} = \frac{b^2 - a^2}{2} \quad (4-12)$$

which is precisely the value of E1(a, b, k) when $k=0$. Therefore the imaginary part of E1 must go to zero as k goes to zero.

The imaginary part of E1 can be written as

$$IM = \frac{\sin(kb) - kb \cos(kb) - \sin(ka) + ka \cos(ka)}{k^2} \quad (4-13)$$

$$= \frac{a \left\{ \cos(ka) - \frac{\sin(ka)}{ka} \right\} - b \left\{ \cos(kb) - \frac{\sin(kb)}{kb} \right\}}{k}$$

Note that as $k \rightarrow 0$ there is a distinct possibility of roundoff error in computing the function

$$\cos(\theta) - \frac{\sin(\theta)}{\theta} \quad (4-14)$$

converges to 1. Clearly, as $k \rightarrow 0$, the imaginary part of E_1 , IM , converges to zero, as expected.

We will select a value of $|\theta| = .01 \cong .573^\circ$ as the point below which we evaluate a truncated portion of (4-16). The tradeoff here is to select a value of $|\theta|$ small enough so that a truncated portion of (4-16) will not require many terms for sufficient accuracy yet $|\theta|$ is not too small to result in round off error when evaluating (4-13) directly. We have selected the value to be $|\theta| = .01$ and will truncate the series in (4-16) to

$$\left(1 - \frac{\theta^2}{10}\right) \quad (4-17)$$

For $|\theta| = .01$, the $\cos \theta$ and $\frac{\sin \theta}{\theta}$ terms in (4-14) are identical to only 4 digits. This should provide sufficient accuracy to prevent any significant roundoff error in (4-14). In evaluating (4-16), we will obtain accuracy to 10 digits by using the truncation in (4-17). (Note, for $\theta = .01$, $\theta^2/10 = 10^{-5}$, $\theta^4/280 = 3.57 \times 10^{-11}$, $\theta^6/15120 = 6.61 \times 10^{-17}$, and terms with higher powers of θ affect only those digits well to the right of 16 places.) Thus this criterion seems to provide sufficient accuracy while limiting the roundoff error in evaluating IM . Therefore, our result is

$$IM = IMA - IMB \quad (4-18)$$

where

$$\begin{aligned} IMA &= \frac{a}{k} \left\{ \cos(ka) - \frac{\sin(ka)}{ka} \right\} \quad |ka| > .01 \\ &= -\frac{ka^3}{3} \left\{ 1 - \frac{(ka)^2}{10} \right\} \quad |ka| \leq .01 \end{aligned} \quad (4-19a)$$

$$\text{IMB} = \frac{b}{k} \left\{ \cos(kb) - \frac{\sin(kb)}{kb} \right\} \quad |kb| > .01 \quad (4-19b)$$

$$= -\frac{kb^3}{3} \left\{ 1 - \frac{(ka)^2}{10} \right\} \quad |kb| \leq .01$$

$$\text{IMB} = \frac{b}{k} \left\{ \cos(kb) - \frac{\sin(kb)}{kb} \right\} \quad |kb| > .01 \quad (4-19b)$$

$$= -\frac{kb^3}{3} \left\{ 1 - \frac{(ka)^2}{10} \right\} \quad |kb| \leq .01$$

5.1 Transmission Line Structure Characteristics Cards, Group I

WIRE considers $(n+1)$ conductor transmission lines consisting of n wires in a lossless, homogeneous surrounding medium and a reference conductor for the line voltages. The n wires and the reference conductor are considered to be perfect (lossless) conductors. There are three choices for the reference conductor type:

TYPE = 1: The reference conductor is a wire.

TYPE = 2: The reference conductor is an infinite ground plane.

TYPE = 3: The reference conductor is an overall, cylindrical shield.

Cross-sectional views of each of these three structure types are shown in Figure 5-1, 5-2 and 5-3, respectively.

For the TYPE 1 structure shown in Figure 5-1, an arbitrary rectangular coordinate system is established with the center of the coordinate system at the center of the reference conductor. The radii of all $(n+1)$ wires, r_{wi} , as well as the Z and Y coordinates of each of the n wires serve to completely describe the structure. Negative coordinate values must be input as negative data items. For example, Z_i and Y_j in Figure 5-1 would be negative numbers.

For the TYPE 2 structure shown in Figure 5-2, an arbitrary coordinate system is established with the ground plane as the Z axis. The coordinates Y_i and Y_j (positive quantities) define the heights of the i -th and j -th wires, respectively, above the ground plane. The necessary data are the

TYPE = 1

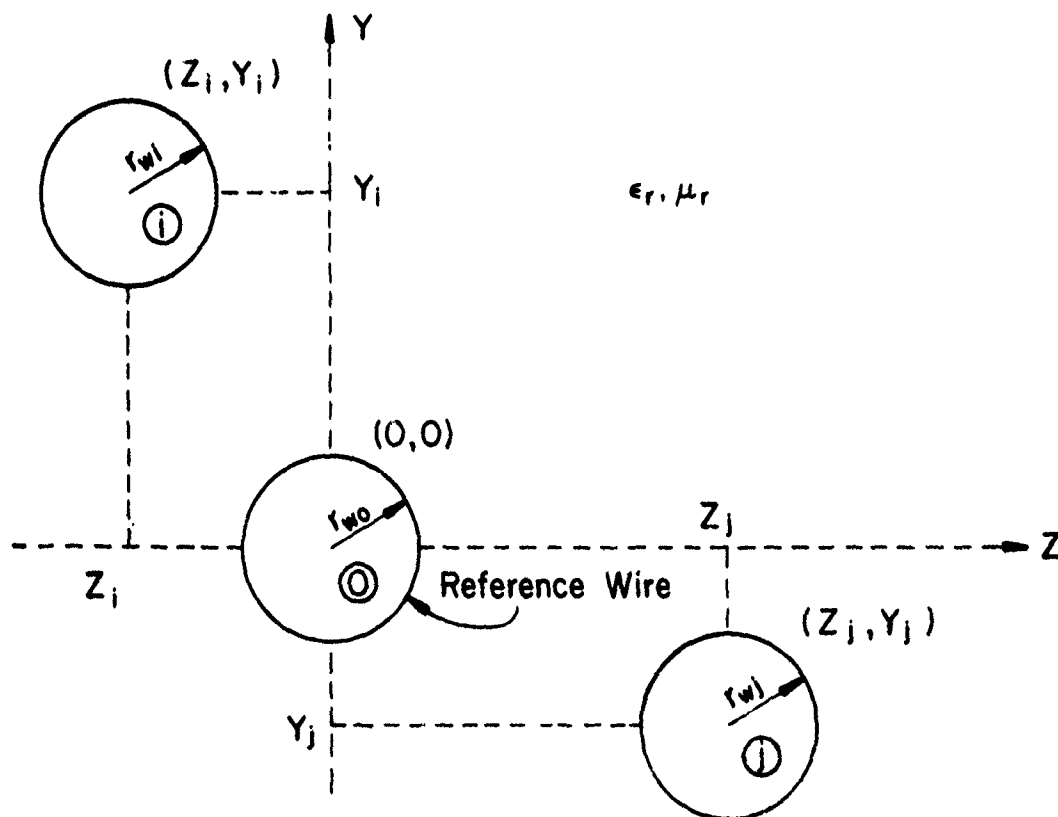


Figure 5-1. The TYPE 1 structure.

TYPE = 2

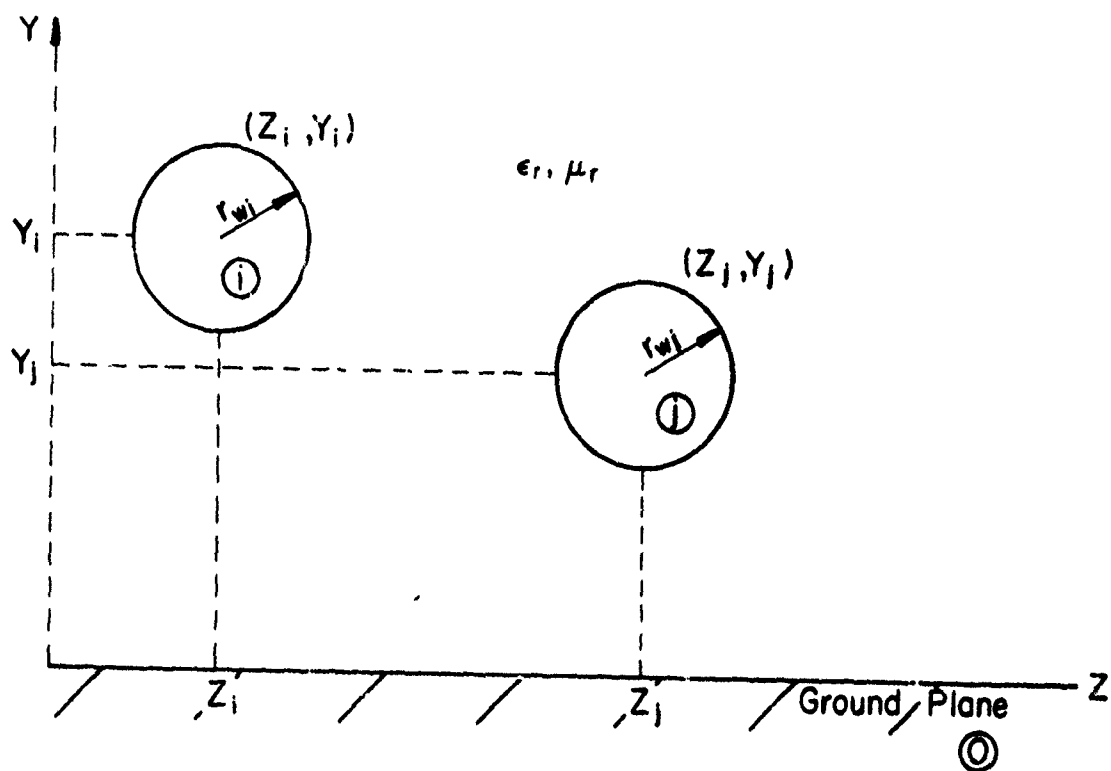


Figure 5-2. The TYPE 2 structure.

TYPE = 3

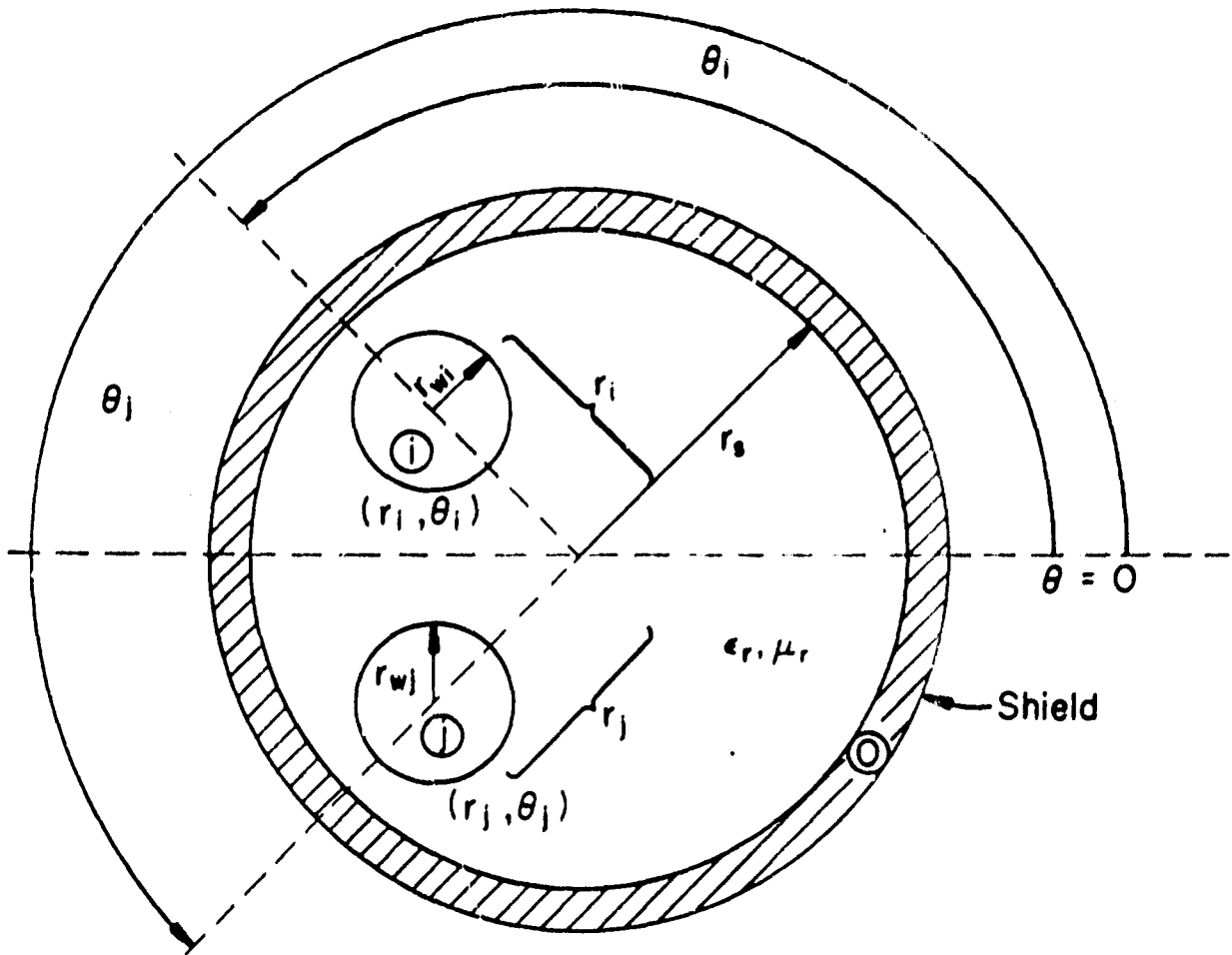


Figure 5-3. The TYPE 3 structure.

Z and Y coordinates and the radius, r_{wi} , of each wire.

For the TYPE 3 structure shown in Figure 5-3, an arbitrary cylindrical coordinate system is established with the center of the coordinate system at the center of the shield. The necessary parameters are the radii of the wires, r_{wi} , the angular position, θ_i , the radial position, r_i , of each wire and the interior radius of the shield, r_s .

The format of the structural characteristics cards, Group I, is shown in TABLE 1. The first card contains the structure TYPE number (1, 2, or 3), the load structure option number, LSO, (11, 12, 21, or 22), the field specification option number, FSO, (1 or 2), the number of wires, n , the relative dielectric constant of the surrounding medium (homogeneous), ϵ_r , the relative permeability of the surrounding medium (homogeneous), μ_r , and the total length of the transmission line, L , (meters). If TYPE 1 or 3 is selected, a second card is required which contains the radius of the reference wire, r_{w0} , (mils) for TYPE 1 structures or the interior radius of the shield, r_s , (meters) for TYPE 3 structures. For TYPE 2 structures, this card is absent. These cards are followed by n cards each of which contain the radii of the n wires, r_{wi} , (mils) and the Z_i and Y_i coordinates of each wire (meters) for TYPE 1 and 2 structures or the angular coordinates r_i (meters) and θ_i (degrees) of the i -th wire for TYPE 3 structures. These n cards must be arranged in the order $i = 1, i = 2, \dots, i = n$.

5.2 The Termination Network Characterization Cards, Group II

This group of cards conveys the terminal characteristics of the termination networks at the ends of the line, $x = 0$ and $x = L$. The termination networks are characterized by either the Thevenin Equivalent or the Norton

TABLE 1

Format of the Structure Characteristics Cards, Group I

<u>Card Group #1 (total = 1):</u>	<u>card column</u>	<u>format</u>
(a) TYPE (1,2,3)	10	I
(b) LOAD STRUCTURE OPTION, LSO, (11,12,21, or 22)	19 - 20	I
(c) FIELD SPECIFICATION OPTION, FSO, (1 or 2)	30	I
(d) n (number of wires)	39 - 40	I
(e) ϵ_r (relative dielectric constant of the surrounding medium)	41 - 50	E
(f) μ_r (relative permeability of the surrounding medium)	51 - 60	E
(g) \mathcal{L} (line length in <u>meters</u>)	61 - 70	E
<u>Card Group #2 (total = 1 if TYPE = 1 or 3)</u> <u>(total = 0 if TYPE = 2)</u>		
(a) TYPE = 1: r_{w0} (radius of reference wire in <u>mils</u>)	6 - 15	E
(b) TYPE = 2: absent		
(c) TYPE = 3: r_s (interior radius of shield in <u>meters</u>)	6 - 15	E
<u>Card Group #3 (total = n)</u>		
(a) r_{w1} (wire radius in <u>mils</u>)	6 - 15	E
(b) Z_1 for TYPE 1 or 2 in <u>meters</u> r_1 for TYPE 3 in <u>meters</u>	21 - 30	E
(c) Y_1 for TYPE 1 or 2 in <u>meters</u> θ_1 for TYPE 3 in <u>degrees</u>	36 - 45	E

Note: Cards in Group #3 must be arranged in the order:
wire 1, wire 2, ..., wire n

Equivalent characterization. These characterizations are of the form

$$\left. \begin{aligned} \underline{V}(0) &= - \underline{Z}_0 \underline{I}(0) \\ \underline{V}(x) &= \underline{Z}_x \underline{I}(x) \end{aligned} \right\} \begin{array}{l} \text{Thevenin} \\ \text{Equivalent} \end{array} \quad (5-1a)$$

$$\left. \begin{aligned} \underline{I}(0) &= - \underline{Y}_0 \underline{V}(0) \\ \underline{I}(x) &= \underline{Y}_x \underline{V}(x) \end{aligned} \right\} \begin{array}{l} \text{Norton} \\ \text{Equivalent} \end{array} \quad (5-1b)$$

(See Volume VII or Chapter II for a more complete discussion of determining the entries in \underline{Z}_0 , \underline{Z}_x , \underline{Y}_0 and \underline{Y}_x [2].) The transmission line consists of n wires which are numbered from 1 to n and a reference conductor for the line voltages. The reference conductor is numbered as the zero (0) conductor. Thus \underline{Z}_0 , \underline{Z}_x , \underline{Y}_0 , \underline{Y}_x are $n \times n$ matrices which are assumed to be symmetric. The n entries in each of the $n \times n$ vectors, $\underline{V}(0)$ and $\underline{V}(x)$, are the line voltages with respect to the reference conductor at $x=0$ and $x=x$, respectively. The n entries in each of the $n \times n$ vectors, $\underline{I}(0)$ and $\underline{I}(x)$, are the line currents at $x=0$ and $x=x$, respectively. The currents at $x=0$ are directed out of the termination networks whereas the currents at $x=x$ are directed into the termination networks. The entries in these four vectors are arranged in the order wire 1, wire 2, ---, wire n .

The impedance or admittance matrices, \underline{Z}_0 and \underline{Z}_x or \underline{Y}_0 and \underline{Y}_x , respectively, may either be "full" in which all entries are not necessarily zero or may be diagonal in which only the entries on the main diagonals are not necessarily zero and the off-diagonal entries are zero. The user may select one of four LOAD STRUCTURE OPTIONS (LSO) for communicating the

entries in the vectors and matrices in (5-1). These are:

- LSO = 11 { Thevenin Equivalent representation;
 diagonal impedance matrices, \underline{Z}_0 and \underline{Z}_1 . }
- LSO = 12 { Thevenin Equivalent representation;
 full impedance matrices, \underline{Z}_0 and \underline{Z}_1 . }
- LSO = 21 { Norton Equivalent representation;
 diagonal admittance matrices, \underline{Y}_0 and \underline{Y}_1 . }
- LSO = 22 { Norton Equivalent representation;
 full admittance matrices, \underline{Y}_0 and \underline{Y}_1 . }

The structure and ordering of the data in Group II are given in Table 2 and can be summarized in the following manner. The first group of cards in Group II, Group II(a), will describe the entries on the main diagonal in $\underline{Y}_0(\underline{Z}_0)$, $\underline{Y}_{0ii}(\underline{Z}_{0ii})$, and $\underline{Y}_1(\underline{Z}_1)$, $\underline{Y}_{1ii}(\underline{Z}_{1ii})$. These cards must be in the order from $i = 1$ to $i = n$. Each of these entries is in general, complex. Therefore two card blocks are assigned for each entry; one for the real part and one for the imaginary part. For example, consider a 4 conductor line (3 wires and a reference conductor). Here n would be 3. Suppose the Thevenin Equivalent characterization is selected, with the following entries in the characterization matrices:

$$\underline{Z}_0 = \begin{bmatrix} 7 + j8 & 0 & 0 \\ 0 & j9 & 0 \\ 0 & 0 & 10 + j11 \end{bmatrix}$$

$$\underline{Z}_1 = \begin{bmatrix} 16 & 0 & 0 \\ 0 & 17 + j18 & 0 \\ 0 & 0 & j19 \end{bmatrix}$$

TABLE 2 (continued)

Format of the Termination Network Characterization Cards, Group IIGroup II(a) (total = n)

		<u>card column</u>	<u>format</u>
$Y_{011}(Z_{011})$	{ real part	1 - 10	E
	{ imaginary part	11 - 20	E
$Y_{111}(Z_{111})$	{ real part	41 - 50	E
	{ imaginary part	51 - 60	E

Note: A total of n cards must be present for an n wire line and must be arranged in the order:

wire 1

wire 2

.

wire n

TABLE 2

Group II(b) $\left\{ \begin{array}{l} \text{total} = n(n-1)/2 \text{ if OPTION} = 12 \text{ or } 22, \\ \text{total} = 0 \text{ if OPTION} = 11 \text{ or } 21 \end{array} \right\}$

	<u>card column</u>	<u>format</u>
$Y_{0ij}(Z_{0ij})$ $\left\{ \begin{array}{l} \text{real part} \\ \text{imaginary part} \end{array} \right.$	1 - 10 11 - 20	E E
$Y_{1ij}(Z_{1ij})$ $\left\{ \begin{array}{l} \text{real part} \\ \text{imaginary part} \end{array} \right.$	41 - 50 51 - 60	E E

Note: If LSO = 12 or 22, a total of $n(n-1)/2$ cards must be present and must follow Group II(a). If LSO = 11 or 21, this card group is omitted.

The cards must be arranged so as to describe the entries in the upper triangle portion of $Y_0(Z_0)$ and $Y_1(Z_1)$ by rows, i.e., the cards must contain the 12 entries, the 13 entries, ---, the 1n entries, the 23 entries, ---, the 2n entries, --- etc. The ordering of the cards is therefore:

wires 1,2

wires 1,3

.

.

wires 1,n

wires 2,3

wires 2,4

.

.

One would have selected LSO=11. The n=3 cards would be arranged (in this order)

Group II(a)	{	7.E0	8.E0	16.E0	0.E0
		0.E0	9.E0	17.E0	18.E0
Card column		10.E0	11.E0	0.E0	19.E0
		↑ 10	↑ 20	↑ 50	↑ 60

If the terminal impedance matrices were not diagonal, e.g., LSO=12 is selected, then $n(n-1)/2$ additional cards, Group II(b), would follow the above n cards comprising Group II(a). These cards describe the entries in the upper triangle portion of the termination impedance or admittance matrices by rows. Suppose the networks are characterized by the Z_0 and Z_L matrices:

$$Z_0 = \begin{bmatrix} 7 + j8 & 20 + j21 & 22 + j23 \\ 20 + j21 & j9 & 24 + j25 \\ 22 + j23 & 24 + j25 & 10 + j11 \end{bmatrix}$$

$$Z_L = \begin{bmatrix} 16 & 26 + j27 & 28 \\ 26 + j27 & 17 + j18 & j29 \\ 28 & j29 & j19 \end{bmatrix}$$

The following $n(n-1)/2 = 3$ cards must follow the above 3 cards in the order of the 12 entries first, the 13 entries next and then the 23 entries:

Group II(b)	20.E0	21.E0	26.E0	27.E0
	22.E0	23.E0	28.E0	0.E0
	24.E0	25.E0	0.E0	29.E0
Card column	↑ 10	↑ 20	↑ 50	↑ 60

5.3 The Field Specification Cards, Group III

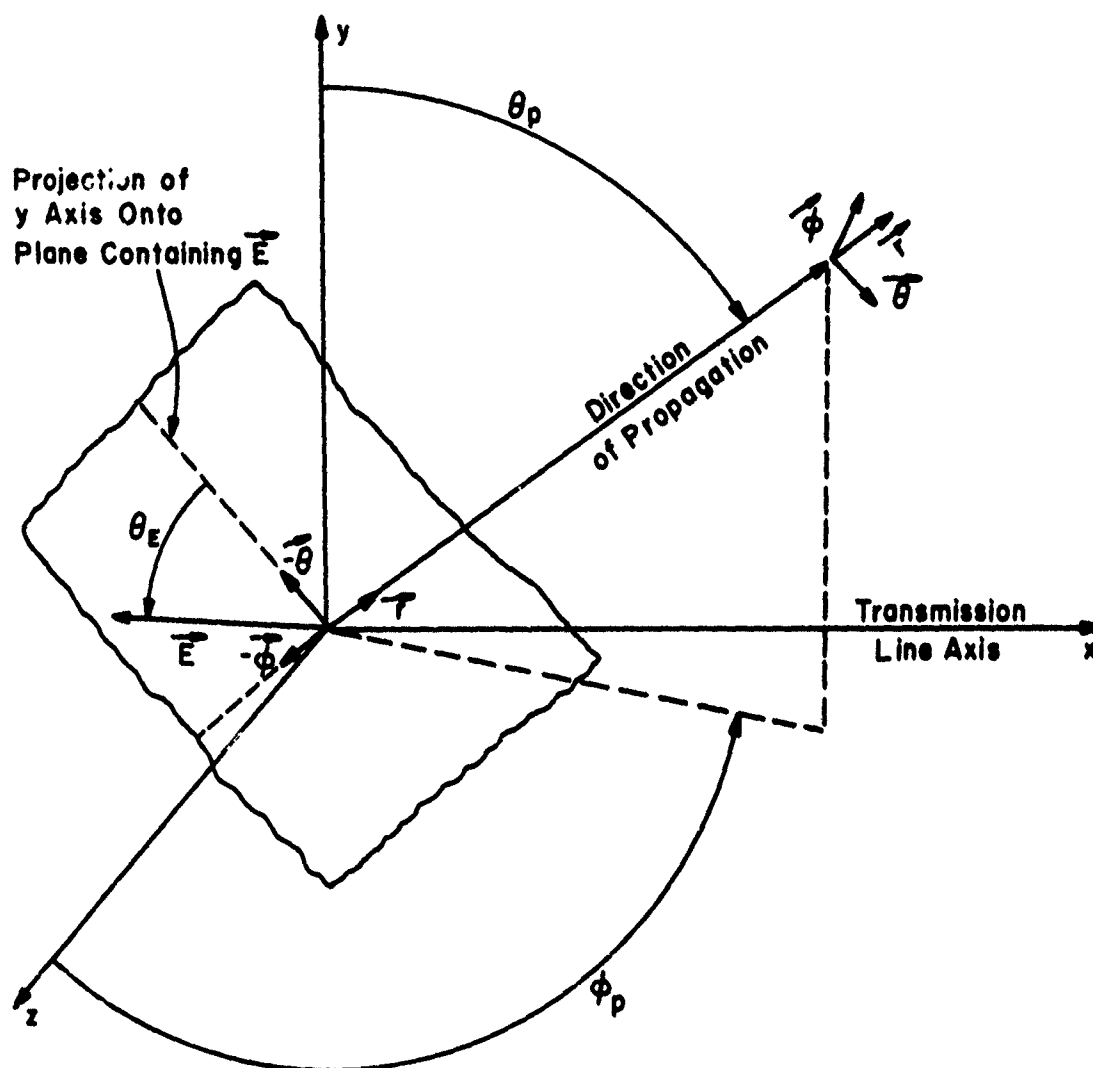
There are two Field Specification Options (FSO) for specifying the form of the excitation field:

FSO = 1 { Uniform plane wave illumination
 of the line (TYPE 1 or TYPE 2 structures
 only) }

FSO = 2 { Nonuniform field illumination of
 the line (all structure types) }

5.3.1 Uniform Plane Wave Illumination, FSO=1

For uniform plane wave illumination of the line, FSO=1, the format of the data cards is shown in Table 3 and consists of two card groups. Card Group #1 consists of one card containing the magnitude of the electric field intensity vector, E_m , the angle between this vector and the projection of the y axis on the plane containing \vec{E} (this plane is perpendicular to the propagation direction), the angle between the y axis and the direction of propagation, and the angle between the z axis and the projection of the propagation vector onto the x,z plane. (See Figure 5-4.) The x coordinate is parallel to the n wires and reference conductor, and the y,z plane forms the cross-section of the line. The origin of the coordinate system,



Note: Zero Phase Reference Taken at $x=0, y=0, z=0$.

Figure 5-4. Definition of the uniform plane wave parameters.

TABLE 3

Format of the Field Specification Cards, Group III, for Uniform Plane Wave

Illumination, FSO=1, (See Figure 5-4)

<u>Card Group #1 (total = 1):</u>	<u>card column</u>	<u>format</u>
(a) E_m (magnitude of the electric field intensity vector in <u>volts/meter</u>)	1 - 10	E
(b) θ_E (angle of electric field intensity vector in <u>degrees</u>)	16 - 25	E
(c) θ_P (angle of propagation direction from y axis in <u>degrees</u>)	31 - 40	E
(d) ϕ_P (angle of projection of propagation direction on the x,z plane from z axis in <u>degrees</u>)	46 - 55	E
 <u>Card Group #2 (total = unlimited)</u>		
(a) Frequency of incident wave in <u>Hertz</u>	1 - 10	E

$x=0, y=0, z=0$, is fixed by the user according to the specification on Card Group I. (See Figure 5-1 and 5-2.) The zero phase of the incident wave is taken at the origin of this coordinate system.

Card Group #2 for $FSO=1$ consists of an unlimited number of cards with each frequency of the incident wave on each card. More than one frequency card may be included in this frequency card group. The program will process the data provided by Groups I and II and the wave orientation data in Group #1 in Table 3 and compute the response at the frequency on the first frequency card. It will then recompute the response at each frequency on the remaining frequency cards. The program assumes that the data on card Groups I and II and the wave orientation data in Group #1 in Table 3 are to be used for all the remaining frequencies. If this is not intended by the user, then one may only run the program for one frequency at a time. This feature, however, can be quite useful. If the termination networks are purely resistive, i.e., frequency independent, then one may use as many frequency cards as desired in Group #2 and the program will compute the response of the line at each frequency without the necessity for the user to input the data in Groups I and II and the wave orientation data for each additional frequency. Many of the time-consuming calculations which are independent of frequency need to be computed only once so that this mode of useage will save considerable computation time when the response at many frequencies is desired. If, however, the termination network characteristics (in Group II) are complex-valued (which implies frequency dependent), one must run the program for only one frequency at a time.

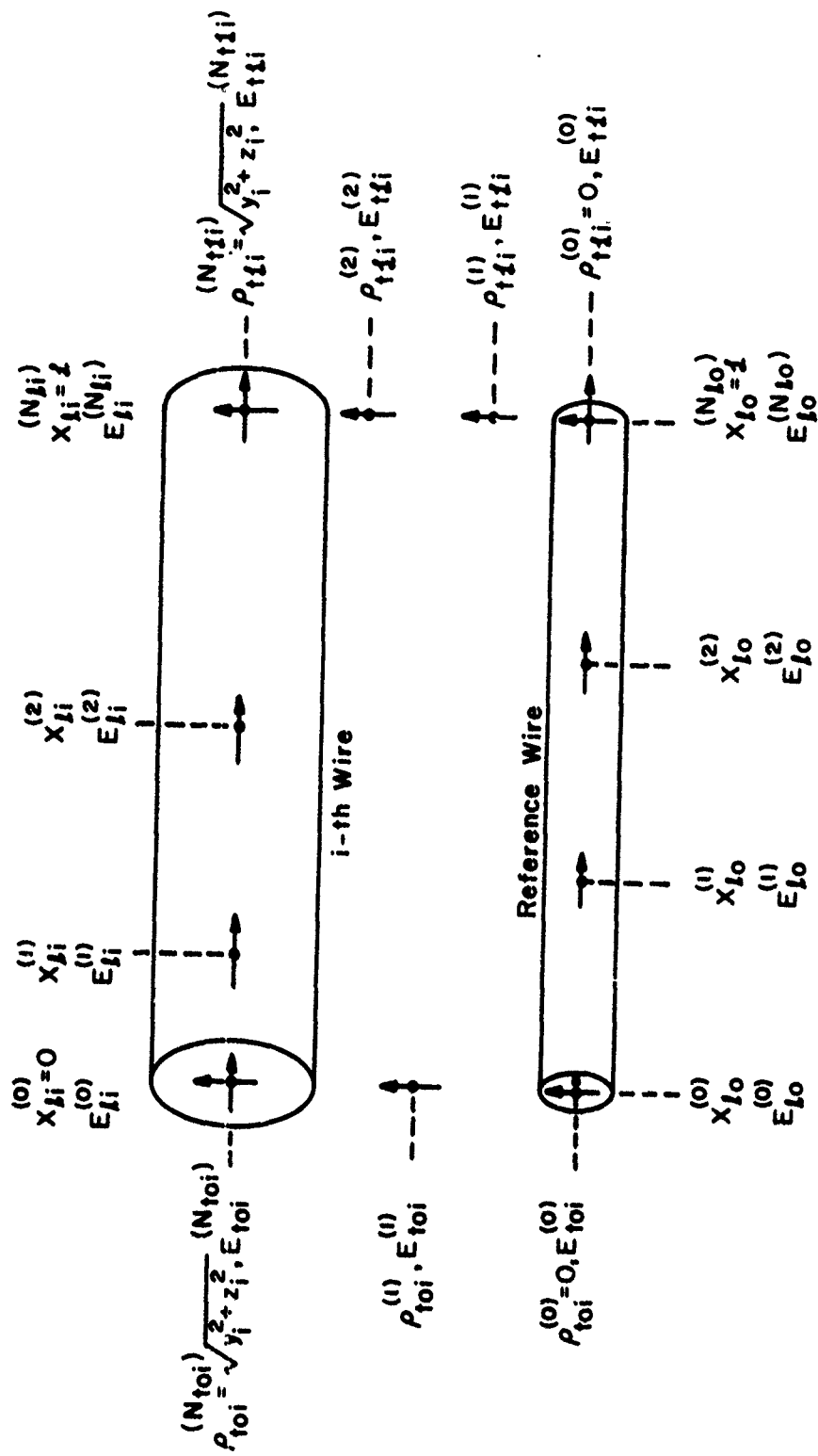
5.3.2 Nonuniform Field Illumination, $FSO=2$

The format of the Field Specification Cards, Group III, for nonuniform

field illumination, $FSO=2$, is shown in Table 4. The first card group, Group #1, consists of one and only one card which contains the frequency of the field.

The remaining cards contain the values of the longitudinal electric field (magnitude and phase) along the n wires (and reference wire for TYPE 1 structures) which are directed in the $+x$ direction, and the transverse electric field along straight line contours joining the i -th wire and the reference conductor at $x=0$ and $x=L$. The directions of the transverse field at these specification points are tangent to the contours and directed from the reference conductor to the i -th wire. For TYPE 1 structures, the precise location and orientation of the transverse field specification contours should be clear. For TYPE 2 structures, the transverse field specification contours should comprise the shortest path in the y,z plane between the ground plane and the i -th wire, i.e., it should be perpendicular to the ground plane or directly beneath the i -th wire. For TYPE 3 structures, the transverse field specification contours should comprise the shortest path in the y,z plane between the interior wall of the cylindrical shield and the i -th wire. (See Figure 5-5.)

The ordering of the card Groups #2-#9 is quite logical but somewhat involved to describe. The philosophy of the ordering is as follows. If TYPE 1 structures are selected, we first describe the longitudinal electric field (magnitude and phase) along the reference wire at $(N_{10}+1)$ specification points. This is done in Groups #2 and #3. (If TYPE = 2 or 3, Groups #2 and #3 are omitted and it is assumed that the net incident electric field is obtained, i.e., the electric field tangent to the ground plane (TYPE=2) and the interior of the cylindrical shield (TYPE=3) is zero.) In Group #2,



(a)

Figure 5-5. Nonuniform field specification for TYPE 1 structures.

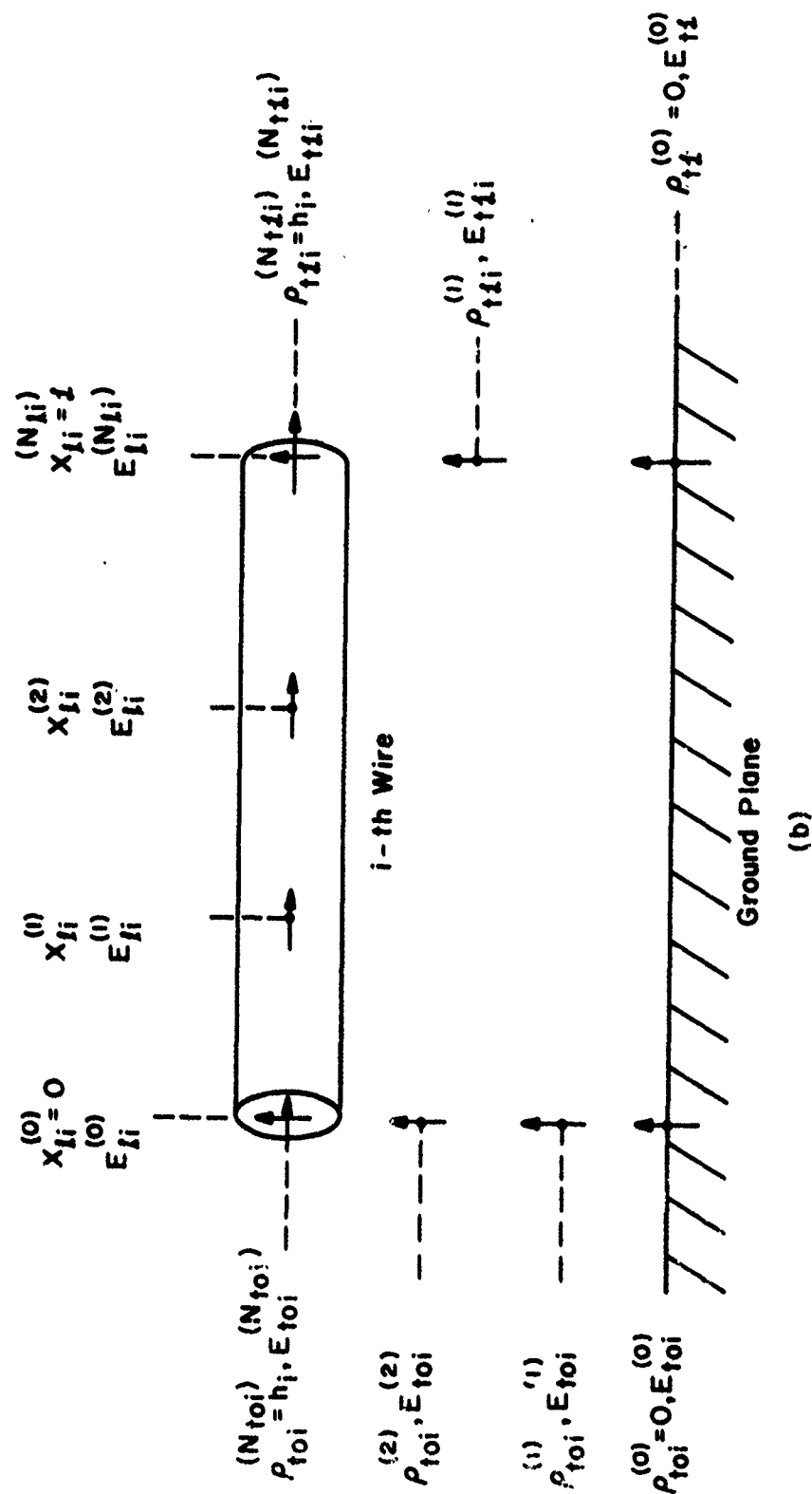


Figure 5-5. Nonuniform field specification for TYP 2 structures.

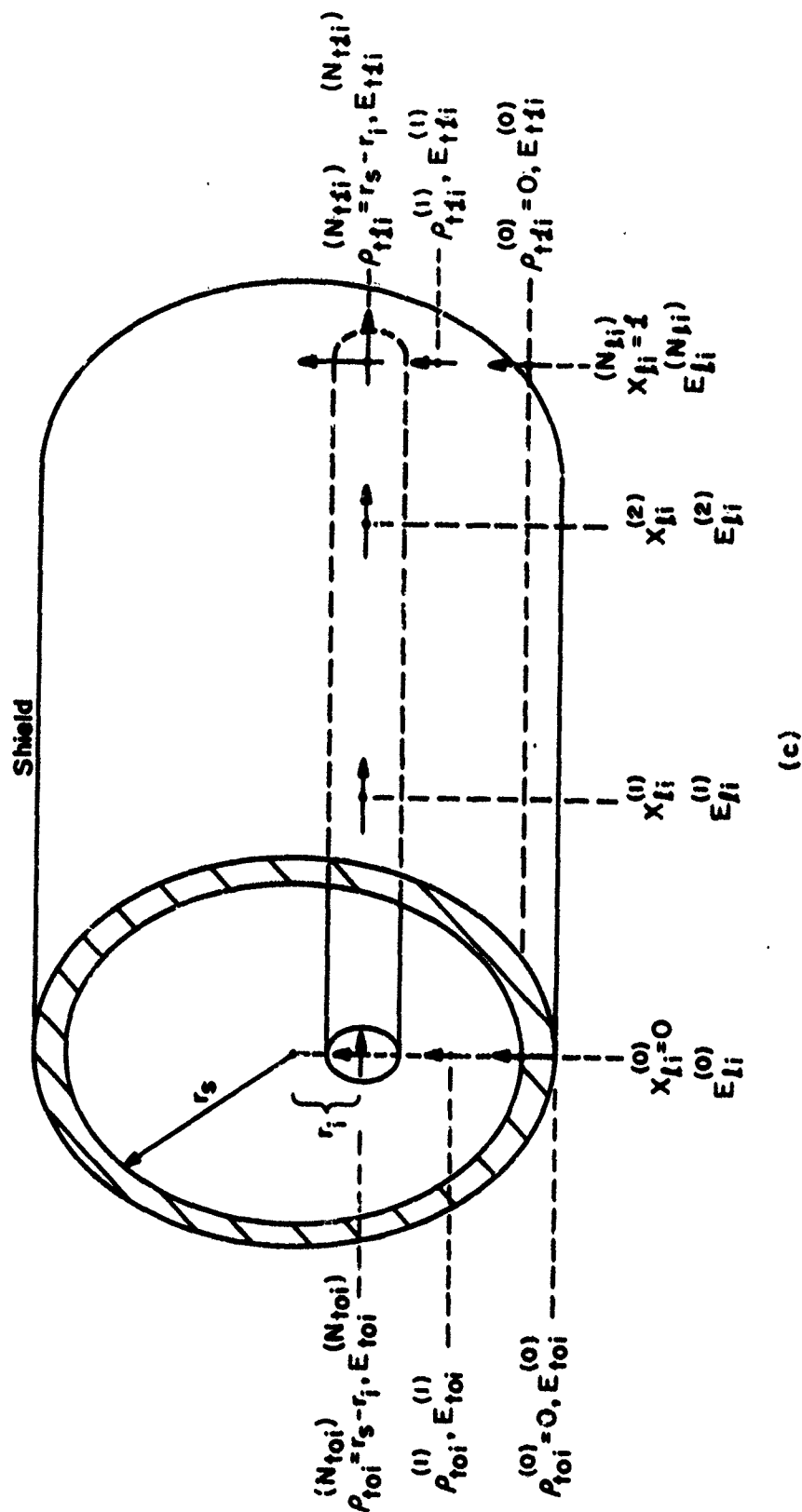


Figure 5-5. Nonuniform field specification for TYPE 3 structures.

we communicate the number N_{l0} and the magnitude and phase of the field at the first specification point at $x=0$. In Group #3, we compute the locations of the remaining N_{l0} specification points and the magnitude and phase of the field at each of these specification points. The cards in this group must be arranged sequentially so that each specification point is located to the right of the previous point. In addition, the last $(N_{l0}+1)$ specification point must be equal to the line length, l , i.e., located at $x=l$.

The remaining card groups (#4-#9) use the same philosophy as Group #2 and #3 and describe, for each wire from 1 to n , the quantities (in this order):

- (1) longitudinal field on i -th wire,
- (2) transverse field at $x=0$ between the reference conductor and i -th wire, and
- (3) transverse field at $x=l$ between the reference conductor and i -th wire.

For example, after Group #3 we must have Groups #4-#9 for wire 1, Groups #4-#9 for wire 2, ---, Groups #4-#9 for wire n . This is illustrated in Figure 5-6.

It should be noted that the incident electric field which one specifies in Card Groups #2-#9 is the incident field with the n wires (and the reference wire for TYPE 1 structures) removed. This is inherent in the derivations of Chapter II. Thus one specifies the longitudinal electric field at points along the positions of each wire.

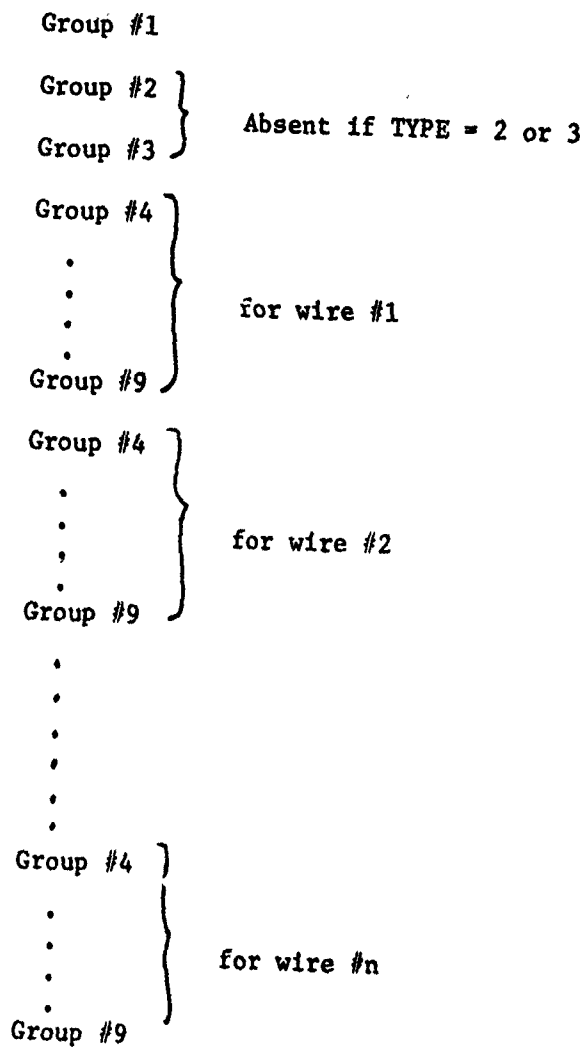


Figure 5-6. Ordering of Card Groups in Group III for FSO = 2.

TABLE 4 (continued)

Format of the Field Specification Cards, Group III, for Nonuniform Fields,

FSO = 2 (see Figure 5-5)

<u>Card Group #1 (total = 1):</u>	<u>card column</u>	<u>format</u>
(a) <u>Frequency of incident field in Hertz</u>	1 - 10	E
<u>Card Group #2 (total = 1 if TYPE = 1 absent if TYPE = 2 or 3)</u>		
(a) N_{20} (number of field specification points along reference wire = $N_{20}+1$)	1 - 10	I
(b) $ E_{20}^{(0)} $ (magnitude of electric field along reference wire in +x direction at $x=0$ in <u>volts/meter</u>)	21 - 30	E
(c) $\angle E_{20}^{(0)}$ (phase of electric field along reference wire at $x=0$ in <u>degrees</u>)	41 - 50	E
<u>Card Group #3 (total = N_{20} if TYPE=1 absent if TYPE = 2 or 3)</u>		
(a) $x_{20}^{(m)}$ (electric field specification point along reference wire in <u>meters</u>)	1 - 10	E
(b) $ E_{20}^{(m)} $ (magnitude of electric field at $x_{20}^{(m)}$ in +x direction in <u>volts/meter</u>)	21 - 30	E
(c) $\angle E_{20}^{(m)}$ (phase of electric field at $x_{20}^{(m)}$ in <u>degrees</u>)	41 - 50	E

Note: $m = 1, 2, \dots, N_{20}$ and $x_{20}^{(N_{20})}$ (the last specification point) must equal the line length, l . The cards in Group #3 must be arranged such that

$$x_{20}^{(m)} < x_{20}^{(m+1)}$$

TABLE 4 (continued)

<u>Card Group #4 (total = 1)</u>	<u>card column</u>	<u>format</u>
(a) N_{li} (number of field specification points along i-th wire = $N_{li}+1$)	1 - 10	I
(b) $ E_{li}^{(0)} $ (magnitude of electric field in +x direction along i-th wire at x=0 in <u>volts/meter</u>)	21 - 30	E
(c) $\angle E_{li}^{(0)}$ (phase of electric field along i-th wire at x=0 in <u>degrees</u>)	41 - 50	E

Card Group #5 (total = N_{li})

(a) $x_{li}^{(m)}$ (electric field specification point along i-th wire in <u>meters</u>)	1 - 10	E
(b) $ E_{li}^{(m)} $ (magnitude of electric field at $x_{li}^{(m)}$ in +x direction in <u>volts/meter</u>)	21 - 30	E
(c) $\angle E_{li}^{(m)}$ (phase of electric field at $x_{li}^{(m)}$ in <u>degrees</u>)	41 - 50	E

Note: $m = 1, 2, \dots, N_{li}$ and $x_{li}^{(N_{li})}$ (the last specification point) must equal the line length, l . The cards in Group #5 must be arranged such that

$$x_{li}^{(m)} < x_{li}^{(m+1)}$$

Card Group #6 (total = 1)

(a) N_{t0i} (number of field specification points at x=0 on straight line contour between reference conductor and i-th wire = $N_{t0i}+1$)	1 - 10	I
(b) $ E_{t0i}^{(0)} $ (magnitude of electric field on contour at x=0 in <u>volts/meter</u>)	21 - 30	E

TABLE 4 (continued)

<u>Card Group #6 (total = 1) continued</u>	<u>card column</u>	<u>format</u>
(c) $\angle E_{t0i}^{(0)}$ (phase of electric field on contour at $x=0$ in <u>degrees</u>)	41 - 50	E
<u>Card Group #7 (total = N_{t0i})</u>		
(a) $\rho_{t0i}^{(m)}$ (electric field specification point on contour between reference conductor and i -th wire at $x=0$ in <u>meters</u>)	1 - 10	E
(b) $ E_{t0i}^{(m)} $ (magnitude of electric field on contour at $x=0$ at $\rho_{t0i}^{(m)}$ in <u>volts/meter</u>)	21 - 30	E
(c) $\angle E_{t0i}^{(m)}$ (phase of electric field on contour at $\rho_{t0i}^{(m)}$ in <u>degrees</u>)	41 - 50	E

Note: $m = 1, 2, \dots, N_{t0i}$ and $\rho_{t0i}^{(N_{t0i})}$ (the last specification point) must be located at the center of the i -th wire at $x=0$. The cards in Group #7 must be arranged such that

$$\rho_{t0i}^{(m)} < \rho_{t0i}^{(m+1)}$$

Card Group #8 (total = 1)

(a) N_{tzi} (number of field specification points on straight line contour at $x=z$ between reference conductor and i -th wire = $N_{tzi} + 1$)	1 - 10	I
(b) $ E_{tzi}^{(0)} $ (magnitude of electric field on contour at $x=z$ in <u>volts/meter</u>)	21 - 30	E
(c) $\angle E_{tzi}^{(0)}$ (phase of electric field on contour at $x=z$ in <u>degrees</u>)	41 - 50	E

Card Group #9 (total = N_{tzi})		TABLE 4 (continued)	<u>card column</u>	<u>format</u>
(a)	$\rho_{tzi}^{(m)}$ (electric field specification point on contour between reference conductor and i-th wire at $x=\lambda$ in <u>meters</u>)		1 - 10	E
(b)	$ E_{tzi}^{(m)} $ (magnitude of electric field on contour at $x=\lambda$ at $\rho_{tzi}^{(m)}$ in <u>volts/meter</u>)		21 - 30	E
(c)	$\angle E_{tzi}^{(m)}$ (phase of electric field on contour at $x=\lambda$ at $\rho_{tzi}^{(m)}$ in <u>degrees</u>)		41 - 50	E

Note: $m=1,2,---,N_{tzi}$ and $\rho_{tzi}^{(N_{tzi})}$ (the last specification point) must be located at the center of the i-th wire at $x=\lambda$. The cards in Group #9 must be arranged such that

$$\rho_{tzi}^{(m)} < \rho_{tzi}^{(m+1)}$$

Note: Card Groups #4 - 9 must be repeated for wires 1 to n and arranged sequentially for wire 1, wire 2, ---, wire n.

VI. EXAMPLES OF PROGRAM USAGE

Several examples of program usage will be described in this Chapter. These examples will serve to illustrate preparation of the data input cards as well as provide partial checks on the proper functioning of the program. The data input cards as well as the computed results will be shown for each example.

6.1 Example I

In this Chapter we will show an example of a two wire line above a ground plane (TYPE=2) illuminated by a uniform plane wave (FS0=1). The solution for the terminal currents for a 1 volt/meter field with several angles of incidence will be shown. The image problem will also be considered by replacing the ground plane with the images of the wires resulting in a four wire line (N=3,TYPE=1). The corresponding currents in the wires for the problem of two wires above a ground plane should be twice those for the image problem.

6.1.1 Two Wires Above a Ground Plane

The problem considered here is shown in Figure 6-1. Wire #1 has a radius of 30 mils and is 5 cm above the ground plane. Wire #2 has a radius of 10 mils and is 2 cm above the ground plane. The two wires are separated horizontally by 4 cm. The cross-section of wire #1 is located at $y=5$ cm, $z=0$. The cross-section of wire #2 is located at $y=2$ cm, $z=4$ cm. The line length is 5m and $\mu_r=1$, $\epsilon_r=1$ (a logical choice although any ϵ_r and μ_r may be used in the program). Each wire is terminated with a single impedance (in this case purely resistive) between the wire and the ground plane. Clearly one may chose the load structure option of LS0=11 with the

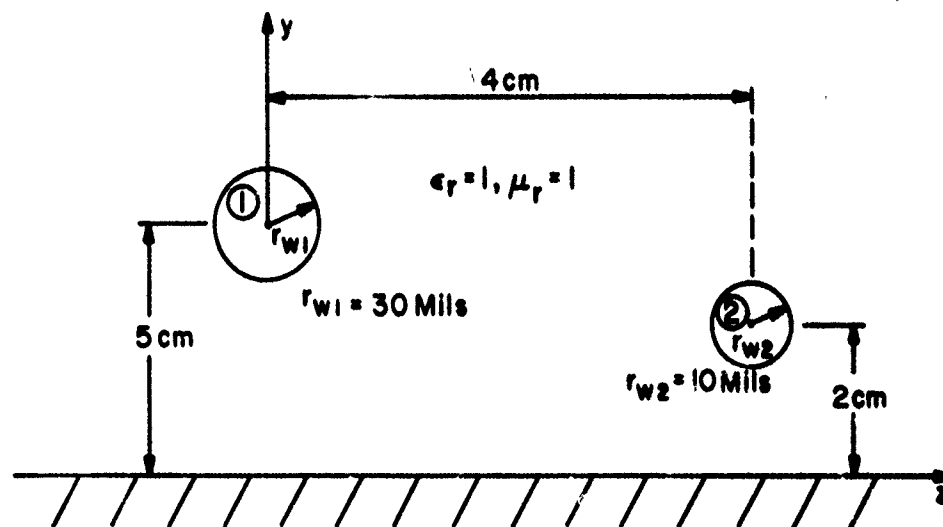
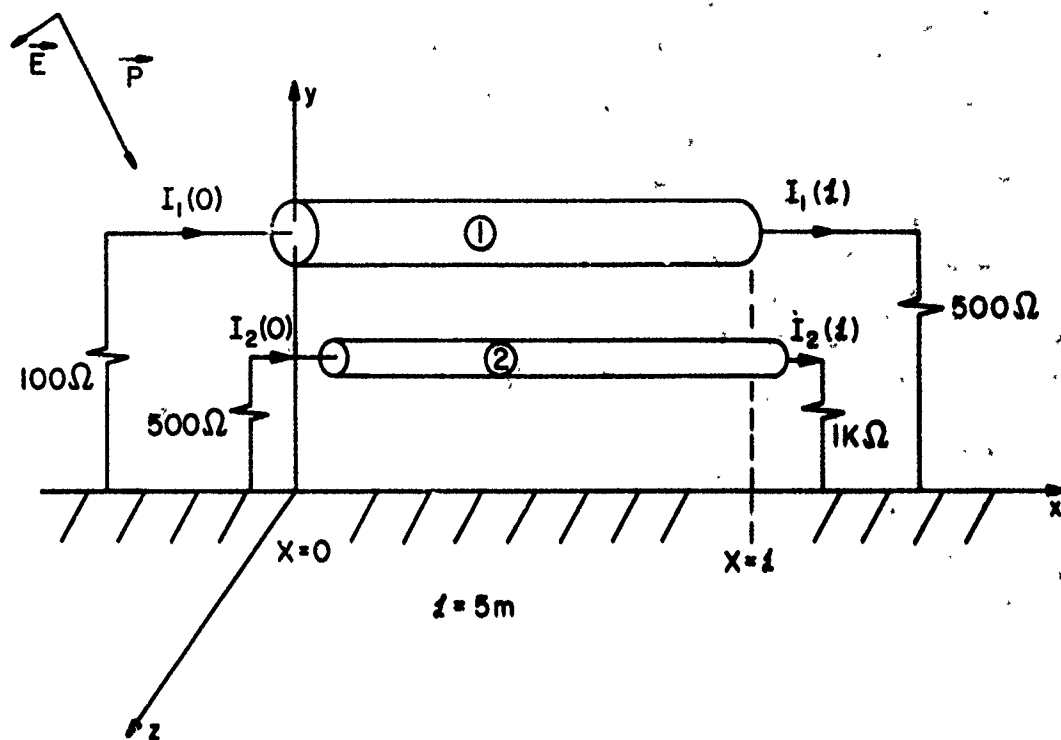


Figure 6-1. Example I.

terminal impedance matrices

$$\underline{Z}_0 = \begin{bmatrix} 100 & 0 \\ 0 & 500 \end{bmatrix} \quad \underline{Z}_L = \begin{bmatrix} 500 & 0 \\ 0 & 1000 \end{bmatrix}$$

Three orientations of the incident field will be considered:

- (a) $E_m = 1 \text{ V/m}$, $\theta_E = 30^\circ$, $\theta_p = 150^\circ$, $\phi_p = 40^\circ$
- (b) $E_m = 1 \text{ V/m}$, $\theta_E = 0^\circ$, $\theta_p = 90^\circ$, $\phi_p = 90^\circ$
- (c) $E_m = 1 \text{ V/m}$, $\theta_E = 0^\circ$, $\theta_p = 180^\circ$, $\phi_p = 90^\circ$

Notice that case (b) has the wave propagating in the +x direction along the line axis with \vec{E} in the +y direction, i.e.,

$$\vec{E} = e^{-jkx} \hat{y}$$

Case (c) has the wave propagating broadside to the line (in the -y direction) with \vec{E} in the +x direction, i.e.,

$$\vec{E} = e^{jky} \hat{x}$$

Four frequencies of excitation will be investigated:

1 MHz, 10 MHz, 100 MHz, 1GHz
(1E6), (1E7), (1E8), (1E9)

and since the loads are resistive, the frequency iteration feature of the program can be used by simply placing all four frequency cards as a group at the end of the program.

The reason for using these frequencies is that for 1 MHz, the cross-sectional dimensions of the line are electrically small. For 1 GHz, they are not. This will serve to further illustrate why we require that the cross-sectional dimensions of the line be electrically small. To illustrate this let us arbitrarily select the distance between wire #1 and the image of wire #1 to be the "largest" cross-sectional dimension of the line. This distance

is given by

$$d_{\max} = 10 \text{ cm}$$

The quantities kd_{\max} (in degrees) at the above four frequencies are:

<u>frequency</u>	<u>kd_{\max} (degrees)</u>	<u>d_{\max}/λ</u>
1 E6	.12	.000334
1 E7	1.2	.003336
1 E8	12.0	.033356
1 E9	120.0	.333564

Notice that for the frequency of 1 E9, the cross-sectional dimensions of the line are certainly not electrically small. For the other frequencies, they probably are.

The input data cards for the angles of incidence in (a), (b) and (c) are shown in Figure 6-2(a), (b) and (c), respectively. The results are shown in Figure 6-3.

6.1.2 Two Wires Above a Ground Plane by the Method of Images

Here we solve the problem considered in the previous section by the method of images. The image problem becomes a four wire problem ($N=3$, TYPE=1) as shown in Figure 6-4. Here we choose (arbitrarily) the image wire of wire #1 in the previous problem as the reference wire. The various wire radii, and coordinates are:

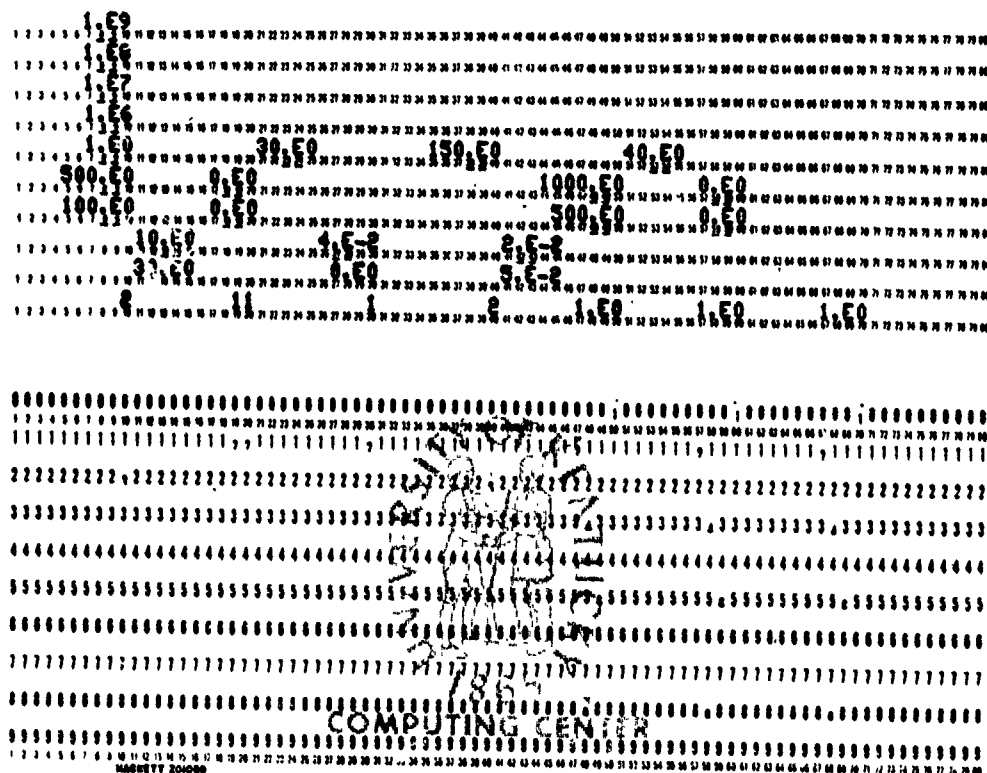


Figure 6-2(a). Data cards for the problem in Figure 6-1
with $E_m = 1V/m$, $\theta_E = 30^\circ$, $\theta_p = 150^\circ$, $\phi_p = 40^\circ$.

Figure 6-2(b). Data cards for the problem in Figure 6-1 with $E_m = 1$ V/m, $\theta_E = 0^\circ$, $\theta_p = 90^\circ$, $\phi_p = 90^\circ$.

Figure 6-2(c). Data cards for the problem in Figure 6-1 with $E_m = 1$ V/m, $\Theta_E = 0^\circ$, $\Theta_p = 180^\circ$, $\phi_p = 90^\circ$.

$$(a) \quad E_m = 1 \text{ V/m}, \theta_E = 30, \theta_p = 150, \phi_p = 40$$

$$\underline{f = 1 \text{ MHz}}$$

$$\begin{aligned} I_1(0) &= 3.298\text{E-}6 \angle 89.41 & I_1(z) &= 2.837\text{E-}7 \angle 86.22 \\ I_2(0) &= 7.336\text{E-}7 \angle 88.68 & I_2(z) &= 1.782\text{E-}7 \angle -91.58 \end{aligned}$$

$$\underline{f = 10 \text{ MHz}}$$

$$\begin{aligned} I_1(0) &= 3.315\text{E-}5 \angle 84.07 & I_1(z) &= 3.116\text{E-}6 \angle 53.64 \\ I_2(0) &= 7.191\text{E-}6 \angle 76.96 & I_2(z) &= 1.732\text{E-}6 \angle -105.55 \end{aligned}$$

$$\underline{f = 100 \text{ MHz}}$$

$$\begin{aligned} I_1(0) &= 2.495\text{E-}4 \angle -1.650 & I_1(z) &= 1.024\text{E-}4 \angle -142.78 \\ I_2(0) &= 3.450\text{E-}5 \angle 4.802 & I_2(z) &= 1.101\text{E-}5 \angle -177.51 \end{aligned}$$

$$\underline{f = 1 \text{ GHz}}$$

$$\begin{aligned} I_1(0) &= 2.089\text{E-}4 \angle 3.521 & I_1(z) &= 9.315\text{E-}5 \angle -139.76 \\ I_2(0) &= 3.317\text{E-}5 \angle -10.474 & I_2(z) &= 1.089\text{E-}5 \angle 172.48 \end{aligned}$$

Figure 6-3. The problem in Figure 6-1.

(b) $E_m = 1 \text{ V/m}$, $\theta_E = 0$, $\theta_p = 90$, $\phi_p = 90$

$f = 1 \text{ MHz}$

$$I_1(0) = 9.294\text{E-}6 \angle 89.09$$

$$I_2(0) = 1.963\text{E-}6 \angle 88.44$$

$$I_1(z) = 2.333\text{E-}6 \angle 87.87$$

$$I_2(z) = 1.432\text{E-}7 \angle -93.46$$

$f = 10 \text{ MHz}$

$$I_1(0) = 9.316\text{E-}5 \angle 80.85$$

$$I_2(0) = 1.920\text{E-}5 \angle 74.56$$

$$I_1(z) = 2.336\text{E-}5 \angle 68.63$$

$$I_2(z) = 1.383\text{E-}6 \angle -124.51$$

$f = 100 \text{ MHz}$

$$I_1(0) = 4.638\text{E-}4 \angle -37.08$$

$$I_2(0) = 6.602\text{E-}5 \angle -24.28$$

$$I_1(z) = 1.150\text{E-}4 \angle -156.86$$

$$I_2(z) = 3.021\text{E-}6 \angle 70.15$$

$f = 1 \text{ GHz}$

$$I_1(0) = 4.587\text{E-}4 \angle -37.91$$

$$I_2(0) = 6.567\text{E-}5 \angle -24.92$$

$$I_1(z) = 1.138\text{E-}4 \angle -158.43$$

$$I_2(z) = 3.054\text{E-}6 \angle 68.47$$

Figure 6-3. The problem in Figure 6-1.

(c) $E_m = 1 \text{ V/m}$, $\theta_E = 0$, $\theta_p = 180$, $\phi_p = 90$

$f = 1 \text{ MHz}$

$$I_1(0) = 3.494\text{E-}6 \text{ } \underline{90.08}$$

$$I_1(\chi) = 3.493\text{E-}6 \text{ } \underline{89.27}$$

$$I_2(0) = 5.590\text{E-}7 \text{ } \underline{89.95}$$

$$I_2(\chi) = 5.589\text{E-}7 \text{ } \underline{89.44}$$

$f = 10 \text{ MHz}$

$$I_1(0) = 3.553\text{E-}5 \text{ } \underline{90.71}$$

$$I_1(\chi) = 3.500\text{E-}5 \text{ } \underline{82.65}$$

$$I_2(0) = 5.656\text{E-}6 \text{ } \underline{89.41}$$

$$I_2(\chi) = 5.581\text{E-}6 \text{ } \underline{84.45}$$

$f = 100 \text{ MHz}$

$$I_1(0) = 5.316\text{E-}4 \text{ } \underline{33.83}$$

$$I_1(\chi) = 1.988\text{E-}4 \text{ } \underline{-6.817}$$

$$I_2(0) = 8.392\text{E-}5 \text{ } \underline{52.80}$$

$$I_2(\chi) = 4.634\text{E-}5 \text{ } \underline{33.77}$$

$f = 1 \text{ GHz}$

$$I_1(0) = 4.402\text{E-}4 \text{ } \underline{33.09}$$

$$I_1(\chi) = 1.632\text{E-}4 \text{ } \underline{-7.429}$$

$$I_2(0) = 8.585\text{E-}5 \text{ } \underline{52.98}$$

$$I_2(\chi) = 4.664\text{E-}5 \text{ } \underline{37.48}$$

Figure 6-3. The problem in Figure 6-1.

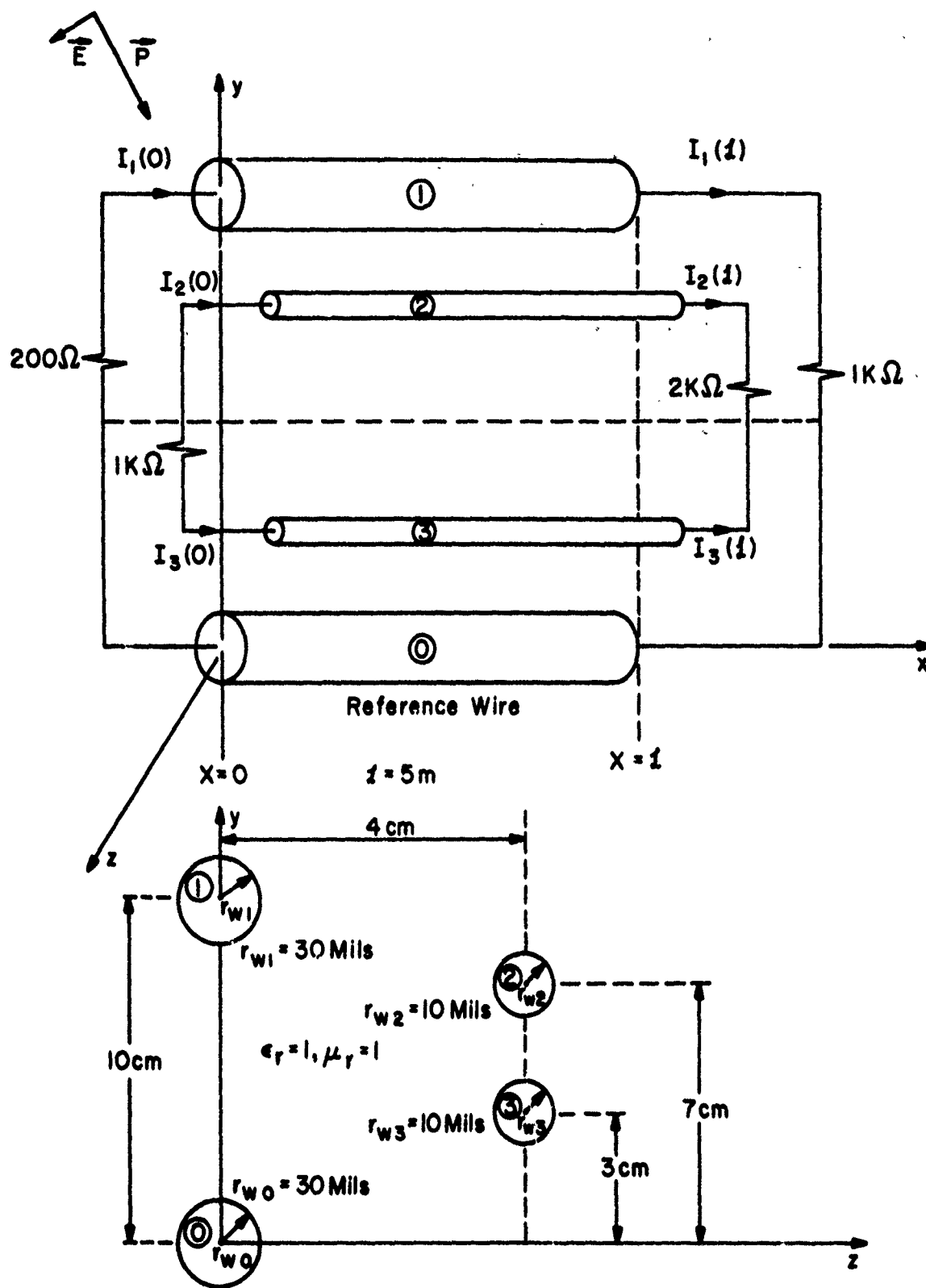


Figure 6-4. Example I, the image problem for Figure 6-1.

<u>Wire</u>	<u>Radius</u>	<u>z_i</u>	<u>y_i</u>
0	30 mils	0	0
1	30 mils	0	10 cm
2	10 mils	4 cm	7 cm
3	10 mils	4 cm	3 cm

The four frequencies of excitation for the ground plane problem in the previous section (1MHz, 10MHz, 100MHz, 1GHz) as well as the three orientations of the plane wave will be considered here. Note here that the zero phase reference for the plane wave is not the same as for the ground plane problem. Here the zero phase reference is displaced downward (in the -y direction) from the zero phase reference for the ground plane problem in the previous section by 5 cm. This means that the phase angles of the currents in this problem will differ from the phase angles of the corresponding currents in the ground plane example by $k(5 \text{ cm})$ degrees or

<u>frequency</u>	<u>$k(5 \text{ cm})$ (degrees)</u>
1 MHz	.0600
10 MHz	.6004
100 MHz	6.0042
1 GHz	60.0415

The next problem remaining is to determine the appropriate representation of the terminal networks. This type of situation was considered in Section 2.6 of Chapter II. From Figure 6-4 we may write (note that the line voltages are with respect to the reference wire here)

$$I_1(0) = -(1/200) V_1(0)$$

$$I_2(0) = (1/1K)(V_3(0) - V_1(0))$$

$$I_3(0) = (1/1K)(V_2(0) - V_3(0))$$

$$I_1(\omega) = (1/1K) V_1(\omega)$$

$$I_2(\omega) = (1/2K)(V_2(\omega) - V_3(\omega))$$

$$I_3(\omega) = (1/2K)(V_3(\omega) - V_2(\omega))$$

Thus we select the load structure option LS0 = 22 and the terminal admittance matrices become

$$Y_0 = \begin{bmatrix} 5E-3 & 0 & 0 \\ 0 & 1E-3 & -1E-3 \\ 0 & -1E-3 & 1E-3 \end{bmatrix} \quad Y_L = \begin{bmatrix} 1E-3 & 0 & 0 \\ 0 & 5E-4 & -5E-4 \\ 0 & -5E-4 & 5E-4 \end{bmatrix}$$

The input data cards are shown in Figure 6-5. The results are shown in Figure 6-6.

Note that for all angles of incidence the magnitudes of $I_2(0)$ and $I_3(0)$ for each frequency are equal as are the magnitudes of $I_2(\omega)$ and $I_3(\omega)$. Further note that $I_2(0)$ and $I_3(0)$ are precisely 180° out of phase as are $I_2(\omega)$ and $I_3(\omega)$. Therefore we have

$$I_2(0) + I_3(0) = 0$$

$$I_2(\omega) + I_3(\omega) = 0$$

for all frequencies as they should be.

MACKEY 201010

-127-

(a) $E_m = 1 \text{ V/m}$, $\theta_E = 30$, $\theta_p = 150$, $\phi_p = 40$

$f = 1 \text{ MHz}$

$$I_1(0) = 1.649\text{E-}6 \angle 89.46$$

$$I_1(\chi) = 1.419\text{E-}7 \angle 86.28$$

$$I_2(0) = 3.668\text{E-}7 \angle 88.79$$

$$I_2(\chi) = 8.912\text{E-}8 \angle -91.43$$

$$I_3(0) = 3.668\text{E-}7 \angle -91.21$$

$$I_3(\chi) = 8.912\text{E-}8 \angle 88.57$$

$f = 10 \text{ MHz}$

$$I_1(0) = 1.658\text{E-}5 \angle 84.57$$

$$I_1(\chi) = 1.558\text{E-}6 \angle 54.19$$

$$I_2(0) = 3.597\text{E-}6 \angle 78.11$$

$$I_2(\chi) = 8.661\text{E-}7 \angle -104.07$$

$$I_3(0) = 3.597\text{E-}6 \angle -101.89$$

$$I_3(\chi) = 8.661\text{E-}7 \angle 75.93$$

$f = 100 \text{ MHz}$

$$I_1(0) = 1.247\text{E-}4 \angle 3.519$$

$$I_1(\chi) = 5.118\text{E-}5 \angle -137.55$$

$$I_2(0) = 1.763\text{E-}5 \angle 15.05$$

$$I_2(\chi) = 5.657\text{E-}6 \angle -165.87$$

$$I_3(0) = 1.76\text{E-}5 \angle -164.95$$

$$I_3(\chi) = 5.657\text{E-}6 \angle 14.13$$

$f = 1 \text{ GHz}$

$$I_1(0) = 1.037\text{E-}4 \angle 55.36$$

$$I_1(\chi) = 4.631\text{E-}5 \angle -87.41$$

$$I_2(0) = 2.591\text{E-}5 \angle 74.23$$

$$I_2(\chi) = 1.024\text{E-}5 \angle -93.50$$

$$I_3(0) = 2.591\text{E-}5 \angle -105.77$$

$$I_3(\chi) = 1.024\text{E-}5 \angle 86.50$$

Figure 6-6. The problem in Figure 6-4.

(b) $E_m = 1 \text{ V/m}$, $\theta_E = 0$, $\theta_p = 90$, $\phi_p = 90$

$f = 1 \text{ MHz}$

$$I_1(0) = 4.647\text{E-}6 \angle 89.09$$

$$I_2(0) = 9.813\text{E-}7 \angle 88.44$$

$$I_3(0) = 9.813\text{E-}7 \angle -91.56$$

$$I_1(z) = 1.166\text{E-}6 \angle 87.87$$

$$I_2(z) = 7.158\text{E-}8 \angle -93.46$$

$$I_3(z) = 7.158\text{E-}8 \angle 86.54$$

$f = 10 \text{ MHz}$

$$I_1(0) = 4.658\text{E-}5 \angle 80.85$$

$$I_2(0) = 9.599\text{E-}6 \angle 74.56$$

$$I_3(0) = 9.599\text{E-}6 \angle -105.44$$

$$I_1(z) = 1.168\text{E-}5 \angle 68.63$$

$$I_2(z) = 6.913\text{E-}7 \angle -124.51$$

$$I_3(z) = 6.913\text{E-}7 \angle 55.49$$

$f = 100 \text{ MHz}$

$$I_1(0) = 2.319\text{E-}4 \angle -37.08$$

$$I_2(0) = 3.301\text{E-}5 \angle -24.28$$

$$I_3(0) = 3.301\text{E-}5 \angle 155.72$$

$$I_1(z) = 5.751\text{E-}5 \angle -156.86$$

$$I_2(z) = 1.510\text{E-}6 \angle 70.15$$

$$I_3(z) = 1.510\text{E-}6 \angle -109.85$$

$f = 1 \text{ GHz}$

$$I_1(0) = 2.294\text{E-}4 \angle -37.91$$

$$I_2(0) = 3.284\text{E-}5 \angle -24.92$$

$$I_3(0) = 3.284\text{E-}5 \angle 155.08$$

$$I_1(z) = 5.689\text{E-}5 \angle -158.43$$

$$I_2(z) = 1.527\text{E-}6 \angle 68.47$$

$$I_3(z) = 1.527\text{E-}6 \angle -111.53$$

Figure 6-6. The problem in Figure 6-4.

(c) $E_m = 1 \text{ V/m}$, $\theta_E = 0$, $\theta_p = 180$, $\phi_p = 90$

$f = 1 \text{ MHz}$

$$I_1(0) = 1.747\text{E-}6 \angle 90.14$$

$$I_2(0) = 2.795\text{E-}7 \angle 90.01$$

$$I_3(0) = 2.795\text{E-}7 \angle -89.99$$

$$I_1(\chi) = 1.747\text{E-}6 \angle 89.33$$

$$I_2(\chi) = 2.794\text{E-}7 \angle 89.50$$

$$I_3(\chi) = 2.794\text{E-}7 \angle -90.50$$

$f = 10 \text{ MHz}$

$$I_1(0) = 1.776\text{E-}5 \angle 91.31$$

$$I_2(0) = 2.828\text{E-}6 \angle 90.01$$

$$I_3(0) = 2.828\text{E-}6 \angle -89.99$$

$$I_1(\chi) = 1.750\text{E-}5 \angle 83.25$$

$$I_2(\chi) = 2.791\text{E-}6 \angle 85.05$$

$$I_3(\chi) = 2.791\text{E-}6 \angle -94.95$$

$f = 100 \text{ MHz}$

$$I_1(0) = 2.658\text{E-}4 \angle 39.83$$

$$I_2(0) = 4.196\text{E-}5 \angle 58.80$$

$$I_3(0) = 4.196\text{E-}5 \angle -121.20$$

$$I_1(\chi) = 9.938\text{E-}5 \angle -81.27$$

$$I_2(\chi) = 2.317\text{E-}5 \angle 41.78$$

$$I_3(\chi) = 2.317\text{E-}5 \angle -138.22$$

$f = 1 \text{ GHz}$

$$I_1(0) = 2.201\text{E-}4 \angle 93.14$$

$$I_2(0) = 4.293\text{E-}5 \angle 113.03$$

$$I_3(0) = 4.293\text{E-}5 \angle -66.97$$

$$I_1(\chi) = 8.161\text{E-}5 \angle 52.61$$

$$I_2(\chi) = 2.332\text{E-}5 \angle 97.52$$

$$I_3(\chi) = 2.332\text{E-}5 \angle -82.48$$

Figure 6-6. The problem in Figure 6-4.

6.1.3 Comparison of the Two Solutions

The terminal currents (I_1, I_2) in Figure 6-1 (the ground plane problem) should be exactly twice the magnitude of the corresponding currents (I_1, I_2) in Figure 6-4 (the image problem). For the case of propagation in the $+x$ direction with \vec{E} in the $+y$ direction:

$$(b) \quad \theta_E = 0, \theta_p = 90, \phi_p = 90$$

$$\vec{E} = e^{-jkx} \vec{y}$$

and the case of propagation in the $-y$ direction with \vec{E} in the $+x$ direction:

$$(c) \quad \theta_E = 0, \theta_p = 180, \phi_p = 90$$

$$\vec{E} = e^{jky} \vec{x}$$

this is precisely the case for all frequencies. (Although not shown here, the results were printed out to 16 digits and agreed to 15 digits.)

However, consider the case of

$$(a) \quad \theta_E = 30, \theta_p = 150, \phi_p = 40$$

Note that the corresponding currents for the ground plane problem in Figure 6-1 are precisely twice those for the image problem in Figure 6-4 for 1 MHz and 10 MHz. For 100 MHz, $I_1(0)$ and $I_1(z)$ correspond exactly and $I_2(0)$ and $I_2(z)$ correspond very closely. However, for 1 GHz, only currents $I_1(0)$ and $I_1(z)$ correspond whereas $I_2(0)$ and $I_2(z)$, although within a factor of two, do not correspond. The reason for this becomes clear when we consider the definition of line voltages used for the two problems.

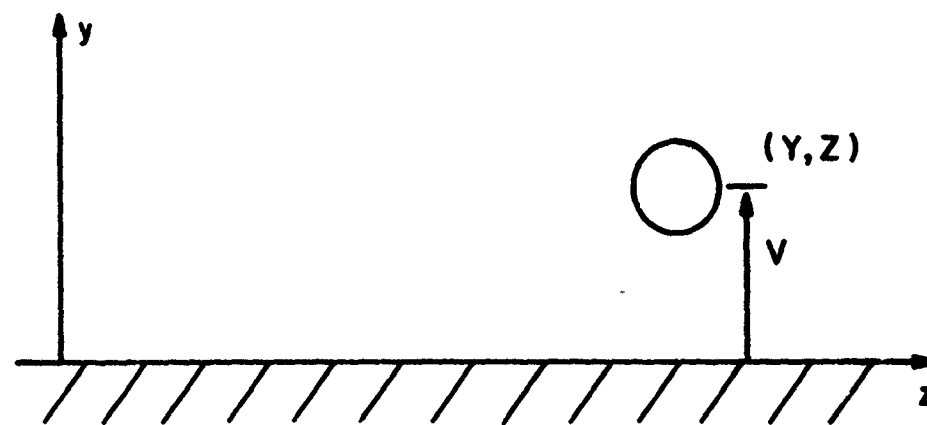
Consider Figure 6-7. We have shown the cross-section of particular wire above a ground plane in Figure 6-7(a), the wire voltage, V , is shown and the potential difference between the wire and its image is $2V$. In Figure 6-7(b), we have shown the corresponding image problem and the voltage of each wire is defined with respect to the reference wire, i.e., V_1 and V_2 . For the two representations to yield corresponding results, one would expect that

$$2V \stackrel{?}{=} (V_1 - V_2)$$

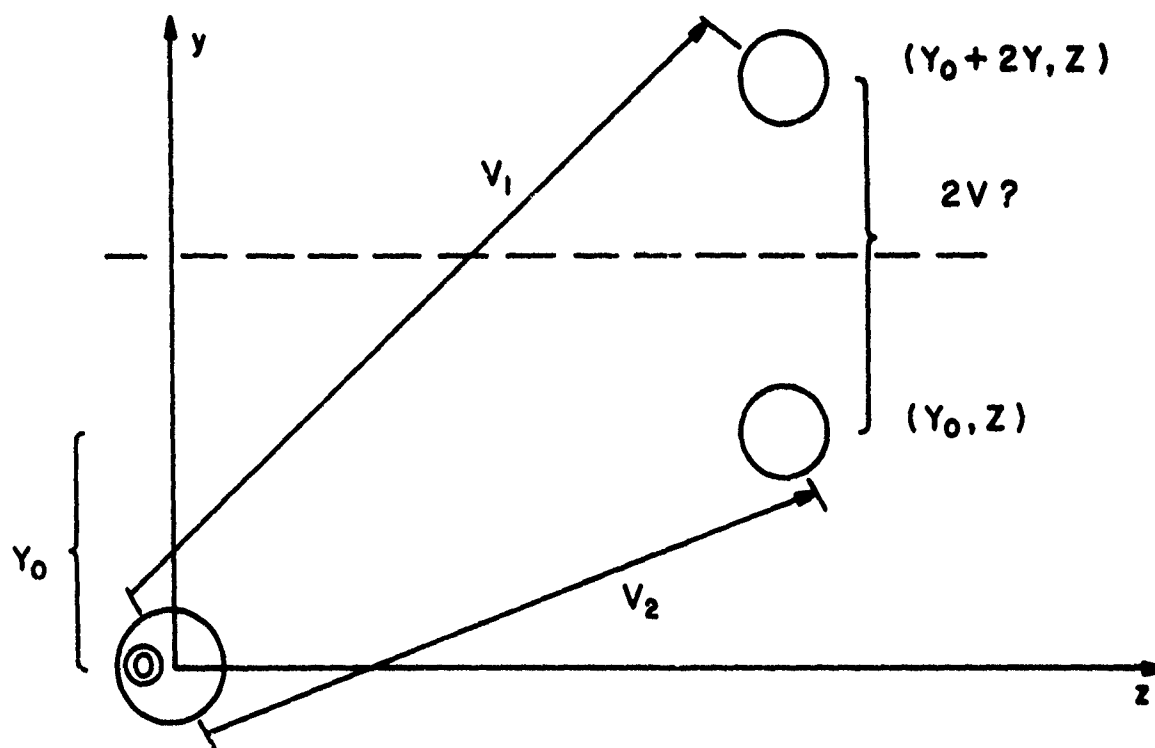
These voltages are related to the integral of $\vec{E}^{(inc)}$ in the transverse (y, z) plane along the contours shown in Figure 6-7 and are included in the vectors $\underline{E}_t^{(inc)}(0)$ and $\underline{E}_t^{(inc)}(x)$. Clearly these will correspond only if $\vec{E}^{(inc)}$ is curl free in the transverse (y, z) plane, i.e., only if there is no component of $\vec{H}^{(inc)}$ in the x direction which penetrates a transverse contour. For angles of incidence $\theta_E = 0$, $\theta_p = 90$, $\phi_p = 90$ and $\theta_E = 0$, $\theta_p = 180$, $\phi_p = 90$, this is clearly the case and the results show this. However, for $\theta_E = 30$, $\theta_p = 150$, $\phi_p = 40$, there is a component of $\vec{H}^{(inc)}$ in the x direction. However, for $f = 1\text{MHz}$, 10 MHz 100 MHz , the cross-sectional dimensions of the line are electrically small and the fact that $\vec{E}^{(inc)}$ is not curl free in the y, z plane does not matter. For 1 GHz , the cross-sectional dimensions of the line are not electrically small and it does matter as is evidenced in the computed results.

6.2 Example II

In this Section we will consider a problem which was investigated by Harrison using an alternate formulation [5,8]. The problem consists of three wires in free space all of radius 10^{-3} m which lie in the x, y plane with adjacent wire separations of 10^{-2} m as shown in Figure 6-8. The line is 10 m



(a)



(b)

Figure 6-7.

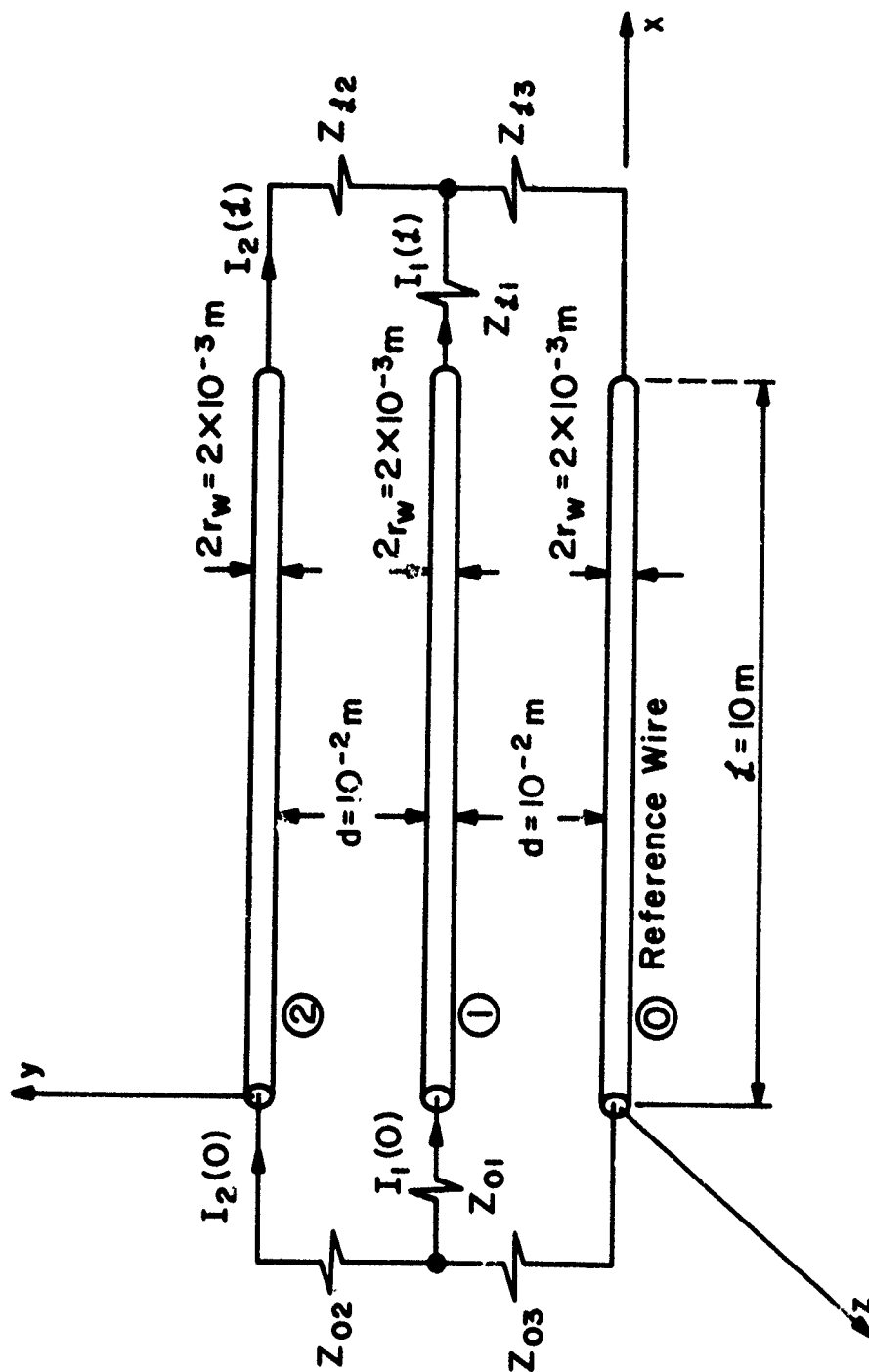


Figure 6-8. Example II.

long and various loads connect each wire to a central point.

The termination impedances are

$$\begin{aligned} Z_{01} &= 50 - j 25 & Z_{02} &= 100 + j 100 & Z_{03} &= 25 + j 25 \\ Z_{21} &= 50 + j 25 & Z_{22} &= 100 - j 50 & Z_{23} &= 150 - j 50 \end{aligned}$$

Obviously we should select $LS0 = 12$ and the termination impedance matrices become

$$\begin{aligned} Z_0 &= \begin{bmatrix} (Z_{01} + Z_{03}) & Z_{03} \\ Z_{03} & (Z_{02} + Z_{03}) \end{bmatrix} = \begin{bmatrix} 75 + j0 & 25 + j 25 \\ 25 + j 25 & 125 + j 125 \end{bmatrix} \\ Z_{\chi} &= \begin{bmatrix} (Z_{\chi 1} + Z_{\chi 3}) & Z_{\chi 3} \\ Z_{\chi 3} & (Z_{\chi 2} + Z_{\chi 3}) \end{bmatrix} = \begin{bmatrix} 200 - j 25 & 150 - j 50 \\ 150 - j 50 & 250 - j 100 \end{bmatrix} \end{aligned}$$

A V/m uniform plane wave is propagating in the $+y$ direction with \vec{E} in the $+x$ direction, i.e., $\vec{E}^{(inc)} = e^{-jky} \vec{x}$. Therefore $E_m = 1$, $\theta_E = 180$, $\theta_p = 0$, $\phi_p = 90$. Harrison showed the result for the terminal currents computed by his method for $k\chi = 1.5$. The line is 10 m long. Therefore the frequency is 7157018.74 Hz. The input data cards are shown in Figure 6-9. The computed results are shown in Figure 6-10 and compared with those obtained by Harrison. Note that the results computed by this method agree with those computed by Harrison to within three digits. The main reason that the results do not agree precisely is that the ratio of line length to wavelength at this frequency is .239. Thus we are entering a frequency range where the variation of line responses with frequency is generally quite rapid

$$\underline{E_m = 1 \text{ V/m}, \theta_E = 180, \theta_p = 0, \phi_p = 90}$$

$$\underline{f = 7157018.74 \text{ Hz } (k\lambda \approx 1.5)}$$

Computed with WIRE:

$$I_1(0) = 1.066\text{E-}5 \angle -99.83$$

$$I_2(0) = 5.647\text{E-}5 \angle -159.07$$

$$I_1(\lambda) = 1.221\text{E-}5 \angle 158.65$$

$$I_2(\lambda) = 2.784\text{E-}5 \angle -148.26$$

Computed by Harrison:

$$|I_1(0)| = 1.065\text{E-}5$$

$$|I_2(0)| = 5.644\text{E-}5$$

$$|I_1(\lambda)| = 1.220\text{E-}5$$

$$|I_2(\lambda)| = 2.784\text{E-}5$$

Figure 6-10. The problem in Figure 6-8 with FSO = 1.

and any seemingly insignificant approximations in the input data ($k\lambda \approx 1.5$) can cause significant changes in the result. In fact the program was internally modified (temporarily) such that $k\lambda$ was precisely 1.5 and the results agreed exactly.

One additional case will be computed in which $E_m = 1$, $\theta_E = 0$, $\theta_p = 90$, $\phi_p = 90$, i.e., the wave is propagating in the $+x$ direction with \vec{E} in the plane of the wires, i.e., the $+y$ direction,

$$\vec{E}(\text{inc}) = e^{-jkx} \vec{y}$$

The input data cards are shown (for $k\lambda = 1.5$) in Figure 6-11 and the computed results are shown in Figure 6-12.

6.2.1 Use of the Nonuniform Field Specification Option, FSO = 2

In this Section we will solve the two problems considered in the previous Section by using the nonuniform field specification option.

For the first example we consider the problem in Figure 6-8 with $E_m = 1$ V/m, $\theta_E = 180$, $\theta_p = 0$, $\phi_p = 90$. To use the nonuniform field specification option, we must describe the magnitude and phase of the incident electric field along the three wires and along straight line contours (the y axis in this case) between each of the two wires and the reference wire at $x = 0$ and $x = \lambda$. Because of this particular field orientation, the specification of these quantities is quite simple. Clearly, the transverse fields are zero. The longitudinal field at all points along the reference wire are $1/0$; along wire 1 are $1/k \times 10^{-2} = 1/-8.5944E-2$ and along wire 2 are $1/k \times 2 \times 10^{-2} = 1/-1.7189E-1$. Although redundant, 11 specification points for the longitudinal fields and 6 specification points for the transverse fields will be used. The data cards are shown in Figure

$$\underline{E_m = 1 \text{ V/m}, \theta_E = 0, \theta_p = 90, \phi_p = 90}$$

$$\underline{f = 7157018.74 \text{ Hz} \text{ (} k\omega \approx 1.5 \text{)}}$$

$$I_1(0) = 1.216\text{E-}5 \angle 17.18$$

$$I_1(\omega) = 1.572\text{E-}5 \angle -49.19$$

$$I_2(0) = 6.708\text{E-}5 \angle -13.76$$

$$I_2(\omega) = 2.849\text{E-}5 \angle -129.84$$

Figure 6-12. The problem of Figure 6-5 with FS0 = 1.

6-13 and the computed results are shown in Figure 6-14. These results compare (and should compare) exactly to those in Figure 6-10 where the uniform plane wave option was used.

The next problem is to use the field orientation of $\theta_E = 0$, $\theta_p = 90$, $\phi_p = 90$. In this case, the longitudinal fields along all wires will be zero whereas the transverse fields at all points along the contours at $x = 0$ will be $1/0$ whereas those of $x = Z$ will be $1/kZ = 1/-85.943669$. The data cards are shown in Figure 6-15 and the computed results are shown in Figure 6-16. These results compare (and should compare) exactly to those in Figure 6-12 where the uniform plane wave option was used.

Figure 6-13. Data cards for the problem in Figure 6-8
with $E_m = 1$ V/m, $\Theta_E = 180^\circ$, $\Theta_p = 0^\circ$, $\phi_p = 90^\circ$, FSO=2 (cont.)

[illegible]

-144-

$$\underline{E_m = 1, \theta_E = 180, \theta_p = 0, \phi_p = 90}$$

$$\underline{f = 7157018.74 \text{ Hz}} \quad (k\gamma \approx 1.5)$$

$$I_1(0) = 1.066\text{E-}5 \angle -99.83$$

$$I_1(\gamma) = 1.221\text{E-}5 \angle 158.65$$

$$I_2(0) = 5.647\text{E-}5 \angle -159.07$$

$$I_2(\gamma) = 2.784\text{E-}5 \angle -148.26$$

Figure 6-14. The problem of Figure 6-8 using the nonuniform field specification option.

[illegible]

-148-

$$\underline{E_m = 1, \theta_E = 0, \theta_p = 90, \phi_p = 90}$$

$$\underline{f = 7157018.74 \text{ Hz}} \quad (k\mathcal{L} \approx 1.5)$$

$$I_1(0) = 1.216\text{E-}5 \underline{/17.18}$$

$$I_1(\mathcal{L}) = 1.572\text{E-}5 \underline{/ -49.19}$$

$$I_2(0) = 6.708\text{E-}5 \underline{/ -13.76}$$

$$I_2(\mathcal{L}) = 2.849\text{E-}5 \underline{/ -129.84}$$

Figure 6-16. The problem of Figure 6-8 using the nonuniform field specification option.

VII. SUMMARY

A digital computer program, WIRE, which is designed to compute the terminal currents induced in a multiconductor transmission line by a single frequency, incident electromagnetic field has been described. The transmission line consists of n wires (cylindrical conductors) and a reference conductor. The reference conductor may be a wire (TYPE=1), an infinite ground plane (TYPE=2) or an overall, cylindrical shield (TYPE=3). All $(n+1)$ conductors are assumed to be perfect conductors and the surrounding medium is assumed to be linear, isotropic, homogeneous and lossless. The line is assumed to be uniform in that all $(n+1)$ conductors have no variation in their cross-sections along the line length and are parallel to each other.

Two types of incident field specification are provided for. Uniform plane wave excitation can be specified for TYPE 1 and TYPE 2 structures whereas nonuniform field excitation can be specified for all structure types.

The primary restrictions on the program validity is that the cross-sectional dimensions of the line, e.g., wire spacings, must be electrically small and the smallest ratio of wire separation to wire radius must be larger than approximately 5.

General linear termination networks are provided for at the two ends of the line.

REFERENCES

- [1] C. R. Paul, "Applications of Multiconductor Transmission Line Theory to the Prediction of Cable Coupling, Volume I, Multiconductor Transmission Line Theory", Technical Report, RADC-TR-76-101, Rome Air Development Center, Griffiss AFB, N.Y., April 1976, A025028.
- [2] C. R. Paul, "Applications of Multiconductor Transmission Line Theory to the Prediction of Cable Coupling, Volume VII, Digital Computer Programs for the Analysis of Multiconductor Transmission Lines", Technical Report, RADC-TR-76-101, Rome Air Development Center, Griffiss AFB, N.Y., July 1977, A046662.
- [3] C. D. Taylor, R. S. Satterwhite, and C. W. Harrison, "The Response of a Terminated Two-Wire Transmission Line Excited by a Nonuniform Electromagnetic Field", IEEE Trans. on Antennas and Propagation, Vol. AP-13, pp. 987-989, November 1965.
- [4] A. A. Smith, "A More Convenient Form of the Equations for the Response of a Transmission Line Excited by Nonuniform Fields", IEEE Trans. on Electromagnetic Compatibility, Vol. EMC-15, pp. 151-152, August 1973.
- [5] C. W. Harrison, "Generalized Theory of Impedance Loaded Multiconductor Transmission Lines in an Incident Field", IEEE Trans. on Electromagnetic Compatibility, Vol. EMC-14, pp. 56-63, May 1972.
- [6] C. R. Paul, "Efficient Numerical Computation of the Frequency Response of Cables Illuminated by an Electromagnetic Field", IEEE Trans. on Microwave Theory and Techniques, Vol. MTT-22, pp. 454-457, April 1974.
- [7] C. R. Paul, "Useful Matrix Chain Parameter Identities for the Analysis of Multiconductor Transmission Lines", IEEE Trans. on Microwave Theory and Techniques, Vol. MTT-23, pp. 756-760, September 1975.

- [8] C. R. Paul, "Frequency Response of Multiconductor Transmission Lines Illuminated by an Electromagnetic Field", IEEE Trans. on Electromagnetic Compatibility, Vol. EMC-18, pp. 183-190, November 1976.
- [9] C. R. Paul and A. E. Feather, "Computation of the Transmission Line Inductance and Capacitance Matrices from the Generalized Capacitance Matrix", IEEE Trans. on Electromagnetic Compatibility, Vol. EMC-18, pp. 175-183, November 1976.
- [10] W. Kaplan, Advanced Calculus. Reading, MA: Addison Wesley, 1952.
- [11] J. C. Clements and C. R. Paul, "Computation of the Capacitance Matrix for Dielectric-Coated Wires", Technical Report, RADC-TR-74-59, Rome Air Development Center, Griffiss AFB, N.Y., March 1974, 778948.
- [12] D. T. Paris and F. K. Hurd, Basic Electromagnetic Theory. McGraw Hill: New York, 1969.
- [13] IMSL, Sixth Floor, GNB Building, 7500 Bellaire Boulevard, Houston, Texas 77036 (Fifth Edition, November 1975).
- [14] C. W. Harrison and R. W. P. King, "Folded Dipoles and Loops", IRE Trans. on Antennas and Propagation, pp. 171-187, March 1961.

APPENDIX A

A Note on Common Mode and Differential Mode

Currents

An important assumption in this method is that the sum of the currents in all $(n+1)$ conductors at a particular x along the line is equal to zero. This is the conventional notion of transmission line currents. The purpose of this Appendix is to provide some justification for the assumption.

As a prelude, consider the two conductor line ($n=1$) shown in Figure A-1(a). At a particular longitudinal coordinate, x , we have separated the total current into a common mode component, I_C , and a differential mode component, I_D . This is purely a mathematical operation and given the currents $I_1(x)$ and $I_2(x)$, one can always resolve them into these components as shown by the following. We are simply looking for a unique transformation which performs this separation. If we write

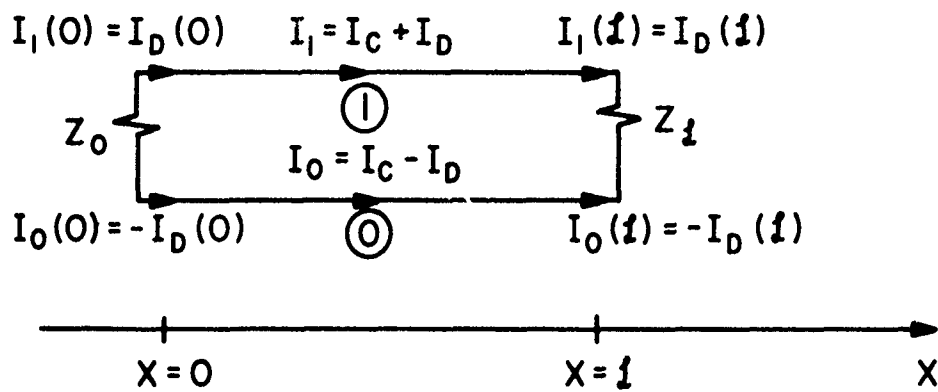
$$I_1(x) = I_C(x) + I_D(x) \quad (A-1a)$$

$$I_2(x) = I_C(x) - I_D(x) \quad (A-1b)$$

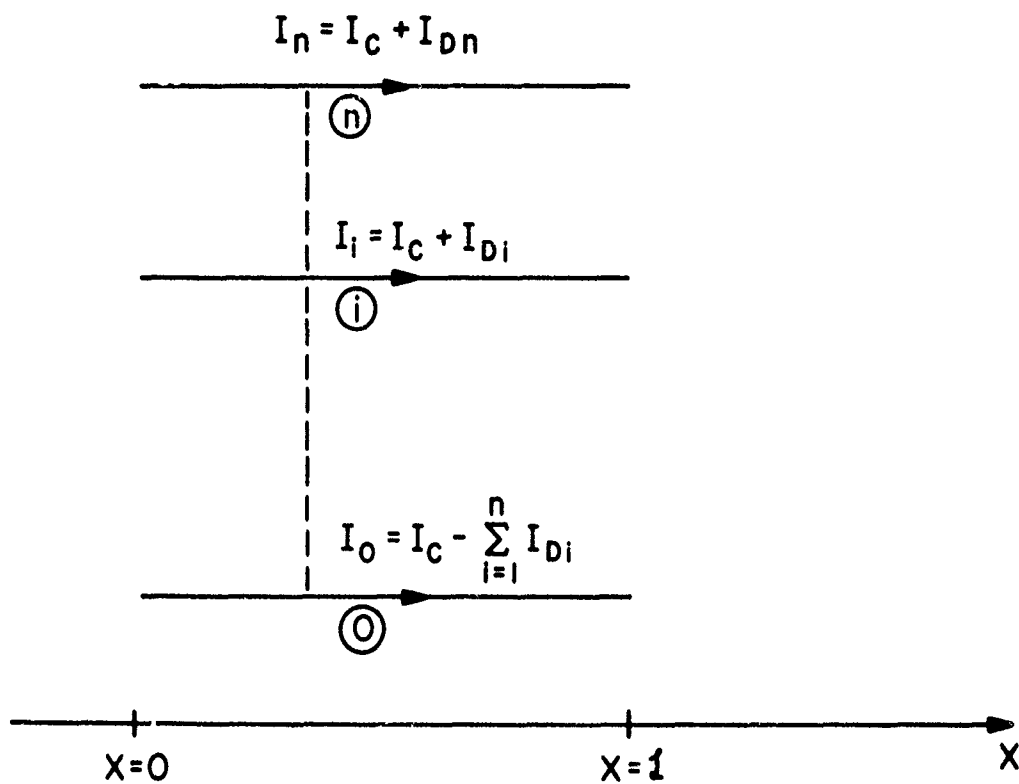
then in matrix form the equations become

$$\begin{bmatrix} I_1(x) \\ I_2(x) \end{bmatrix} = \underbrace{\begin{bmatrix} 1 & 1 \\ -1 & 1 \end{bmatrix}}_{\tilde{T}} \begin{bmatrix} I_D(x) \\ I_C(x) \end{bmatrix} \quad (A-2)$$

The essential question here is whether \tilde{T} is nonsingular which would represent a unique transformation between the two sets of currents. Clearly \tilde{T} is



(a) $n = 1$



(b) n

Figure A-1. Illustration of common mode and differential mode currents.

nonsingular and we may write (multiplying (A-2) on the left by \tilde{T}^{-1})

$$\begin{bmatrix} I_D(x) \\ I_C(x) \end{bmatrix} = \frac{1}{2} \begin{bmatrix} 1 & -1 \\ 1 & 1 \end{bmatrix} \begin{bmatrix} I_1(x) \\ I_2(x) \end{bmatrix} \quad (A-3)$$

Therefore, given $I_1(x)$ and $I_2(x)$ for a particular x , one can uniquely determine $I_D(x)$ and $I_C(x)$.

The question of physical significance of I_D and I_C is essentially irrelevant since this is merely a transformation of variables. The essential point is that as far as the terminal responses are concerned, we need only consider the differential mode (transmission line type) current, I_D , since the common mode current (commonly called antenna type current) has essentially no effect on the terminal responses. The justification for this statement lies in our fundamental assumption that the cross-sectional dimensions (wire separation) of the line are much less than a wavelength. Therefore we may consider the terminal impedances (Z_0 and Z_L) as lumped and if we apply Kirchoff's current law to the "nodes" containing the impedance we can only conclude that the common mode current is zero at the endpoints of the line, i.e., $I_C(0) = I_C(L) = 0$. At points along the line, this is not generally true and the line currents will not be simply due to the differential mode current but will be a combination of $I_D(x)$ and $I_C(x)$ as shown in Figure A-1(a). The essential point here is that if we are only interested in computing the terminal response of the line (as we are in this report), we may disregard or omit consideration of the common mode current.

The extension of this result to multiconductor lines is quite similar. Consider Figure A-1(b) where we have decomposed each line current into a

differential mode current, I_{D1} , and a common mode current, I_C . Note that we have taken the common mode currents to be the same at corresponding points (values of the x coordinate) along the line in all line conductors. The justification for this is our primary assumption that the maximum cross-sectional dimension of the line is "electrically small", i.e., much less than a wavelength. The essential question here is whether we can define a unique (nonsingular) transformation between the actual line currents, I_0, I_1, \dots, I_n , and the decomposition components, $I_{D1}, I_{D2}, \dots, I_{Dn}, I_C$. This is easily found from Figure A-1(b) from

$$I_n(x) = I_C(x) + I_{Dn}(x)$$

$$I_i(x) = I_C(x) + I_{Di}(x)$$

(A-4)

$$I_1(x) = I_C(x) + I_{D1}(x)$$

$$I_0(x) = I_C(x) - \sum_{i=1}^n I_{Di}(x)$$

which becomes in matrix notation

$$\begin{bmatrix} I_n(x) \\ \cdot \\ \cdot \\ \cdot \\ I_i(x) \\ \cdot \\ \cdot \\ I_1(x) \\ I_0(x) \end{bmatrix} = \underbrace{\begin{bmatrix} 1 & 0 & \cdots & 0 & 1 \\ 0 & 1 & 0 & & 0 & 1 \\ & \ddots & \ddots & \ddots & \vdots & \vdots \\ & & \ddots & 0 & 1 \\ & & & 0 & 1 & 1 \\ -1 & \cdots & \cdots & -1 & 1 \end{bmatrix}}_T \begin{bmatrix} I_{Dn}(x) \\ \cdot \\ \cdot \\ \cdot \\ I_{D1}(x) \\ \cdot \\ \cdot \\ I_{D1}(x) \\ I_C(x) \end{bmatrix} \quad (A-5)$$

One can easily show (use elementary row operations to reduce \tilde{T} to echelon or upper diagonal form) that \tilde{T} is nonsingular and therefore represents a unique transformation. Thus for a particular x , given the actual line currents, $I_n(x), \dots, I_1(x), I_0(x)$, one can obtain the components, $I_{Dn}(x), \dots, I_{D1}(x), I_C(x)$ from

$$\begin{bmatrix} I_{Dn}(x) \\ \vdots \\ I_{D1}(x) \\ \vdots \\ I_C(x) \end{bmatrix} = \tilde{T}^{-1} \begin{bmatrix} I_n(x) \\ \vdots \\ I_1(x) \\ \vdots \\ I_0(x) \end{bmatrix} \quad (\text{A-6})$$

Again, assuming the line cross-sectional dimensions to be electrically small, we may conclude that the common mode currents at the endpoints of the line, $I_C(0)$ and $I_C(L)$, are essentially zero and have no effect on the terminal networks. Therefore it suffices to consider only the differential mode (transmission line mode) currents when computing only the terminal responses of the line.

For a parallel discussion of this problem see [14].

APPENDIX B

WIRE

Program Listing

Flowchart

```

C*****WIRE0001
C
C      PROGRAM WIRE                                WIRE0002
C      (FORTRAN IV, DOUBLE PRECISION)              WIRE0003
C      WRITTEN BY                                  WIRE0004
C      CLAYTON R. PAUL                             WIRE0005
C      DEPARTMENT OF ELECTRICAL ENGINEERING        WIRE0006
C      UNIVERSITY OF KENTUCKY                       WIRE0007
C      LEXINGTON, KENTUCKY 40506                   WIRE0008
C
C      A DIGITAL COMPUTER PROGRAM TO COMPUTE THE TERMINAL CURRENTS
C      AT THE ENDS OF A MULTICONDUCTOR TRANSMISSION LINE WHICH IS
C      EXCITED BY AN INCIDENT ELECTROMAGNETIC FIELD. WIRE0009
C
C      THE DISTRIBUTED PARAMETER, MULTICONDUCTOR TRANSMISSION LINE
C      EQUATIONS ARE SOLVED FOR STEADY STATE, SINUSOIDAL EXCITATION
C      OF THE LINE.                                WIRE0010
C
C      THE LINE CONSISTS OF N WIRES (CYLINDRICAL CONDUCTORS) AND A
C      REFERENCE CONDUCTOR. THE REFERENCE CONDUCTOR MAY BE A WIRE
C      (TYPE=1), AN INFINITE GROUND PLANE (TYPE=2), OR AN OVERALL
C      CYLINDRICAL SHIELD (TYPE=3).                 WIRE0011
C
C      THE INCIDENT FIELD MAY BE IN THE FORM OF A UNIFORM PLANE WAVE
C      FOR TYPE 1 AND TYPE 2 STRUCTURES OR A NONUNIFORM FIELD FOR ALL
C      STRUCTURE TYPES.                             WIRE0012
C
C      THE N WIRES ARE ASSUMED TO BE PARALLEL TO EACH OTHER AND THE
C      REFERENCE CONDUCTOR.                         WIRE0013
C
C      THE N WIRES AND THE REFERENCE CONDUCTOR ARE ASSUMED TO BE
C      PERFECT CONDUCTORS.                          WIRE0014
C
C      THE LINE IS IMMERSSED IN A LINEAR, ISOTROPIC, AND HOMOGENEOUS
C      MEDIUM WITH A RELATIVE PERMEABILITY OF  $\mu_r$  AND A RELATIVE
C      DIELECTRIC CONSTANT OF  $\epsilon_r$ . THE MEDIUM IS ASSUMED TO BE LOSSLESS. WIRE0015
C
C      LOAD STRUCTURE OPTION (LSO) DEFINITIONS:     WIRE0016
C      LSO=11,THEVENIN EQUIVALENT LOAD STRUCTURES WITH DIAGONAL
C      IMPEDANCE MATRICES                           WIRE0017
C      LSO=12,THEVENIN EQUIVALENT LOAD STRUCTURES WITH FULL
C      IMPEDANCE MATRICES                           WIRE0018
C      LSO=21,NORTON EQUIVALENT LOAD STRUCTURES WITH DIAGONAL
C      ADMITTANCE MATRICES                          WIRE0019
C      LSO=22,NORTON EQUIVALENT LOAD STRUCTURES WITH FULL
C      ADMITTANCE MATRICES                          WIRE0020
C
C      FIELD SPECIFICATION OPTION (FSO) DEFINITIONS: WIRE0021
C      FSO=1,UNIFORM PLANE WAVE (TYPE=1,2)          WIRE0022
C      FSO=2,NONUNIFORM FIELD (TYPE=1,2,3)          WIRE0023
C
C      FUNCTION SUBPROGRAMS USED: E1,E2              WIRE0024
C      SUBROUTINES USED: LEQ1C                      WIRE0025
C
C*****WIRE0055
C
C      ALL VECTORS AND MATRICES IN THE FOLLOWING DIMENSION STATEMENTS
C      SHOULD BE OF SIZE N WHERE N IS THE NUMBER OF WIRES (EXCLUSIVE OF
C      THE REFERENCE CONDUCTOR), I.E., V1(N), V2(N), Y0(N,N), YL(N,N), B(N),
C      A(N,N), WA(N), M1(N,N), M2(N,N), ETL(N), ETO(N), Y3(N,N), V3(N), V4(N)
C
C      WIRE0026
C      WIRE0027
C      WIRE0028
C      WIRE0029
C      WIRE0030
C      WIRE0031
C      WIRE0032
C      WIRE0033
C      WIRE0034
C      WIRE0035
C      WIRE0036
C      WIRE0037
C      WIRE0038
C      WIRE0039
C      WIRE0040
C      WIRE0041
C      WIRE0042
C      WIRE0043
C      WIRE0044
C      WIRE0045
C      WIRE0046
C      WIRE0047
C      WIRE0048
C      WIRE0049
C      WIRE0050
C      WIRE0051
C      WIRE0052
C      WIRE0053
C      WIRE0054
C      WIRE0056
C      WIRE0057
C      WIRE0058
C      WIRE0059
C      WIRE0060
C      WIRE0061

```

IMPLICIT REAL*8 (A-H,O-Z)	WIRE0062
INTEGER TYPE,PSO	WIRE0063
REAL*8 L,V3(2),V4(2),IOM,ILM,IOR,IOT,ILR,ILI,IOA,ILA,MUR,MUO2PI	WIRE0064
1,M1,M2,MH,NP	WIRE0065
COMPLEX*16 XJ,V1(2),V2(2),Y0(2, 2),YL(2, 2),A(2, 2),B(2),	WIRE0066
1SUMO,SUHL,IO,IL,ZEROC,WA(2),M1(2, 2),M2(2, 2),ETL(2),ETO(2),	WIRE0067
2C,A1,A2,ONEC,M3(2, 2),EBXL,EBL,V1H,V2H,EP,RN,EJ8Z,EBTPBZ,EPBL,	WIRE0068
3ENBL,EJCI,SUNC,SUNS,ELOC,ELOS,E1,E2,EJBY	WIRE0069
CONHON XJ,ZERO,TWO,ONE,ONEC	WIRE0070
DATA CHTH/2.54D-5/,MUO2PI/2.D-7/,P5/.5D0/,FOUR/*.D0/,	WIRE0071
1ONE80/180.D0/,V/2.997925D8/	WIRE0072
ZERO=0.D0	WIRE0073
ONE=1.D0	WIRE0074
TWO=2.D0	WIRE0075
ONEC=DCHPLX(1.D0,0.D0)	WIRE0076
ZEROC=DCHPLX(0.D0,0.D0)	WIRE0077
XJ=DCHPLX(0.D0,1.D0)	WIRE0078
PI=FOUR*DATAH(ONE)	WIRE0079
RADeg=ONE80/PI	WIRE0080
C	WIRE0081
C*****FREQUENCY INDEPENDENT CALCULATIONS*****	WIRE0082
C	WIRE0083
C READ AND PRINT INPUT DATA	WIRE0084
C	WIRE0085
READ(5,1) TYPE,LSO,PSO,M,ER,MUR,L	WIRE0086
1 FORMAT(9X,I1,8X,I2,9X,I1,8X,I2,3(E10.3))	WIRE0087
IF (TYPE.GE.1.AND.TYPE.LE.3) GO TO 3	WIRE0088
WRITE(6,2)	WIRE0089
2 FORMAT(' STRUCTURE TYPE ERROR'/// TYPE MUST EQUAL 1,2,OR 3'///)	WIRE0090
GO TO 121	WIRE0091
3 IF (LSO.EQ.11.OR.LSO.EQ.12) GO TO 5	WIRE0092
IF (LSO.EQ.21.OR.LSO.EQ.22) GO TO 5	WIRE0093
WRITE(6,4)	WIRE0094
4 FORMAT(' LOAD STRUCTURE OPTION ERROR'/// LSO MUST EQUAL 11,12,21,OR 22'///)	WIRE0095
GO TO 121	WIRE0096
5 IF (PSO.EQ.1.OR.PSO.EQ.2) GO TO 7	WIRE0097
WRITE(6,6)	WIRE0098
6 FORMAT(' FIELD SPECIFICATION OPTION ERROR'/// PSO MUST EQUAL 1,2,OR 3'///)	WIRE0099
GO TO 121	WIRE0100
7 IF (TYPE.EQ.3.AND.PSO.EQ.1) GO TO 8	WIRE0101
GO TO 10	WIRE0102
8 WRITE(6,9)	WIRE0103
9 FORMAT(' UNIFORM PLANE WAVE EXCITATION CANNOT BE SPECIFIED FOR TYPE 3 STRUCTURE'///)	WIRE0104
GO TO 121	WIRE0105
10 WRITE(6,11) M,TYPE,LSO,PSO,L,ER,MUR	WIRE0106
11 FORMAT(16X,51X,' WIRE'///	WIRE0107
145X,I2,' PARALLEL WIRES'///	WIRE0108
243X,' TYPE OF STRUCTURE= ',I1///	WIRE0109
341X,' LOAD STRUCTURE OPTION= ',I2///	WIRE0110
440X,' FIELD SPECIFICATION OPTION= ',I1///	WIRE0111
539X,' LINE LENGTH= ',1PE13.6,' METERS'///	WIRE0112
633X,' DIELECTRIC CONSTANT OF THE MEDIUM= ',1PE10.3///	WIRE0113
733X,'RELATIVE PERMEABILITY OF THE MEDIUM= ',1PE10.3///)	WIRE0114
GO TO (12,20,16),TYPE	WIRE0115
12 READ(5,13) RW0	WIRE0116
13 FORMAT(5X,E10.3)	WIRE0117
WRITE(6,14) RW0	WIRE0118
14 FORMAT(' REFERENCE CONDUCTOR FOR LINE VOLTAGES IS A WIRE WITH RADI	WIRE0119
	WIRE0120
	WIRE0121
	WIRE0122

1	US= ' ,1PE10.3, ' MILS'////)	WIRE0123
	RW0=RW0*CHTH	WIRE0124
	WRITE(6,15)	WIRE0125
15	FORMAT(' WIRE NUMBER',4X,'WIRE RADIUS (MILS)',18X,	WIRE0126
	'Z COORDINATE (METERS)',24X,'Y COORDINATE (METERS)',//)	WIRE0127
	GO TO 23	WIRE0128
16	READ(5,17) RS	WIRE0129
17	FORMAT(5X,E10.3)	WIRE0130
	WRITE(6,18) RS	WIRE0131
18	FORMAT(' REFERENCE CONDUCTOR FOR LINE VOLTAGES IS A CYLINDRICAL O	WIRE0132
	VERALL SHIELD WITH INTERIOR RADIUS= ' ,1PE10.3, ' METERS'////)	WIRE0133
	RS2=RS*RS	WIRE0134
	WRITE(6,19)	WIRE0135
19	FORMAT(' WIRE NUMBER',2X,'WIRE RADIUS (MILS)', 2X,'SEPARATION BETWEEN	WIRE0136
	TEEN WIRE AND CENTER OF SHIELD (METERS)',6X,'ANGULAR COORDINATE (DE	WIRE0137
	GREES)'//)	WIRE0138
	GO TO 23	WIRE0139
20	WRITE(6,21)	WIRE0140
21	FORMAT(' REFERENCE CONDUCTOR FOR LINE VOLTAGES IS AN INFINITE GROU	WIRE0141
	ND PLANE'////)	WIRE0142
	WRITE(6,22)	WIRE0143
22	FORMAT(' WIRE NUMBER',4X,'WIRE RADIUS (MILS)',18X,	WIRE0144
	'HORIZONTAL COORDINATE (METERS)',16X,'WIRE HEIGHT (METERS)'//)	WIRE0145
C		WIRE0146
C	READ AND PRINT LINE DIMENSIONS AND COMPUTE THE CHARACTERISTIC	WIRE0147
C	IMPEDANCE MATRIX,ZC (STORE ZC IN REAL PART OF ARRAY M1)	WIRE0148
C		WIRE0149
23	C=MU02PI*QMEC*V*DSQRT(MUR/ER)	WIRE0150
	DO 29 I=1,N	WIRE0151
	READ(5,24) RW,Z,Y	WIRE0152
24	FORMAT(3(5X,E10.3))	WIRE0153
	WRITE(6,25) I,RW,Z,Y	WIRE0154
25	FORMAT(2X,I2,13X,1PE10.3,27X,1PE10.3,35X,1PE10.3/)	WIRE0155
	V3(I)=Z	WIRE0156
	V4(I)=Y	WIRE0157
	RW=RW*CHTH	WIRE0158
	GO TO (26,27,28),TYPE	WIRE0159
26	DI2=Z*Z+Y*Y	WIRE0160
	M1(I,I)=C*DLOG(DI2/(RW*RW0))	WIRE0161
	GO TO 29	WIRE0162
27	M1(I,I)=C*DLOG(TWO*Y/RW)	WIRE0163
	GO TO 29	WIRE0164
28	M1(I,I)=C*DLOG((RS2-Z*Z)/(RS*RW))	WIRE0165
29	CONTINUE	WIRE0166
	IF(N.EQ.1) GO TO 34	WIRE0167
	K1=N-1	WIRE0168
	DO 33 I=1,K1	WIRE0169
	K2=I+1	WIRE0170
	DO 33 J=K2,N	WIRE0171
	ZI=V3(I)	WIRE0172
	ZJ=V3(J)	WIRE0173
	YI=V4(I)	WIRE0174
	YJ=V4(J)	WIRE0175
	GO TO (30,31,32),TYPE	WIRE0176
30	DI2=ZI*ZI+YI*YI	WIRE0177
	DJ2=ZJ*ZJ+YJ*YJ	WIRE0178
	ZD=ZI-ZJ	WIRE0179
	YD=YI-YJ	WIRE0180
	DIJ2=ZD*ZD+YD*YD	WIRE0181
	M1(I,J)=P5*C*DLOG(DI2*DJ2/(RW0*RW0*DIJ2))	WIRE0182
	M1(J,I)=M1(I,J)	WIRE0183

	GO TO 33	WIRE0184
31	ZD=ZI-ZJ	WIRE0185
	YD=YI-YJ	WIRE0186
	DIJ2=ZD*ZD+YD*YD	WIRE0187
	M1(I,J)=P5*C*DLOG(ONE+FOUR*YI*YJ/DIJ2)	WIRE0188
	M1(J,I)=M1(I,J)	WIRE0189
	GO TO 33	WIRE0190
32	THETA=(YI-YJ)/RADEG	WIRE0191
	RI2=ZI*ZI	WIRE0192
	RJ2=ZJ*ZJ	WIRE0193
	M1(I,J)=P5*C*DLOG((RJ2/RS2)*(RI2*RJ2+RS2*RS2-TWO*ZI*ZJ*RS2* 1DCOS(THETA))/(RI2*RJ2+RJ2*RJ2-TWO*ZI*ZJ*RJ2*DCOS(THETA)))	WIRE0194
	M1(J,I)=M1(I,J)	WIRE0195
33	CONTINUE	WIRE0196
C		WIRE0197
C	COMPUTE THE INVERSE OF THE CHARACTERISTIC IMPEDANCE MATRIX,ZCINV	WIRE0198
C	(STORE ZCINV IN ARRAYS M2 AND M3)	WIRE0199
C		WIRE0200
	34 DO 36 I=1,N	WIRE0201
	DO 35 J=1,N	WIRE0202
	A(I,J)=M1(I,J)	WIRE0203
35	M2(I,J)=ZEROC	WIRE0204
36	M2(I,I)=ONEC	WIRE0205
	CALL LEQ1C(A,N,N,M2,N,N,0,WA,KER)	WIRE0206
	KER=KER-128	WIRE0207
	DO 37 I=1,N	WIRE0208
	DO 37 J=1,N	WIRE0209
37	M3(I,J)=M2(I,J)	WIRE0210
	IF(KER.NE.1) GO TO 39	WIRE0211
	WRITE(6,38)	WIRE0212
	38 FORMAT(//,' *****CHARACTERISTIC IMPEDANCE MATRIX INVERSION ERROR**	WIRE0213
	1***',//)	WIRE0214
	GO TO 121	WIRE0215
C		WIRE0216
C	READ AND PRINT ENTRIES IN LOAD ADMITTANCE(IMPEDANCE) MATRICES	WIRE0217
C	(STORE ADMITTANCE(IMPEDANCE) MATRICES AT X=0 IN ARRAY Y0 AND	WIRE0218
C	THOSE AT X=L IN ARRAY YL)	WIRE0219
C		WIRE0220
	39 IF(LSO.EQ.11.OR.LSO.EQ.12) GO TO 42	WIRE0221
	WRITE(6,40)	WIRE0222
40	FORMAT(//,18X,' ADMITTANCE AT X=0',43X,' ADMITTANCE AT X=L'//)	WIRE0223
	WRITE(6,41)	WIRE0224
41	FORMAT(21X,' (SIEMENS)',51X,' (SIEMENS)'//)	WIRE0225
	GO TO 45	WIRE0226
42	WRITE(6,43)	WIRE0227
43	FORMAT(//,18X,' IMPEDANCE AT X=0',44X,' IMPEDANCE AT X=L'//)	WIRE0228
	WRITE(6,44)	WIRE0229
44	FORMAT(23X,' (OHMS)',54X,' (OHMS)'//)	WIRE0230
45	WRITE(6,46)	WIRE0231
46	FORMAT(' ENTRY',10X,' REAL',11X,' IMAG',41X,' REAL',11X,' IMAG'//)	WIRE0232
	DO 49 I=1,N	WIRE0233
	READ(5,47) Y0R,Y0I,YLR,YLI	WIRE0234
47	FORMAT(2(E10.3),20X,2(E10.3))	WIRE0235
	Y0(I,I)=Y0R+XJ*Y0I	WIRE0236
	YL(I,I)=YLR+XJ*YLI	WIRE0237
	WRITE(6,48) I,I,Y0(I,I),YL(I,I)	WIRE0238
48	FORMAT(1X,I2,2X,I2,2(5X,1PE10.3),30X,2(5X,1PE10.3)//)	WIRE0239
49	CONTINUE	WIRE0240
	IF(LSO.EQ.11.OR.LSO.EQ.21) GO TO 52	WIRE0241
	IF(N.EQ.1) GO TO 52	WIRE0242
	DO 51 I=1,K1	WIRE0243
		WIRE0244

K2=I+1	WIRE0245
DO 51 J=K2,N	WIRE0246
READ(5,50) YOR,YOI,YLR,YLI	WIRE0247
50 FORMAT(2(E10.3),20X,2(E10.3))	WIRE0248
Y0(I,J)=YOR+XJ*YOI	WIRE0249
YL(I,J)=YLR+XJ*YLI	WIRE0250
Y0(J,I)=Y0(I,J)	WIRE0251
YL(J,I)=YL(I,J)	WIRE0252
WRITE(6,48) I,J,Y0(I,J),YL(I,J)	WIRE0253
51 CONTINUE	WIRE0254
C	WIRE0255
C IF THEVENIN EQUIVALENT SPECIFIED, SWAP ENTRIES IN ARRAYS M1 AND M2	WIRE0256
C M1 WILL CONTAIN THE INVERSE OF ZC AND M2 WILL CONTAIN ZC	WIRE0257
C	WIRE0258
52 IF (LSO.EQ.21.OR.LSO.EQ.22) GO TO 54	WIRE0259
DO 53 I=1,N	WIRE0260
DO 53 J=I,N	WIRE0261
A1=M1(I,J)	WIRE0262
A2=M2(I,J)	WIRE0263
M1(I,J)=A2	WIRE0264
M1(J,I)=A2	WIRE0265
M2(I,J)=A1	WIRE0266
53 M2(J,I)=A1	WIRE0267
C	WIRE0268
C COMPUTE THE MATRIX ZC+ZL*ZCINV*Z0 FOR THE THEVENIN EQUIVALENT	WIRE0269
C OR ZCINV+YL*ZC*Y0 FOR NORTON EQUIVALENT	WIRE0270
C STORE IN ARRAY M2	WIRE0271
C	WIRE0272
54 IF (LSO.EQ.12.OR.LSO.EQ.22) GO TO 57	WIRE0273
DO 55 I=1,N	WIRE0274
DO 55 J=1,N	WIRE0275
55 A(I,J)=M1(I,J)*Y0(J,J)	WIRE0276
DO 56 I=1,N	WIRE0277
DO 56 J=1,N	WIRE0278
56 M2(I,J)=YL(I,I)*A(I,J)+M2(I,J)	WIRE0279
GO TO 62	WIRE0280
57 DO 59 I=1,N	WIRE0281
DO 59 J=1,N	WIRE0282
SUML=ZEROC	WIRE0283
DO 58 K=1,N	WIRE0284
58 SUML=SUML+M1(I,K)*Y0(K,J)	WIRE0285
59 A(I,J)=SUML	WIRE0286
DO 61 I=1,N	WIRE0287
DO 61 J=1,N	WIRE0288
SUML=ZEROC	WIRE0289
DO 60 K=1,N	WIRE0290
60 SUML=SUML+YL(I,K)*A(K,J)	WIRE0291
61 M2(I,J)=SUML+M2(I,J)	WIRE0292
62 BB=TWO*PI*DSQRT(ER*MUR)/V	WIRE0293
BBL=BB*L	WIRE0294
C	WIRE0295
C IF FIELD SPECIFICATION IS A UNIFORM PLANE WAVE, READ DATA AND	WIRE0296
C COMPUTE THE COMPONENTS OF THE ELECTRIC FIELD INTENSITY AND THE	WIRE0297
C PHASE CONSTANT(FOR ONE HERTZ) IN THE X,Y, AND Z DIRECTIONS	WIRE0298
C	WIRE0299
IF (PSO.EQ.2) GO TO 66	WIRE0300
READ(5,63) EM,THE,THP,PHP	WIRE0301
63 FORMAT(4(E10.3,5X))	WIRE0302
WRITE(6,64)	WIRE0303
64 FORMAT(///' EXCITATION SOURCE IS A UNIFORM PLANE WAVE'//)	WIRE0304
WRITE(6,65) EM,THE,THP,PHP	WIRE0305

```

65 FORNAT(' MAGNITUDE OF ELECTRIC FIELD = ',1PE10.3,' (VOLTS/METER)' / WIRE0306
1' THETA = ',1PE10.3,' (DEGREES)' / THETA = ',1PE10.3,' (DEGREES)' / WIRE0307
2' PHIP = ',1PE10.3,' (DEGREES)' / WIRE0308
THE=THE/RADEG WIRE0309
THP=THP/RADEG WIRE0310
PHP=PHP/RADEG WIRE0311
CTE=DCOS (THE) WIRE0312
CTP=DCOS (THP) WIRE0313
CPP=DCOS (PHP) WIRE0314
STE=DSIN (THE) WIRE0315
STP=DSIN (THP) WIRE0316
SPP=DSIN (PHP) WIRE0317
EYN=EN*CTE*STP WIRE0318
EZB=-EN*(CTE*CTP*CPP+STE*SPP) WIRE0319
EIN=-EN*(CTE*CTP*SPP+STE*CPP) WIRE0320
BBX=BB*STP*SPP WIRE0321
BBY=BB*CTP WIRE0322
BBZ=BB*STP*CPP WIRE0323
C WIRE0324
C*****FREQUENCY DEPENDENT CALCULATIONS***** WIRE0325
C WIRE0326
66 CONTINUE WIRE0327
READ(5,67,END=121) F WIRE0328
67 FORNAT(E10.3) WIRE0329
BETA=BB*F WIRE0330
BETAL=BBL*F WIRE0331
DS=DSIN (BETA) WIRE0332
DC=DCOS (BETAL) WIRE0333
GO TO (68,74),FSO WIRE0334
C WIRE0335
C COMPUTE THE EQUIVALENT FORCING FUNCTIONS FOR UNIFORM PLANE WAVE WIRE0336
C EXCITATION WIRE0337
C WIRE0338
C COMPUTE THE X,Y, AND Z COMPONENTS OF THE PHASE CONSTANT FOR WIRE0339
C UNIFORM PLANE WAVE EXCITATION AND A FREQUENCY OF F HERTZ WIRE0340
C WIRE0341
68 BX=BBX*F WIRE0342
BY=BBY*F WIRE0343
BZ=BBZ*F WIRE0344
EBXL=CDEXP (-XJ*BX*L) WIRE0345
BP=BETA+BX WIRE0346
BN=BETA-BX WIRE0347
EPBL=CDEXP (XJ*BETAL) WIRE0348
ENBL=CDEXP (-XJ*BETAL) WIRE0349
EP=EPBL*E2 (ZERO,L,-BP) WIRE0350
EN=ENBL*E2 (ZERO,L,BN) WIRE0351
69 GO TO (70,72),TYPE WIRE0352
C WIRE0353
C COMPUTE FORCING FUNCTIONS FOR UNIFORM PLANE WAVE EXCITATION AND WIRE0354
C TYPE 1 STRUCTURES WIRE0355
C WIRE0356
70 DO 71 I=1,N WIRE0357
YI=V4 (I) WIRE0358
ZI=V3 (I) WIRE0359
BYPBZ=BY*YI+BZ*ZI WIRE0360
EBYPBZ=CDEXP (-XJ*BYPBZ) -ONE WIRE0361
EJBZ=CDEXP (-XJ*BZ*ZI) WIRE0362
EJBY=CDEXP (-XJ*BY*YI) WIRE0363
V1N=EXN*EBYPBZ/TWO WIRE0364
V2N=-XJ*V1N WIRE0365
V1 (I)=V1N*(EP+EN) WIRE0366

```

	V2(I)=V2H*(EP-EN)	WIRE0367
	ETO(I)=(EYH*YI+EZH*ZI)*E2(ZERO,ONE,-BYPBZ)	WIRE0368
71	ETL(I)=ETO(I)*EBXL	WIRE0369
	GO TO 96	WIRE0370
C		WIRE0371
C	COMPUTE FORCING FUNCTIONS FOR UNIFORM PLANE WAVE EXCITATION AND	WIRE0372
C	TYPE 2 STRUCTURES	WIRE0373
C		WIRE0374
72	DO 73 I=1,N	WIRE0375
	YI=V4(I)	WIRE0376
	ZI=V3(I)	WIRE0377
	SBY=DSIN(BY*YI)	WIRE0378
	EJBZ=CDEXP(-XJ*BZ*ZI)	WIRE0379
	V2H=-EYH+EJBZ*SBY	WIRE0380
	V1H=XJ*V2H	WIRE0381
	V1(I)=V1H*(EP+EN)	WIRE0382
	V2(I)=V2H*(EP-EN)	WIRE0383
	ETO(I)=EYH+EJBZ*E2(-YI,YI,BY)	WIRE0384
73	ETL(I)=ETO(I)*EBXL	WIRE0385
	GO TO 96	WIRE0386
C		WIRE0387
C	COMPUTE THE EQUIVALENT FORCING FUNCTIONS FOR NONUNIFORM EXCITATION	WIRE0388
C		WIRE0389
74	EPBL=CDEXP(XJ*BETAL)	WIRE0390
	ENBL=CDEXP(-XJ*BETAL)	WIRE0391
	WRITE(6,75)	WIRE0392
75	FORMAT(///' EXCITATION SOURCE IS A NONUNIFORM FIELD'//)	WIRE0393
	GO TO (76,83,83), TYPE	WIRE0394
C		WIRE0395
C	COMPUTE THE CONTRIBUTION DUE TO THE LONGITUDINAL ELECTRIC FIELD	WIRE0396
C	FOR THE REFERENCE WIRE	WIRE0397
C		WIRE0398
76	READ(5,77) NLO,E0,T0	WIRE0399
77	FORMAT(10,2(10X,E10.3))	WIRE0400
	WRITE(6,78)	WIRE0401
78	FORMAT(' LONGITUDINAL ELECTRIC FIELD ON REFERENCE WIRE'//)	WIRE0402
	WRITE(6,79)	WIRE0403
79	FORMAT(5X,'SPECIFICATION POINT(METERS)',	WIRE0404
	15X,'ELECTRIC FIELD INTENSITY(VOLTS/METER)',5X,'PHASE(DEGREES)'//)	WIRE0405
	XL=ZERO	WIRE0406
	EL=E0	WIRE0407
	TL=T0	WIRE0408
	SUMC=ZEROC	WIRE0409
	SUMS=ZEROC	WIRE0410
	WRITE(6,80) XL,E0,T0	WIRE0411
80	FORMAT(13X,1PE10.3,24X,1PE10.3,25X,1PE10.3)	WIRE0412
	DO 82 I=1,NLO	WIRE0413
	READ(5,81) XI,EI,TI	WIRE0414
81	FORMAT(3(E10.3,10X))	WIRE0415
	WRITE(6,80) XI,EI,TI	WIRE0416
	XP=XI	WIRE0417
	EP=EI	WIRE0418
	TP=TI	WIRE0419
	XD=XP-XL	WIRE0420
	NI=(EP-EL)/XD	WIRE0421
	BI=(EL*XP-EP*XL)/XD	WIRE0422
	NI=(TP-TL)/(RADEG*XD)	WIRE0423
	CI=(TL*XP-TP*XL)/(RADEG*XD)	WIRE0424
	NH=NI-BETA	WIRE0425
	NP=NI+BETA	WIRE0426
	EJCI=CDEXP(XJ*CI)	WIRE0427

	SUNC=SUNC+EJCI*P5*(NI*EPBL*E1(XL,XP,NH)+NI*ENBL*E1(XL,XP,NP)	WIRE0428
	1+BI*EPBL*E2(XL,XP,NH)+BI*ENBL*E2(XL,XP,NP))	WIRE0429
	SUNS=SUNS-XJ*P5+EJCI*(NI*EPBL*E1(XL,XP,NH)-NI*ENBL*E1(XL,XP,NP)	WIRE0430
	1+BI*EPBL*E2(XL,XP,NH)-BI*ENBL*E2(XL,XP,NP))	WIRE0431
	XL=XP	WIRE0432
	EL=EP	WIRE0433
82	TL=TP	WIRE0434
	ELOC=SUNC	WIRE0435
	ELOS=SUNS	WIRE0436
	GO TO 84	WIRE0437
83	ELOC=ZEROC	WIRE0438
	ELOS=ZEROC	WIRE0439
C		WIRE0440
C	COMPUTE THE CONTRIBUTION DUE TO THE LONGITUDINAL ELECTRIC FIELD	WIRE0441
C	FOR THE WIRES	WIRE0442
C		WIRE0443
84	DO 95 I=1,N	WIRE0444
	READ(5,85) NLO,ELO,TLO	WIRE0445
85	FORMAT(I10,2(10X,E10.3))	WIRE0446
	XL=ZERO	WIRE0447
	WRITE(6,86) I	WIRE0448
86	FORMAT(// ' LONGITUDINAL ELECTRIC FIELD ON WIRE ',3X,I2/)	WIRE0449
	WRITE(6,79)	WIRE0450
	WRITE(6,80) XL,ELO,TLO	WIRE0451
	EL=ELO	WIRE0452
	TL=TLO	WIRE0453
	SUNC=ZEROC	WIRE0454
	SUNS=ZEROC	WIRE0455
	DO 88 J=1,NLO	WIRE0456
	READ(5,87) XI,EI,TI	WIRE0457
87	FORMAT(3(E10.3,10X))	WIRE0458
	WRITE(6,80) XI,EI,TI	WIRE0459
	XP=XI	WIRE0460
	EP=EI	WIRE0461
	TP=TI	WIRE0462
	XD=XP-XL	WIRE0463
	NI=(EP-EL)/XD	WIRE0464
	BI=(EL*XP-EP*XL)/XD	WIRE0465
	NI=(TP-TL)/(RADEG*XD)	WIRE0466
	CI=(TL*XP-TP*XL)/(RADEG*XD)	WIRE0467
	NH=NI-BETA	WIRE0468
	NP=NI+BETA	WIRE0469
	EJCI=CDEXP(XJ*CI)	WIRE0470
	SUNC=SUNC+EJCI*P5*(NI*EPBL*E1(XL,XP,NH)+NI*ENBL*E1(XL,XP,NP)	WIRE0471
	1+BI*EPBL*E2(XL,XP,NH)+BI*ENBL*E2(XL,XP,NP))	WIRE0472
	SUNS=SUNS-XJ*P5+EJCI*(NI*EPBL*E1(XL,XP,NH)-NI*ENBL*E1(XL,XP,NP)	WIRE0473
	1+BI*EPBL*E2(XL,XP,NH)-BI*ENBL*E2(XL,XP,NP))	WIRE0474
	XL=XP	WIRE0475
	EL=EP	WIRE0476
88	TL=TP	WIRE0477
	V1(I)=SUNC-ELOC	WIRE0478
	V2(I)=SUNS-ELOS	WIRE0479
C		WIRE0480
C	COMPUTE THE CONTRIBUTION DUE TO THE TRANSVERSE ELECTRIC FIELD	WIRE0481
C	AT X=0 FOR EACH WIRE	WIRE0482
C		WIRE0483
	XL=ZERO	WIRE0484
	WRITE(6,89) I	WIRE0485
89	FORMAT(// ' TRANSVERSE ELECTRIC FIELD AT X=0 FOR WIRE ',3X,I2/)	WIRE0486
	READ(5,85) NTO,ETO,ETO	WIRE0487
	WRITE(6,79)	WIRE0488

```

WRITE(6,80) XL,EET0,TTO
EL=EET0
TL=TTO
SUM0=ZEROC
DO 91 J=1,NT0
READ(5,90) XI,EI,TI
90 FORMAT(3(E10.3,10X))
WRITE(6,80) XI,FI,TI
XP=XI
EP=EI
TP=TI
XD=XP-XL
NI=(EP-EL)/XD
BI=(EL*XP-EP*XL)/XD
NI=(TP-TL)/(RADEG*XD)
CI=(TL*XP-TP*XL)/(RADEG*XD)
EJCI=CDEXP(XJ*CI)
SUM0=SUM0+EJCI*(NI*E1(XL,XP,NI)+BI*E2(XL,XP,NI))
XL=XP
EL=EP
91 TL=TP
ET0(I)=SUM0

C
C   COMPUTE THE CONTRIBUTION DUE TO THE TRANSVERSE ELECTRIC FIELD
C   AT X=L FOR EACH WIRE
C
XL=ZERO
WRITE(6,92) I
92 FORMAT(//' TRANSVERSE ELECTRIC FIELD AT X=L FOR WIRE ',3X,I2/)
READ(5,85) NTL,EETL,TTL
WRITE(6,79)
WRITE(6,80) XL,EETL,TTL
EL=EETL
TL=TTL
SU IL=ZEROC
DO 94 J=1,NTL
READ(5,93) XI,EI,TI
93 FORMAT(3(E10.3,10X))
WRITE(6,80) XI,EI,TI
XP=XI
EP=EI
TP=TI
XD=XP-XL
NI=(EP-EL)/XD
BI=(EL*XP-EP*XL)/XD
NI=(TP-TL)/(RADEG*XD)
CI=(TL*XP-TP*XL)/(RADEG*XD)
EJCI=CDEXP(XJ*CI)
SUML=SUML+EJCI*(NI*E1(XL,XP,NI)+BI*E2(XL,XP,NI))
XL=XP
EL=EP
94 TL=TP
ETL(I)=SUML
95 CONTINUE

C
C   COMPUTE THE TERMINAL CURRENTS
C
C   FORM THE EQUATIONS
C
96 IF (LSO.EQ.12.OR.LSO.EQ.22) GO TO 100
DO 98 I=1,N

```

```

WIRE0489
WIRE0490
WIRE0491
WIRE0492
WIRE0493
WIRE0494
WIRE0495
WIRE0496
WIRE0497
WIRE0498
WIRE0499
WIRE0500
WIRE0501
WIRE0502
WIRE0503
WIRE0504
WIRE0505
WIRE0506
WIRE0507
WIRE0508
WIRE0509
WIRE0510
WIRE0511
WIRE0512
WIRE0513
WIRE0514
WIRE0515
WIRE0516
WIRE0517
WIRE0518
WIRE0519
WIRE0520
WIRE0521
WIRE0522
WIRE0523
WIRE0524
WIRE0525
WIRE0526
WIRE0527
WIRE0528
WIRE0529
WIRE0530
WIRE0531
WIRE0532
WIRE0533
WIRE0534
WIRE0535
WIRE0536
WIRE0537
WIRE0538
WIRE0539
WIRE0540
WIRE0541
WIRE0542
WIRE0543
WIRE0544
WIRE0545
WIRE0546
WIRE0547
WIRE0548
WIRE0549

```

SUM0=ZEROC	WIRE0550
SUML=ZEROC	WIRE0551
DO 97 J=1,N	WIRE0552
A(I,J)=XJ*DS*M2(I,J)	WIRE0553
SUM0=SUM0+M3(I,J)*V2(J)	WIRE0554
97 SUML=SUML+M3(I,J)*ETO(J)	WIRE0555
V1(I)=V1(I)-ETL(I)	WIRE0556
M1(I,I)=SUM0	WIRE0557
ETL(I)=SUML	WIRE0558
98 A(I,I)=A(I,I)+DC*(Y0(I,I)+YL(I,I))	WIRE0559
DO 99 I=1,N	WIRE0560
SUM0=ONEC	WIRE0561
SUML=ONEC	WIRE0562
IF(LSO.EQ.21) SUM0=VL(I,I)	WIRE0563
IF(LSO.EQ.11) SUML=YL(I,I)	WIRE0564
99 B(I)=SUM0*V1(I)+XJ*SUML*M1(I,I)+DC*SUM0*ETO(I)+XJ*DS*SUML*ETL(I)	WIRE0565
GO TO 107	WIRE0566
100 DO 102 I=1,N	WIRE0567
SUM0=ZEROC	WIRE0568
SUML=ZEROC	WIRE0569
DO 101 J=1,N	WIRE0570
A(I,J)=XJ*DS*M2(I,J)+DC*(Y0(I,J)+YL(I,J))	WIRE0571
SUM0=SUM0+M3(I,J)*V2(J)	WIRE0572
101 SUML=SUML+M3(I,J)*ETO(J)	WIRE0573
V1(I)=V1(I)-ETL(I)	WIRE0574
M1(I,I)=SUM0	WIRE0575
102 ETL(I)=SUML	WIRE0576
DO 106 I=1,N	WIRE0577
IF(LSO.EQ.22) GO TO 104	WIRE0578
SUM0=ZEROC	WIRE0579
SUML=ZEROC	WIRE0580
DO 103 J=1,N	WIRE0581
SUM0=SUM0+YL(I,J)*M1(J,J)	WIRE0582
103 SUML=SUML+YL(I,J)*ETL(J)	WIRE0583
B(I)=V1(I)+XJ*SUM0+DC*ETO(I)+XJ*DS*SUML	WIRE0584
GO TO 106	WIRE0585
104 SUM0=ZEROC	WIRE0586
SUML=ZEROC	WIRE0587
DO 105 J=1,N	WIRE0588
SUM0=SUM0+YL(I,J)*V1(J)	WIRE0589
105 SUML=SUML+YL(I,J)*ETO(J)	WIRE0590
B(I)=SUM0+XJ*M1(I,I)+DC*SUML+XJ*DS*ETL(I)	WIRE0591
106 CONTINUE	WIRE0592
C SOLVE THE EQUATIONS	WIRE0593
C	WIRE0594
C	WIRE0595
107 CALL LEQ1C(A,N,N,B,1,N,O,WA,IER)	WIRE0596
IER=IER-128	WIRE0597
WRITE(6,108) F	WIRE0598
108 FORMAT(1H1,' FREQUENCY (HERTZ) = ',1PE16.9,///)	WIRE0599
IF(IER.EQ.1) GO TO 110	WIRE0600
WRITE(6,109)	WIRE0601
109 FORMAT(///,' *****SOLUTION ERROR*****',///)	WIRE0602
GO TO 121	WIRE0603
110 WRITE(6,111)	WIRE0604
111 FORMAT(16X,' WIRE',8X,' IOM(AMPS)',4X,' IOA (DEGREES)',8X,	WIRE0605
' ILN(AMPS)',4X,' ILA (DEGREES)' ///)	WIRE0606
C COMPUTE AND PRINT THE TERMINAL CURRENTS	WIRE0607
C	WIRE0608
C	WIRE0609
DO 114 I=1,N	WIRE0610

IF (LSO.EQ.11.OR.LSO.EQ.21) GO TO 113	WIRE0611
SUM0=ZEROC	WIRE0612
DO 112 J=1,N	WIRE0613
112 SUM0=SUM0+Y0(I,J)*B(J)	WIRE0614
WA(I)=SUM0	WIRE0615
GO TO 114	WIRE0616
113 WA(I)=Y0(I,I)*B(I)	WIRE0617
114 CONTINUE	WIRE0618
DO 120 I=1,N	WIRE0619
IF (LSO.EQ.21.OR.LSO.EQ.22) GO TO 116	WIRE0620
IO=B(I)	WIRE0621
SUM0=ZEROC	WIRE0622
DO 115 J=1,N	WIRE0623
115 SUM0=SUM0+M3(I,J)*WA(J)	WIRE0624
IL=-XJ*(M1(I,I)+DS*ETL(I))+DC*B(I)+XJ*DS*SUM0	WIRE0625
GO TO 118	WIRE0626
116 IO=WA(I)	WIRE0627
SUM0=ZEROC	WIRE0628
DO 117 J=1,N	WIRE0629
117 SUM0=SUM0+M3(I,J)*B(J)	WIRE0630
IL=-XJ*(M1(I,I)+DS*ETL(I))+DC*WA(I)+XJ*DS*SUM0	WIRE0631
118 IOM=CDABS(IO)	WIRE0632
ILM=CDABS(IL)	WIRE0633
IOR=DREAL(IO)	WIRE0634
IOI=DIMAG(IO)	WIRE0635
ILR=DREAL(IL)	WIRE0636
ILI=DIMAG(IL)	WIRE0637
IF (IOR.EQ.ZERO.AND.IOI.EQ.ZERO) IOR=ONE	WIRE0638
IF (ILR.EQ.ZERO.AND.ILI.EQ.ZERO) ILR=ONE	WIRE0639
IOA=DATAN2(IOI,IOR)*RADEG	WIRE0640
ILA=DATAN2(ILI,ILR)*RADEG	WIRE0641
WRITE(6,119) I,IOM,IOA,ILM,ILA	WIRE0642
119 FORMAT(18X,I2,7X,1PE10.3,4X,1PE10.3,9X,1PE10.3,4X,1PE10.3/)	WIRE0643
120 CONTINUE	WIRE0644
GO TO 66	WIRE0645
121 STOP	WIRE0646
END	WIRE0647

APPENDIX B-1

Conversion of WIRE to Single Precision

Delete 0062			
<u>Card</u>		<u>Double Precision</u>	<u>Single Precision</u>
0064		REAL *8	REAL
0066		COMPLEX *16	COMPLEX
0071-0072	Change all	D's to	E's
0073		0.D0	0.E0
0074		1.D0	.E0
0075		2.D0	2.E0
0076		DCMPLX(1.D0,0.D0)	CMPLX(1.E0,0.E0)
0077		DCMPLX(0.D0,0.D0)	CMPLX(0.E0,0.E0)
0078		DCMPLX(0.D0,1.D0)	CMPLX(0.E0,1.E0)
0079		DATAN	ATAN
0150		DSQRT	SQRT
0161		DLOG	ALOG
0163		DLOG	ALOG
0165		DLOG	ALOG
0182		DLOG	ALOG
0188		DLOG	ALOG
0194		DLOG	ALOG
0195		DCOS	COS
0195		DCOS	COS
0293		DSQRT	SQRT
0312		DCOS	COS
0313		DCOS	COS

APPENDIX B-1 (continued)

<u>Card</u>	<u>Double Precision</u>	<u>Single Precision</u>
0314	DCOS	COS
0315	DSIN	SIN
0316	DSIN	SIN
0317	DSIN	SIN
0332	DSIN	SIN
0333	DCOS	COS
0345	CDEXP	CEXP
0348	CDEXP	CEXP
0349	CDEXP	CEXP
0361	CDEXP	CEXP
0362	CDEXP	CEXP
0363	CDEXP	CEXP
0378	DSIN	SIN
0379	CDEXP	CEXP
0390	CDEXP	CEXP
0391	CDEXP	CEXP
0427	CDEXP	CEXP
0470	CDEXP	CEXP
0505	CDEXP	CEXP
0536	CDEXP	CEXP
0632	CDABS	CABS
0633	CDABS	CABS
0634	DREAL	REAL

APPENDIX B-1 (continued)

<u>Card</u>	<u>Double Precision</u>	<u>Single Precision</u>
0635	DIMAG	AIMAG
0636	DREAL	REAL
0637	DIMAG	AIMAG
0640	DATAN2	ATAN2
0641	DATAN2	ATAN2

APPENDIX B-2

Flowchart of WIRE

START

0001

General comments concerning the
applicability of the program.

0055

0057

Array dimension information

0060

0062

Declare variable and array types.
Dimension arrays.

0069

0071

Define constants:

CMTM (conversion from mils to meters)

= 2.54×10^{-5}

MU02PI = $\mu/2\pi$

ONE = .1

P5 = .5

FOUR = 4.

ONE80 = 180.

ZERO = 0.

TWO = 2.

ONEC = $1.+j0.$

0080

ZEROC	= 0.+j0.
XJ	= 0.+j1.
V(velocity of light in free space)	= 2.997925×10^8 m/sec
PI	= π
RADEG(conversion of radians to degrees)	= $180./\pi$

Read and print:

Structure type (1,2,3) = TYPE

Load Structure option
(11,12,21,22) = LSO

Field Specification
option (1,2) = FSO

Number of wires (n) = N

Relative permittivity of
medium (ϵ_r) = ER

Relative permeability of
medium (μ_r) = MUR

Line length (l) = L

TYPE = 1;

Radius of reference wire,
 r_{w0} = RWO

TYPE = 3;

Interior radius of cylindrical
shield = RS

0086

0145

(0150)

Read and print the wire radii and the z_i and y_i (r_i and θ_i for TYPE = 3) coordinates. Store z_i in array V3 and y_i in array V4. Compute entries in characteristic impedance matrix, \tilde{Z}_C . Store \tilde{Z}_C in array M1. See equations (2-40), (2-50), and (2-53). ($\tilde{Z}_C = v L$)

(0197)

(0202)

Compute the inverse of \tilde{Z}_C , \tilde{Z}_C^{-1} , with LEQTLIC and store in arrays M2 and M3.

(0211)

(0222)

Read and print entries in terminal impedance (admittance) matrices at $x=0$, $\tilde{Z}_0(Y_0)$, and $x=L$, $\tilde{Z}_L(Y_L)$. Store $\tilde{Z}_0(Y_0)$ in array Y0 and $\tilde{Z}_L(Y_L)$ in array YL.

(0254)

LS0=11,12

LS0=21,22

(54)

(0259)

If Thevenin Equivalent specification of the termination networks is used, swap entries in arrays M1 and M2. M1 will contain Z_C^{-1} and M2 will contain Z_C .

(0267)

54

(0273)

Compute the matrix $Z_C + Z_C Z_C^{-1} Z_0$ for the Thevenin Equivalent or $Z_C^{-1} + Y_C Z_C Y_0$ for the Norton Equivalent. Store in array M2.

(0292)

FS0=2

66

FS0=1

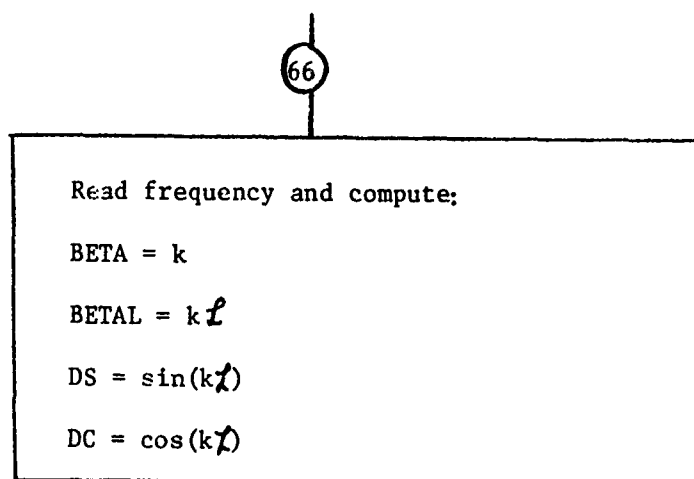
(0300)

If field specification is a uniform plane wave (FS0=1), read wave description data and compute the components of the electric field intensity vector, EXM, EYM, ELM, and propagation constant (for one Hertz), BBX, BBY, BBZ, in the x,y,z directions. See equations (3-12).

(0323)

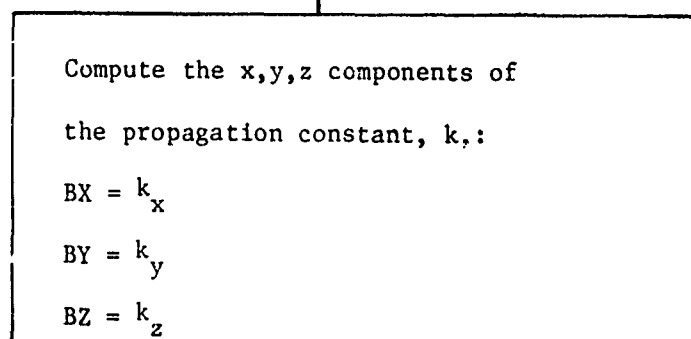
0327

0333



0342

0351



Compute entries in induced source
vectors for TYPE 1 structures:

$$V1 = \underline{M} \quad (3-16)$$

$$V2 = \underline{N} \quad (3-17)$$

$$ET0 = \underline{E}_t(0) \quad (3-22) \quad (I = 0)$$

$$ETL = \underline{E}_t(I) \quad (3-22)$$

96

72

Compute entries in induced source
vectors for TYPE 2 structures:

$$V1 = \underline{M} \quad (3-28)$$

$$V2 = \underline{N} \quad (3-29)$$

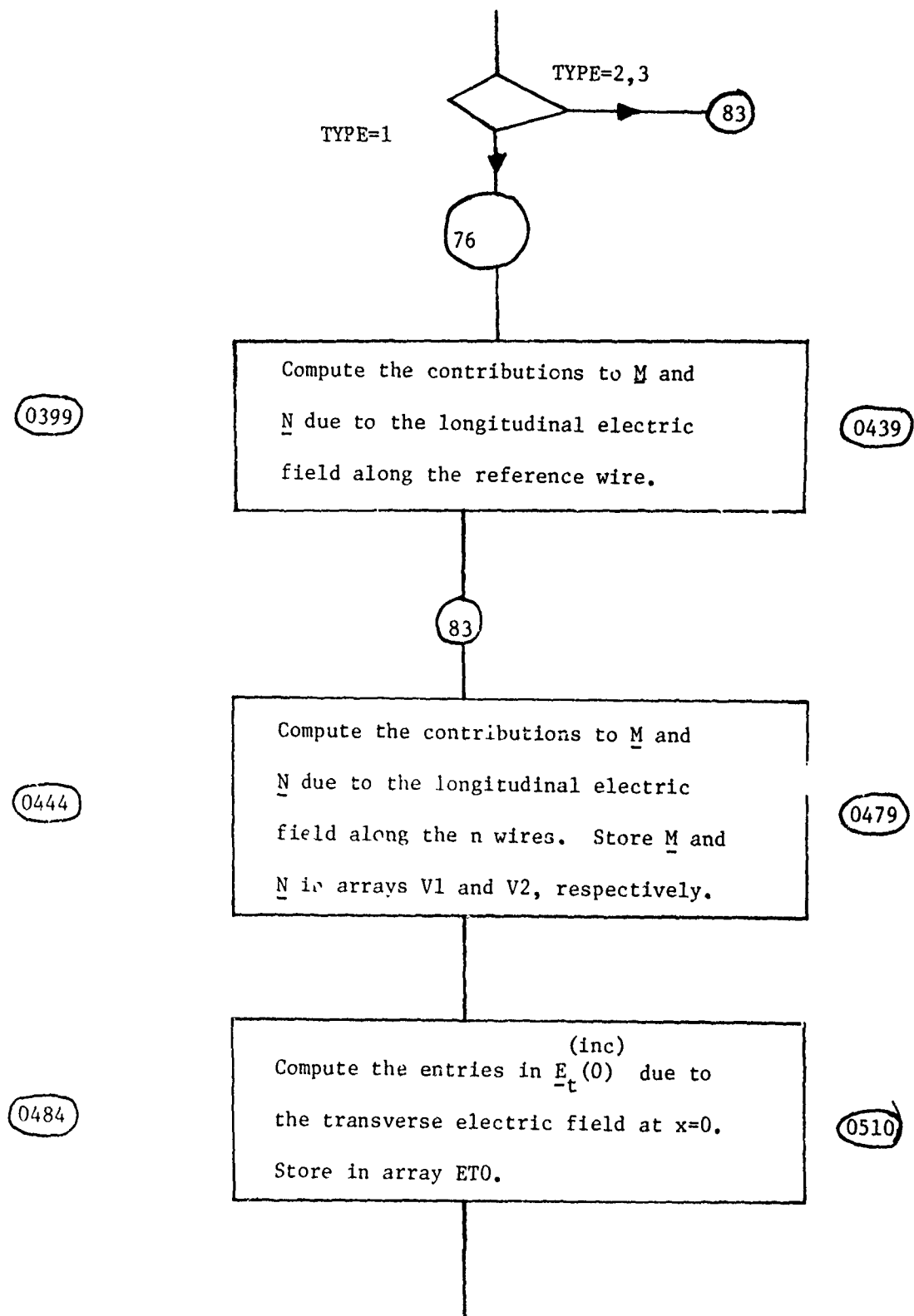
$$ET0 = \underline{E}_t(0) \quad (3-30) \quad (I = 0)$$

$$ETL = \underline{E}_t(I) \quad (3-30)$$

96

74

Compute induced source vectors for
nonuniform field excitation.



0515

(inc)
Compute the entries in $\underline{E}_t(\underline{z})$ due to the
transverse electric field at $x=\underline{z}$. Store
in array ETL.

0542

96

0548

Form the equations (3-2a) or (3-4a).
Arrays \underline{V}_1 , \underline{V}_2 , $\underline{E}0$, ETL now contain
(inc) (inc) (inc)
 $\underline{M}-\underline{E}_t(\underline{z})$, \underline{N} , $\underline{E}_t(0)$ and $\underline{Z}_C^{-1} \underline{E}_t(0)$,
respectively. Array \underline{M} contains on its
main diagonal the entries in $\underline{Z}_C^{-1} \underline{N}$.

0592

0596

Solve the equations with LEQT1C

0596

0610

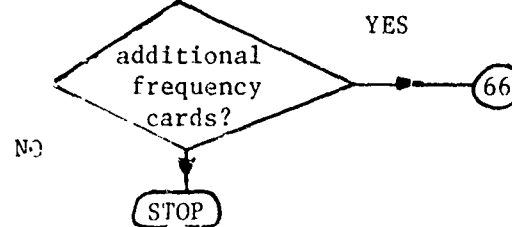
Compute the terminal currents at $x=0$
and those at $x=\underline{z}$ via (3-2b) or (3-4b).

0641

0632

Compute and print the magnitude and
phase of the terminal currents.

0644



APPENDIX C

Function Subprograms

E1, E2

Program Listings

COMPLEX FUNCTION E1*16 (A,B,X)	PNE10001
IMPLICIT REAL*8 (A-H,O-Z)	PNE10002
COMPLEX*16 XJ,ONEC	PNE10003
DATA THREE/3.D0/,PZ1/1.D-2/,TEN/10.D0/	PNE10004
COMMON XJ,ZERO,TWO,ONE,ONEC	PNE10005
B2=B*B	PNE10006
A2=A*A	PNE10007
XB=X*B	PNE10008
XA=X*A	PNE10009
BPA=B+A	PNE10010
XBPA2=X*BPA/TWO	PNE10011
BNA=B-A	PNE10012
XBNA2=X*BNA/TWO	PNE10013
IF (XBPA2.EQ.ZERO) GO TO 1	PNE10014
SBPA=DSIN (XBPA2)/XBPA2	PNE10015
GO TO 2	PNE10016
1 SBPA=ONE	PNE10017
2 IF (XBNA2.EQ.ZERO) GO TO 3	PNE10018
SBNA=DSIN (XBNA2)/XBNA2	PNE10019
GO TO 4	PNE10020
3 SBNA=ONE	PNE10021
4 IF (XB.EQ.ZERO) GO TO 5	PNE10022
SB=DSIN (XB)/XB	PNE10023
GO TO 6	PNE10024
5 SB=ONE	PNE10025
6 IF (XA.EQ.ZERO) GO TO 7	PNE10026
SA=DSIN (XA)/XA	PNE10027
GO TO 8	PNE10028
7 SA=ONE	PNE10029
8 XR=-SBPA*SBNA*(B2-A2)/TWO+B2*SB-A2*SA	PNE10030
IF (X.EQ.ZERO) GO TO 13	PNE10031
IF (DABS (XA).LE.PZ1) GO TO 9	PNE10032
XIA=A*(DCOS (XA)-SA)/X	PNE10033
GO TO 10	PNE10034
9 XIA=-XA*A2*((ONE-XA*XA/TEN)/THREE)	PNE10035
10 IF (DABS (XB).LE.PZ1) GO TO 11	PNE10036
XIB=B*(DCOS (XB)-SB)/X	PNE10037
GO TO 12	PNE10038
11 XIB=-XB*B2*((ONE-XB*XB/TEN)/THREE)	PNE10039
12 XI=XIA-XIB	PNE10040
GO TO 14	PNE10041
13 XI=ZERO	PNE10042
14 E1=XR+XJ*XI	PNE10043
RETURN	PNE10044
END	PNE10045

APPENDIX C-1

Conversion of E1 to Single Precision

Delete Card 0002

001		E1*16		E1
0003		COMPLEX*16		COMPLEX
0004	Change all	D's	to	E's
0015		DSIN		SIN
0019		DSIN		SIN
0023		DSIN		SIN
0027		DSIN		SIN
0032		DABS		ABS
0033		DCOS		COS
0036		DABS		ABS
0037		DCOS		COS

```

COMPLEX FUNCTION E2*16(A,B,X)
IMPLICIT REAL*8 (A-H,O-Z)
COMPLEX*16 XJ,ONEC
COMMON XJ,ZERO,TWO,ONE,ONEC
DIF=B-A
FA=X*DIF/TWO
FB=X*(B+A)/TWO
IF (FA.EQ.ZERO) GO TO 1
E2=DIF*(DSIN(FA)/FA)*CDEXP(XJ*FB)
GO TO 2
1 E2=DIF*ONEC
2 CONTINUE
RETURN
END

```

```

FNE20001
FNE20002
FNE20003
FNE20004
FNE20005
FNE20006
FNE20007
FNE20008
FNE20009
FNE20010
FNE20011
FNE20012
FNE20013
FNE20014

```

APPENDIX C-2

Conversion of E2 to Single Precision

Delete Card 0002

0001	E2*16	E2
0003	COMPLEX*16	COMPLEX
0009	DSIN	SIN
0009	CDEXP	CEXP

MISSION of Rome Air Development Center

RADC plans and conducts research, exploratory and advanced development programs in command, control, and communications (C³) activities, and in the C³ areas of information sciences and intelligence. The principal technical mission areas are communications, electromagnetic guidance and control, surveillance of ground and aerospace objects, intelligence data collection and handling, information system technology, ionospheric propagation, solid state sciences, microwave physics and electronic reliability, maintainability and compatibility.

